ÇUKUROVA UNIVERSITY
INSTITUTE OF NATURAL AND APPLIED SCIENCES

MSc THESIS

Özgür ÇELİK

A NOVEL HYBRID MPPT METHOD FOR GRID CONNECTED PHOTOVOLTAIC SYSTEMS WITH PARTIAL SHADING CONDITIONS

DEPARTMENT OF ELECTRICAL AND ELECTRONICS ENGINEERING

ADANA, 2015

ÇUKUROVA UNIVERSITY
INSTITUTE OF NATURAL AND APPLIED SCIENCES

A NOVEL HYBRID MPPT METHOD FOR GRID CONNECTED PHOTOVOLTAIC SYSTEMS WITH PARTIAL SHADING CONDITIONS

Özgür ÇELİK

MSC THESIS

DEPARTMENT OF ELECTRICAL AND ELECTRONICS ENGINEERING

We certify that the thesis titled above was reviewed and approved for the award of degree of the Master of Science by the board of jury on 03/08/2015.

.....	.....	.....
Assoc. Prof. Dr. Ahmet TEKE	Prof. Dr. Mehmet TÜMAY	Asst. Prof. Dr. Lütfü SARIBULUT
SUPERVISOR	MEMBER	MEMBER

This MSc Thesis is written at the Department of Electrical and Electronics Engineering of Institute of Natural And Applied Sciences of Çukurova University.
Registration Number:

Prof. Dr. Mustafa GÖK
Director
Institute of Natural and Applied Sciences

This thesis was supported by the Scientific Research Project Unit of Cukurova University with a project number of FYL-2014-3485.

ABSTRACT

MSc THESIS

A NOVEL HYBRID MPPT METHOD FOR GRID CONNECTED PHOTOVOLTAIC SYSTEMS WITH PARTIAL SHADING CONDITIONS

Özgür ÇELİK

ÇUKUROVA UNIVERSITY
INSTITUTE OF NATURAL AND APPLIED SCIENCES
DEPARTMENT OF ELECTRICAL AND ELECTRICAL ENGINNERING

Supervisor : Assoc. Prof. Dr. Ahmet TEKE
Year: 2015, Pages: 130
Jury : Assoc. Prof. Dr. Ahmet TEKE
: Prof. Dr. Mehmet TÜMAY
: Asst. Prof. Dr. Lütfü SARIBULUT

Energy efficiency and using alternative energy sources issues have become more crucial due to the world energy supply has been subjected to enormous stress. Photovoltaic (PV) systems are one of the mostly used alternative energy generation option. However, PV systems suffer from low system efficiency, high initial cost and erratic atmospheric conditions. The output power of PV panels highly depends on the ambient temperature and the radiation intensity. The modest changes in operating current and voltage of PV panel, which relies on the temperature and radiation, constitutes visible variations in the output power of the panel. In order to mitigate these variations and force the system to study on maximum power point (MPP), several maximum power point tracking (MPPT) techniques are presented in the literature.

In this thesis, a grid connected PV system, which consists of an artificial neural network (ANN) based MPPT technique and a novel Hybrid MPPT technique, is analyzed, modeled and simulated. The proposed MPPT is integrated to a two stage grid connected PV system. The performance and efficiency of the proposed system are tested with different simulation cases by PSCAD/EMTDC program.

The results obtained from the simulations clearly demonstrates that the presented MPPT algorithm simultaneously performs the tracking of MPP voltage and provide significant efficiency gains under variable atmospheric conditions and partial shading conditions. Furthermore, by employing an interleaved DC-DC boost converter, I^2R losses, ripples in the input and output waveform and electromagnetic interference are substantially reduced, and the transient response, which affects the dynamic performance of the entire system, is improved.

Key Words: Grid-tied photovoltaic systems, MPPT techniques, Hybrid MPPT, ANN based MPPT techniques.

ÖZ

YÜKSEK LİSANS TEZİ

ŞEBEKEYE BAĞLI FOTOVOLTAİK SİSTEMLERDE KISMİ GÖLGELENME ŞARTLARI İÇİN YENİ BİR HİBRİD MGNİ YÖNTEMİ

Özgür ÇELİK

ÇUKUROVA ÜNİVERSİTESİ
FEN BİLİMLERİ ENSTİTÜSÜ
ELEKTRİK ELEKTRONİK MÜHENDİSLİĞİ ANABİLİM DALI

Danışman : Doç. Dr. Ahmet TEKE
Yıl: 2015, Sayfa: 130
Jüri : Doç. Dr. Ahmet TEKE
: Prof. Dr. Mehmet TÜMAY
: Yrd. Doç. Dr. Lütfü SARIBULUT

Dünya enerji arzı çok büyük baskıya maruz kaldığından dolayı enerji verimliliği ve alternatif enerji kaynaklarının kullanılması çok önemli bir konu haline gelmiştir. Fotovoltaik sistemler (FV) en çok kullanılan alternatif enerji üretim seçeneklerinden birisidir. Fakat FV sistemler düşük verimlilik, yüksek kurulum maliyeti ve değişken atmosferik koşullardan negatif olarak etkilenmektedirler. FV panellerin çıkış gücü ortam sıcaklığı ve ışıma şiddetine bağlıdır. Sıcaklık ve ışımaya bağlı olarak, FV panellerin çalışma akım ve gerilimlerinde meydana gelen küçük değişimler çıkış gücünde hissedilir salınımlar oluşturmaktadır. Bu salınımları azaltmak ve sistemi maksimum güç noktasında (MGN) çalışmaya zorlamak için, çeşitli maksimum güç noktası izleyici (MGNİ) teknikleri literatürde sunulmuştur.

Bu tez çalışmasında, yapay sinir ağı (YSA) tabanlı yeni MGNİ tekniği ve yeni bir hibrid MGNİ tekniği içeren şebeke bağlantılı FV sistemin analizi, modellemesi ve benzetimi yapılmıştır. Önerilen MGNİ iki kademeli şebeke bağlı FV sisteme entegre edilmiştir. Önerilen sistemin performansı ve verimliliği PSCAD/EMTDC programında farklı benzetim çalışmalarıyla incelenmiştir.

Benzetimden elde edilen sonuçlar değişken atmosferik koşullar ve kısmi gölgelenme şartları altında sunulan MGNİ algoritmalarının anlık olarak MGN takibini gerçekleştirdiğini açıkça göstermiştir. Ayrıca, paralel bağlı yükseltici DC-DC çeviriciler kullanılmış, I^2R kayıpları, giriş ve çıkış dalga formundaki dalgacıklar, elektromanyetik girişimler önemli ölçüde azaltılmış ve sistemin dinamik performansını etkileyen geçici tepki hızı arttırılmıştır.

Anahtar Kelimeler: Şebeke bağlantılı FV sistemler, MGNİ teknikleri, Hibrid MGNİ, YSA tabanlı MGNİ teknikleri.

ACKNOWLEDGEMENTS

The subject of this thesis was suggested by my supervisor, Assoc. Prof. Dr. Ahmet TEKE to whom I would like to express my heartfelt thanks for his valuable supervision, friendly discussions, guidance, encouragements and extremely useful suggestions throughout this thesis.

I am grateful to Prof. Dr. Mehmet TÜMAY for accepting to be the members of the jury for my thesis.

I would like thanks to Asst. Prof. Dr. Lütfü SARIBULUT for his help, support and accepting to be the members of the jury for my thesis.

My appreciation is also extended to my colleague H. Başak YILDIRIM from university for her valuable advices and supports.

I also gratefully acknowledge the Scientific Research Project Unit of Çukurova University for the financial support (Project Number: FYL-2014-3485).

Finally, I am also indebted to my family for their endless support and encouragements in any respect during the completion of this thesis.

CONTENTS **PAGE**

LIST OF TABLES **PAGE**

LIST OF FIGURES **PAGE**

LIST OF SYMBOLS AND ABBREVIATIONS

A	: Diode Quality Factor
C_{DC}	: DC Link Capacitor
C_{in}	: Input Capacitor of DC-DC Converter
D	: Duty Cycle
f_n	: Nominal Frequency
f_{res}	: Resonance Frequency
f_{sw}	: Switching Frequency
G	: Irradiance
h	: Hour
I_L	: Load Current
I_o	: Dark Saturation Current
I_{op}	: Operation Current
I_{ph}	: Photo Generated Current
I_{pv}	: Photovoltaic Output Current
I_{sc}	: Short Circuit Current
I_{THD}	: Total Harmonic Distortion of Current
k	: Boltzmann's Constant
kWh	: Kilowatthour
L_{boost}	: DC-DC Boost Converter Inductance
L_{dc}	: DC Inductance
L_f	: Filter Inductance
L_g	: Grid Side Inductance
L_i	: Inverter Side Inductance
m_a	: Modulation Index
MW	: Megawatt
P	: Active Power
q	: Charge of Electrons
Q	: Reactive Power
R_d	: Damping Resistor

R_s : Series Resistance

R_{sh} : Parallel Resistance

S : Apparent Power

T : Temperature

T : Time Period

V_{bat} : Battery Voltage

$V_{coupling}$: Voltage Drop Caused by Coupling Impedance

$V_{DC\text{-}link}$: DC Link Voltage

V_{dcref} : Reference DC Voltage

V_{inv} : Inverter Output Voltage

V_{LL} : Line to Line Voltage

V_m : Peak Value of Voltage

V_{mpp} : Maximum Power Point Voltage

V_{oc} : Open Circuit Voltage

V_{op} : Operation Voltage

V_{PCC} : Voltage of Point Of Common Coupling

V_{pv} : Photovoltaic Panel Output Voltage

V_{ref} : Reference Voltage at PCC

V_s : Source Voltage

V_t : Thermal Voltage

V_{THD} : Total Harmonic Distortion of Voltage

w : Fundamental Frequency (rad/s)

w_{sw} : Switching Frequency (rad/s)

α : Temperature Coefficient of Current

γ : Temperature Coefficient of Voltage

AC : Alternating Current

ADALINE : Adaptive Linear Neuron

ANN : Artificial Neural Network

ASD : Adjustable Speed Drive

BP : British Petroleum

BP : Back Propagation Based Theory

CCM	: Continuous Conduction Mode
CSI	: Current Source Inverter
DC	: Direct Current
DCM	: Discontinuous Conduction Mode
DSP	: Digital Signal Processor
EE	: Energy Institute
EI	: Energy Informative
EIA	: Energy Information Administration
EİŞY	: Electricity Market Grid Regulation
et al.	: And Others
GTO	: Gate Turn-Off Thyristor
IEC	: International Electrotechnical Commission
IEEE	: Institute of Electrical and Electronics Engineers
IGBT	: Insulated Gate Bipolar Thyristor
IHD	: Individual Harmonic Distortion
INC	: Incremental Conductance
LM	: Levenberg-Marquardt
LMS	: Least Mean Square
MPP	: Maximum Power Point
MPPT	: Maximum Power Point Tracking
NN	: Neural Network
NREL	: National Renewable Energy Laboratory
P&O	: Perturb and Observation
p.f.	: Power Factor
PCC	: Point of Common Coupling
PCS	: Power Conditioning System
PI	: Proportional-Integral
PLL	: Phase Locked Loop
PV	: Photovoltaic
PWM	: Pulse Width Modulation
REN	: Renewable Energy Policy Network

RMS	: Root Mean Square
SCG	: Scaled Conjugate Gradient
SPWM	: Sinusoidal PWM
STC	: Standard Test Conditions
TDD	: Total Demand Distortion
TEIAS	: Turkish Electricity Transmission Company
THD	: Total Harmonic Distortion
TI	: Texas Instrument
VSI	: Voltage Source Inverter
YEGM	: General Directorate of Renewable Energy

1. INTRODUCTION

1.1. Statement of Problem and Research Motivation

Energy utilization has become a major concern in recent years due to the rapidly increasing demand with population growth and industrialization. Despite this increasing demand, enough amount of energy cannot be supplied and the search for different energy sources is composed. Moreover, the depletion of fossil fuels, racing oil prices, environmental issues of customary energy resources such as global warming, impact of carbon emissions from fossil fuels combustion and environmental pollution direct us to the alternative energy sources (Kjaer et al., 2005; Chiu et al., 2012). Because of the abundance and sustainability of the sun, solar energy is envisaged to a substantial renewable energy source of present and future (Salam et al., 2013; Ishaque et al., 2011).

A photovoltaic (PV) system can directly transforms sunlight into electricity. The fundamental component of this system is PV cell. PV cells basically a semiconductor material, which generates electricity from light owing to the photoelectric effect on this material. Besides having so many advantages like easy to install, no noise, almost maintenance free, inexhaustible and environmentally friendly, PV systems suffer from the initial cost of purchasing and installing PV panels. Also, being inefficiency is the most crucial problem of these systems. The efficiency rating measures what percentage of sunlight absorbed by a panel gets turned into electricity that available to use. Since not all the light from the sun is absorbed by the solar panels therefore most solar panels have a 40% efficiency of conversion and most of PV panels are around 15-18% efficient (REN21, 2014). Although extensive studies have been carried out on increasing PV cell efficiency, growth rates have still not been at the desired level. However, it is equally important to enhance the power generation of PV system by improving its maximum power point tracking capability. Because more advanced applications require power converters to transfer the electricity from PV panels to utility. These converters can be used to regulate the voltage and current at the load, to control the power flow in

both grid connected and stand-alone PV systems, fundamentally to track the maximum power point (MPP) of the device. So it is the most effective and economical way to improve the overall PV system efficiency (Salam et al., 2013; Villalva et al., 2009).

An intermediate DC-DC converter can be attached between PV panels and battery bank or utility grid to deliver maximum energy. DC-DC converter continuously adjusts the voltage or current level to optimize the load match between PV output and load. The unit with the inclusion of a DC-DC converter and a controller is generally named as maximum power point tracking (MPPT) (Rai et al.). A basic PV electric power generation block diagram, which consists of PV panel, DC-DC converter, MPPT and inverter, is exhibited in Figure 1.1.

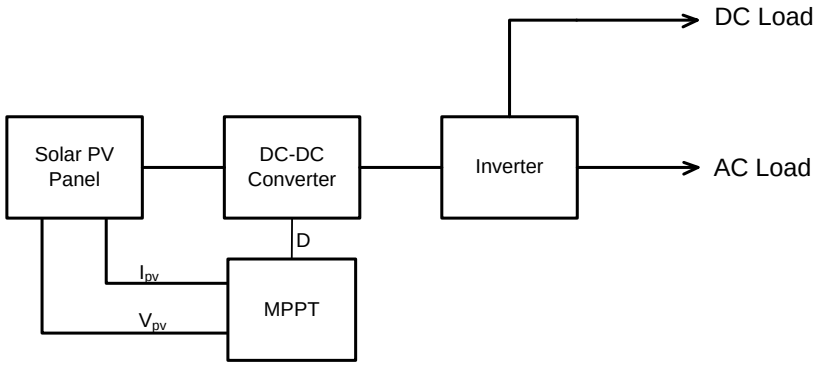

Figure 1.1. A block diagram of MPPT controlled PV electric power generation

The main objective of MPPT controller is to provide that independently of the atmospheric conditions such as temperature and solar irradiance, maximum power is extracted from the PV panels (Salam et al., 2013). MPPT controllers deliver more power, actually lowering the cost per watt and adding reliability. There are many MPPT controllers available commercially and in the literature that can perform task of tracking maximum power point. In these controllers several algorithms working as embedded. These algorithms generally employed the measured voltage and current of the PV array; the power is calculated and duty cycle of the converter is adjusted for tracking MPP. Despite having same objectives, MPPT methods have differences in terms of control variable, complexity level, cost, applications, oscillations around

MPP and convergence speed. With these merits and demerits, MPPT is the most effective ways to increase the overall efficiency of PV systems.

1.2. Objective and Outline of Thesis

The main objective of this thesis is modeling and simulation of a novel MPPT method that utilizes soft computing techniques and developing a hybrid MPPT method. Also to demonstrate the validity of developed method, a three phase grid connected PV model is presented which is convenient for power system dynamic and transient analysis. Furthermore, mostly used conventional MPPT methods are modeled and simulated for demonstrating the superiority of proposed methods. The model has been implemented in an electromagnetic transient software environment, PSCAD/EMTDC. The model consists of PV panels, interleaved DC-DC boost converter, MPPT controller, DC link capacitor, two level three phase inverter, PI based inverter controller, harmonic filter, transformer and utility grid equivalent model.

After an introductory section where the statement of problem, research motivation and contribution of the study are introduced, the structure of this thesis is as follows:

In Chapter 2, the renewable energy term is defined, present and future of the PV panel technologies is discussed. Effect of temperature and irradiation on PV cell's characteristic and parameter extraction of PV cell is introduced. Also PV connection forms and the grid connection limits specified by the regulating standards are examined.

In Chapter 3, overview and extensive literature survey of photovoltaic converters and MPPT controllers are presented in detail. The circuit configuration, operation and basic functions are presented.

In Chapter 4, the power circuit parameters of grid-tied PV system model components are designed in an electromagnetic transient software environment, PSCAD/EMTDC program for simulation cases. The equations and controller

algorithms derived in previous chapters are utilized for the design of different components and blocks in the model.

In Chapter 5, different case studies are performed to validate the performance of proposed MPPT controller and to verify the behavior of modeled grid-tied PV system under various dynamically changing atmospheric conditions. Case studies are presented to test conventional and proposed ANN based – hybrid MPPT method under different solar radiation variables.

In Chapter 6, the significant conclusions of the study are explained and the future work topics on MPPT controller are presented.

1.3. Contributions of Thesis

The main distinctions and important contributions of this thesis can be summarized as follows:

(i) The wide literature survey for grid-tied PV system components and MPPT techniques has been accomplished.

(ii) To overcome the deficiencies of traditional MPPT techniques, a novel ANN (artificial neural network) based MPPT method and a novel hybrid MPPT method are developed.

(iii) The multistring inverter with interleaved boost converters are remarkable choice and not much work has yet been reported on its theoretical, design procedure and analysis for PV system applications. Interleaved DC-DC boost converter is used for each line which reduces the ripple and has a faster transient response when compared to conventional boost converters.

(iv) Optimal layout with the use of a minimum number of solar irradiation measurement sensors is suggested.

2. LITERATURE REVIEW OF THE PHOTOVOLTAIC SYSTEMS

2.1. Renewable Energy

Energy is the basic constituent of life and its supply effects directly on the social and economic development of nations. In modern societies, development level and economic growth are directly measured by energy consumption and generation. It can be clearly said that our prosperity is fundamentally dependent on a continuous, abundant, and economic energy supply (Exposito et al., 2009; Würfel, 2009). Moreover, the tremendous advancement in industry is another reason that raises the energy issue to the foreground. Hence, there is a growing demand to increase the energy generation capacity due to rising of the global energy consumption in all over the world as shown in Figure 2.1. According to the United States Energy Information Administration (EIA), total world consumption of commercial energy is predicted to increase by 49% from 2007 to 2035 in International Energy Outlook 2010 reference case (EIA, 2010).

While there is so much need of energy, fossil fuels are running out, oil prices are getting higher and more importantly environmental issues of customary energy resources such as global warming and impact of carbon emissions are forced people to find different energy sources. Therefore, in the last decades there has been an increasing interest in the field of production and saving of energy. Saving of energy can be one of the cost effective solution but it is not enough to prevent energy crisis and global warming. Furthermore, energy efficiency and energy incentives remain consistently relevant and renewable energies are becoming increasingly important in all over the world (Liu, 2009).

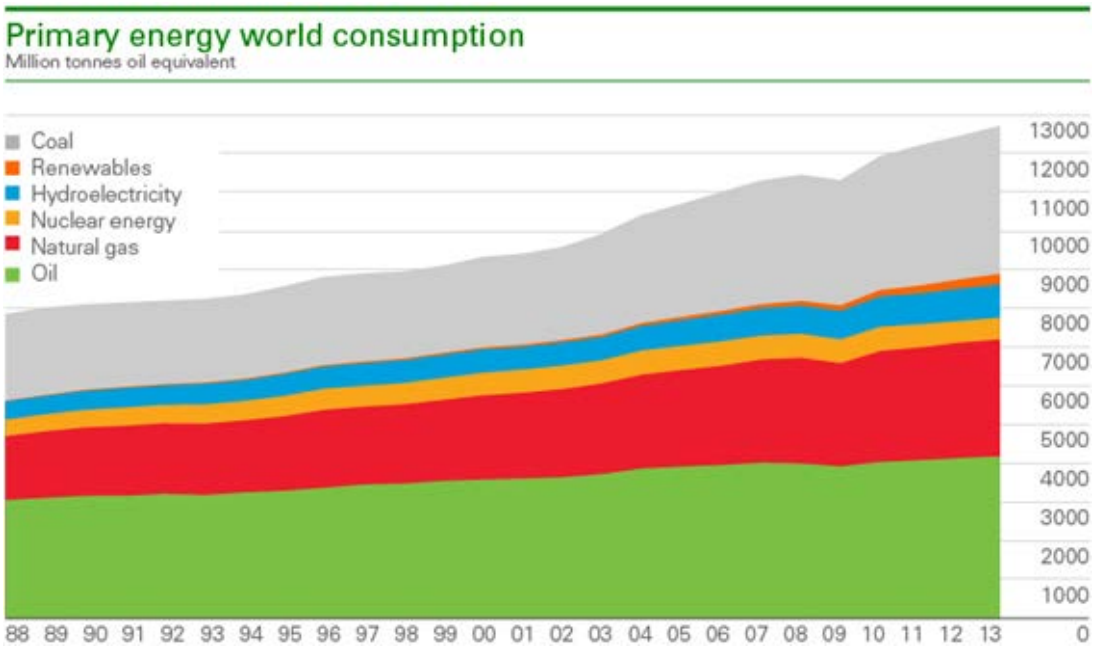

Figure 2.1. Primary energy world consumption (BP, 2014)

In recent years, renewable energy attracts great interest because of being sustainable, abundant, inexhaustible and environmentally friendly. The sources of the renewable energy are inherently renewed on its own accord such as biomass, wind, hydropower, geothermal and solar. Their application areas can be investigated under four main headings, electricity generation, solar heating/solar cooling, rural (off-grid) application and vehicle fuels. So the share of the renewable energy in global energy production and consumption increasing day by day as demonstrated in Figure 2.2 and renewable contributed 19% to our energy consumption and 22% to our electricity generation in 2012 and 2013, respectively (REN21, 2014).

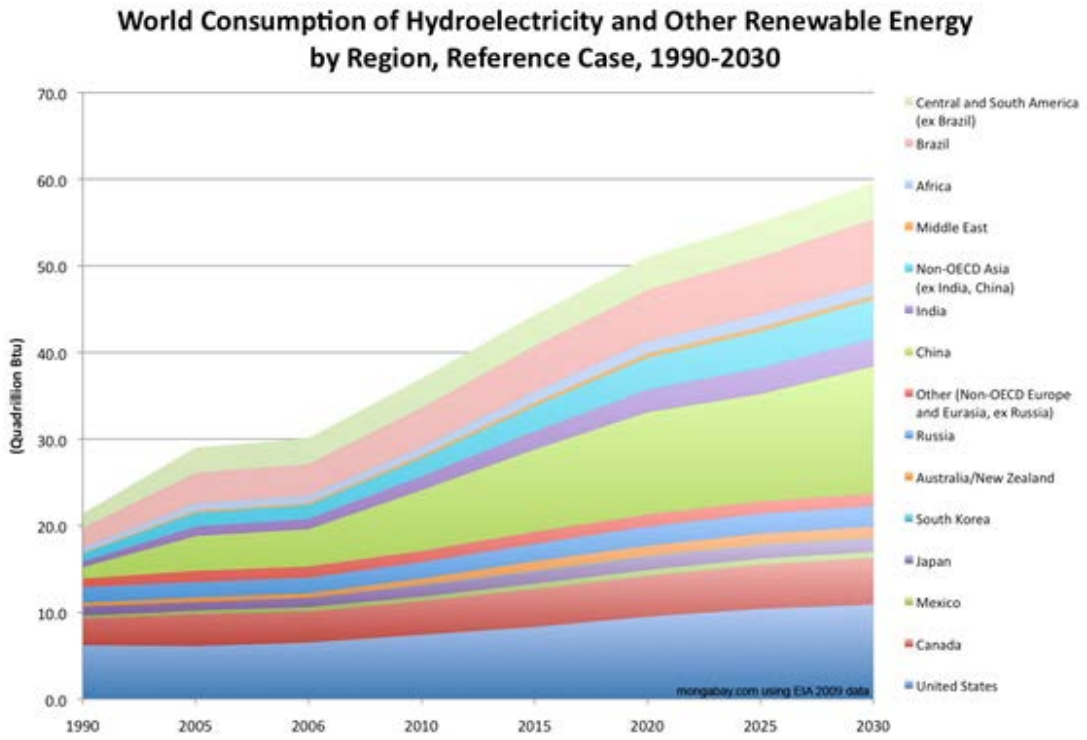

Figure 2.2. Renewable energy world usage (BP, 2014)

Although renewable energy has many advantages compared to conventional fossil fuel based energy, it has some drawbacks such as high initial cost of material purchasing, installing and maintenance. These drawbacks create some prejudices against the renewable energy. When depreciation period is considered, they suffer from long term fulfilling. It is one of the most important parameters for companies However, technical studies in this area for reducing initial installing costs continue.

In all over the world energy demand has been increasing steadily during the past five decades, and it is believed that this trend will continue to rise (Sağbaş and Karamanlıoğlu, 2011). Also it is estimated that global energy consumption in 2055 will increase up to 3 times compared to in 1998. Parallel to this, growing energy demand becomes one of Turkey's most important development precedence. Thus, effective utilization of renewable energy sources has a vital importance for Turkey for reducing the dependence on expensive foreign energy supplies (Kucukali and Baris, 2012). Turkey has a various energy resources, including hard coal, lignite, oil, hydropower, natural gas, geothermal, bioenergy and renewable energy (Kucukali and Baris, 2012). Despite being very rich in terms of renewable energy sources, in our

country these sources are not utilized effectively. When Figure 2.3 is investigated, the distributions of the resources in terms of installed power are not in desired level. To eliminate this situation, The Law of Utilization of Renewable Energy Resources in Electricity Generation is constituted in 2005. Main goals of the law can be summarized as; to expand the utilization of renewable sources for generating electrical energy, to benefit from these resources in secure, economic and qualified manner, to increase the diversification of energy resources (YEGM, 2015).

In addition, for identify the country's energy source potentials, preparing sample application projects and feasibility studies, preparing regulations in the areas of renewable energy and energy efficiency, following development in relevant areas/sector, defining goals and priorities in energy sector and creating specific incentives General Directorate of Renewable Energy was founded in 2011. It is the fundamental governmental body in the areas of renewable energy and energy efficiency.

In Turkey, electricity energy consumption that was 230 billion kWh by the year 2011 is predicted to reach to 450 billion kWh at the beginning of 2023. Turkey's energy policy targets to increase the installed capacity of renewable energy in solar plants to 600 MW, in wind energy plants to 20.000 MW, in geothermal energy plants to 600 MW and in hydraulic power plants to 36.000 MW until 2023. Hence, it is aimed to increase the share of renewable energy in the electricity supply above 30% (YEGM, 2009). The current installed capacity of Turkey is 70.557 MW (EE, 2015).

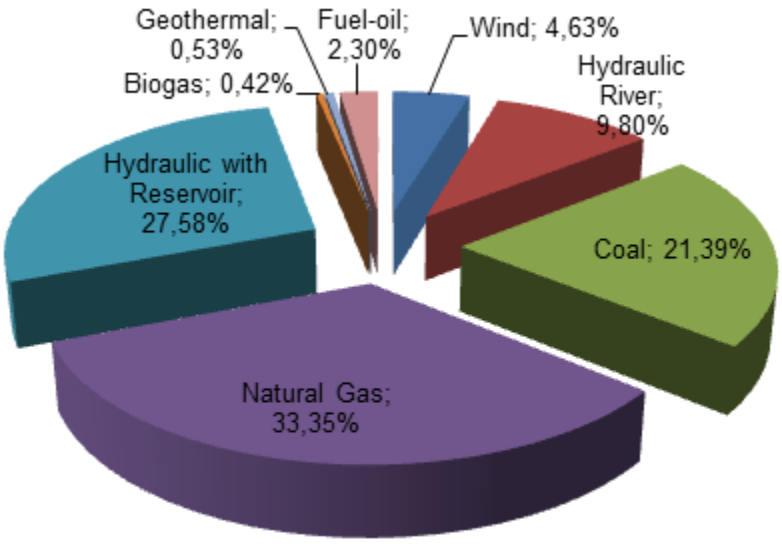

Figure 2.3. Total installed power according to source usage in Turkey (EE, 2015)

2.2. Solar Photovoltaic Technologies

Solar energy is one of the most important renewable sources. The sun emits huge amounts of irradiation, which can be used as direct source of energy, onto the earth surface everyday (Liu, 2009). PV is a technology with the inclusion of the direct conversion of solar radiation into electricity by using solar cells. Some materials demonstrate photoelectric effect, which causes them to absorb photons and snatch electrons from p-n junction. These free electrons are forced to fill the holes on a path and an electric current occurs that can be used as electricity.

Photovoltaic history starts in 1839, Edmund Becquerel discovered that electrical currents occur from certain light induced chemical reactions, and then in 1883 Charles Fritts created the first solid state photovoltaic cell by layering the semiconductor selenium with a thin layer of gold to form the junctions (Chaar et al., 2011). The first practical PV cell was exhibited at Bell laboratories, but it was too expensive to obtain common usage. Up to now, intensive studies have carried out on materials and structure development to expand and improve this energy collector, because minimum depreciation period is desired by maximum power generation (Razykof et al., 2011; Chaar et al., 2011). The rapid growth of the PV market began in the 1980s due to the application of multi-megawatt PV plants for power

generation. As a result of studies, cost reduction and market development have become possible (Maycock, 2015).

Traditional PV cells are made from semiconductor material especially silicon, are usually flat-plate, and generally are the most efficient. Second-generation PV cells are called thin-film solar cells because they are made from amorphous silicon or non-silicon materials such as cadmium telluride. Third-generation PV cells are being made from a variety of new materials besides silicon, including solar inks using conventional printing press technologies, solar dyes, and conductive plastics (NREL, 2015). These leading types of PV cells have merits and demerits relative to each other in terms of efficiency, raw material usage, reasonable cost and technical properties.

2.2.1. Monocrystalline Photovoltaic Modules

It is quite easy to recognize these types of PV modules; PV cells look perfectly rectangular with no rounded edges, in other words the crystalline framework is homogenous. This type of PV panel has many advantages compared to other types. Because of being space-efficient, these PV panels generate much more power than other panels (EI, 2015). Also, in regions dominated by high temperature, monocrystalline PV modules suffer from temperature but demonstrate higher energy yield compared to other types. However, partially covered with shade, dirt or snow seriously decreases energy harvesting and it comes to halt. In addition, they are weak against physical impacts; when a fracture starting at any point, it affects the entire of the panel (EIA, 2015; NREL, 2015; Lynn, 2010).

Figure 2.4. Monocrystalline PV Cell

2.2.2. Polycrystalline Photovoltaic Modules

Production process is differently performed from monocrystalline, raw silicon is melted and poured into a square mold, which is cooled and cut into square wafers. It is quite distinguishable from monocrystalline because of the appearance (EI, 2015). These types of PV modules were first launched in 1981. Due to the less amount of wasted raw material, these type PV modules have simpler and inexpensive manufacturing process. Polycrystalline PV panels are not as efficient as monocrystalline PV panels. Series resistance of the connection points can be shown one of the reason of being less efficient. In addition they are not quite as good as monocrystalline in terms of heat tolerance and being space-efficient (Lynn, 2010; Kolic et al., 1995).

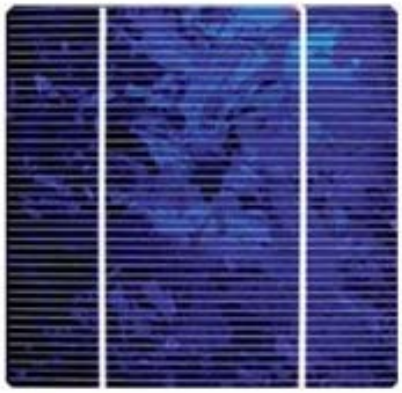

Figure 2.5. Polycrystalline PV Cell

2.2.3. Thin-film Photovoltaic Modules

Amorphous silicon (a-Si) was the first thin-film technology used in PV technology. There are three main types of thin film solar panels are commercially available; Amorphous silicon (a-Si), cadmium telluride (CdTe) and copper indium gallium selenide (CIS/CIGS) (Lynn, 2010). Ease of production process, low cost, raw material savings, lower construction cost and their specific electricity production values (kWp/kWh) make them popular over the PV technologies. However, their square per meter generation (kWh/m^2) is low and consequently installation costs go up due to the need for more panels (NREL, 2015; EIA, 2015).

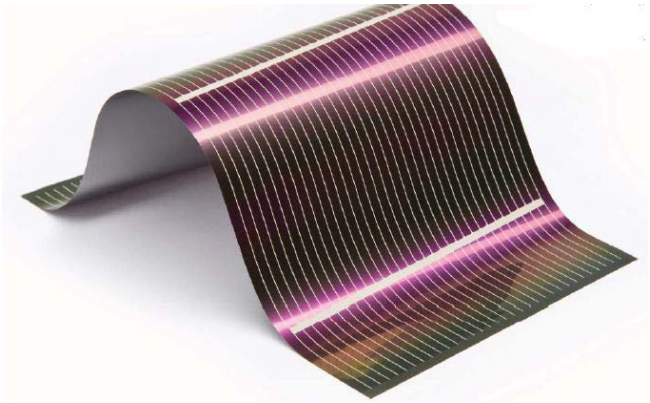

Figure 2.6. Thin-film PV Cell

2.3. Photovoltaic Cell and Module Characteristic

A PV system directly converts sunlight into electricity. The basic component of a PV module is the PV cell. This is fundamentally a semiconductor diode that can generate electricity when its p-n junction exposed to sun light (Villalva et al., 2009). A PV cell's physical cross-sectional view is demonstrated in Figure 2.7.

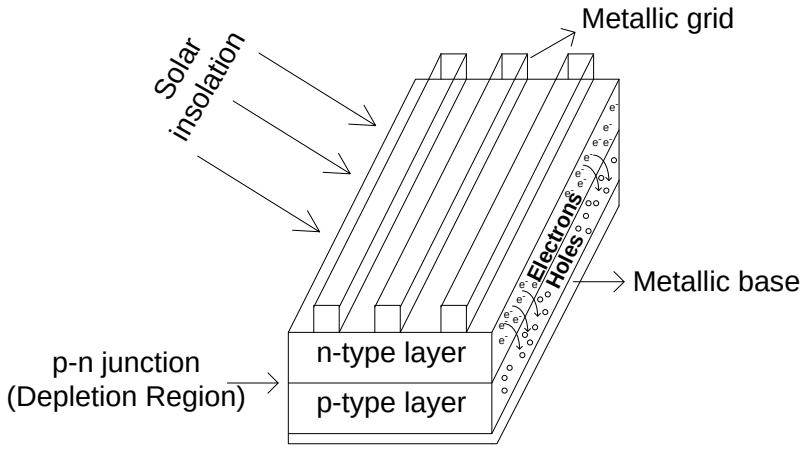

Figure 2.7. PV cell's physical demonstration (Villalva et al., 2009)

To form a PV panel a set of cell is connected in series or parallel, these connection types can exhibit different variations according to the desired output voltage and current.

It is very important to understand and estimate the PV characteristics in order to use a PV plant effectively, regardless of external factors. Therefore effect of atmospheric conditions especially irradiation and temperature should be deeply investigated (Patel and Agarwal, 2008).

2.3.1. Effect of Irradiance and Temperature

PV array's output characteristic curves, current-voltage and power-voltage reflect PV array's dependence on atmospheric conditions such as temperature and radiation. The current and voltage dependence on radiation and temperature is given in Figure 2.8.

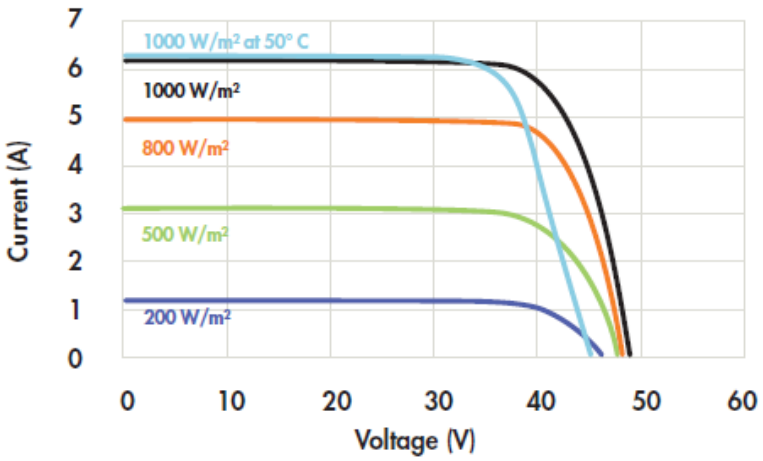

Figure 2.8. Current/voltage characteristics with dependence on irradiance and temperature (Sunpower 19\240 solar panel)

It can be clearly seen that the cell output voltage related with the temperature and the cell output current is affected by irradiation level. Due to these characteristic dependencies, extraction of maximum power from PV modules mainly changed by the temperature and irradiance level (Gow and Manning, 1999 and Villalva et al., 2009) Furthermore, for specifying rating of power electronics equipment, these variations should be taken into consideration.

Open circuit voltage (V_{oc}) is primarily affected by temperature and the relationship between them is inversely proportional whereas the current is only slightly dependent (Massave, 2013; Blas et al., 2001). This relationship can be extracted by using Equation (2.1).

$$V_{oc} = V_{oc-STC} - \gamma * (T - T_{STC}) \tag{2.1}$$

"γ" is a constant which can be obtained from datasheet of a PV module. It is a negative value and shows change of open circuit voltage by increasing or decreasing ambient temperature for 1 ºC.

Short circuit current (I_{sc}) is mostly affected by irradiation level and the relationship between them is directly proportional as shown in Equation (2.2).

$$I_{sc} = I_{sc-STC} * \left(1 + \alpha * (T - T_{STC})\right) * \frac{G}{G_{STC}} \quad (2.2)$$

2.3.2. Equivalent Circuit and Mathematical Model

Modeling of photovoltaic cell is an essential research area for implementing performance analysis, sizing, performance estimation and optimization of PV energy systems (Celik and Acıkgoz, 2007). Because PV panel manufacturers do not supply sufficient information over a large operating conditions except for some electrical quantities and this makes designers to develop a realistic alternative simulations. PV models are generally built up by using four parameter and five parameter model (Blae et al., 2002; Soto et al., 2006; Mahmoud et al., 2012). The five parameters model includes light-generated current, diode reverse saturation-current, series resistance, shunt resistance and diode ideality factor. The four parameters model neglects the shunt resistance and assumes it as infinity (Celik and Acıkgoz, 2007). Moreover, there are one diode and two diode models are available in the literature. One of the models proposed in literature is the double exponential model depicted in Figure 2.9 (Gow and Manning, 1999). The models comprising two or more diode are more sophisticated and constructed for obtaining better accuracy.

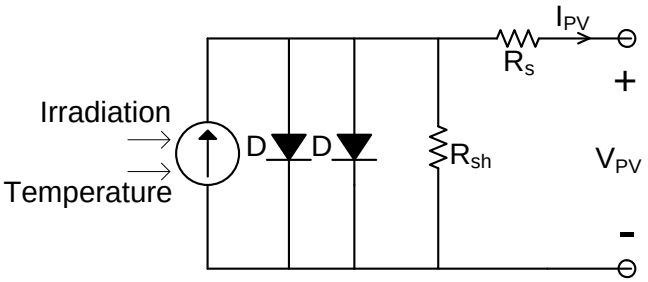

Figure 2.9. The equivalent circuit of a two diode PV cell

However, single diode model has many advantages for designers such as being more simple, easy adjustment of parameters and effective model for the simulations (Villalva et al., 2009; Patel and Agarwal, 2008; Xiao et al., 2004).

In this thesis a well-known one diode model consists of a series and a parallel resistance is implemented. This model expresses a good balance between simplicity and accuracy. The circuit diagram of the model is given in Figure 2.10.

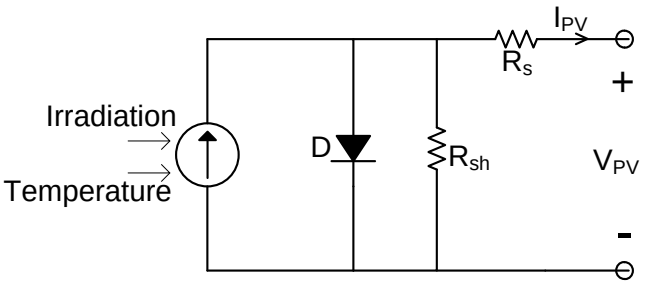

Figure 2.10. The equivalent circuit of a single diode PV cell

The general current-voltage characteristic of a PV panel based on the single diode model is (Said et al., 2012):

$$I_{pv} = I_{ph} - I_o * \left(e^{\frac{V+I_{pv}}{n_s V_t}} - 1 \right) - \frac{V+IR_s}{R_{sh}} \tag{2.3}$$

"V_t" is the junction thermal voltage:

$$V_t = \frac{AkT_{STC}}{q} \tag{2.4}$$

The five parameters of the model are given below:

- "I_{ph}" is the photo generated current in STC
- "I_o" is the dark saturation current in STC
- "R_s" is the series resistance of the PV module
- "R_{sh}" is the shunt resistance of the PV module
- "A" is the diode quality factor

$$I_{ph} = \frac{G}{G_{STC}} (I_{SC-STC} + \alpha * (T - T_{STC})) \tag{2.5}$$

$$I_o = \frac{(I_{SC-STC}+\alpha*(T-T_{STC}))}{e^{(\frac{V_{OC-STC}+\gamma(T-T_{STC})}{AV_t})}-1} \quad (2.6)$$

Other unknowns in the equations are; "k" is the Boltzmann's constant, "q" is the charge of electrons, "n_s" is the number of cells connected in series, "I_{SC-STC}" is the short circuit current value at STC, "V_{OC-STC}" is the open circuit voltage at STC, "G" (W/m^2) is the radiation on the PV surface, "G_{STC}" is the radiation at STC and "T_{STC}" is the temperature at STC in Kelvin.

The following equations summarize how a single-cell model can be extended to represent a PV panel (Can, 2013):

$$I_{pv-tot} = N_p I_{pv} \quad (2.7)$$

$$I_{o-tot} = N_p I_o \quad (2.8)$$

$$R_{s-tot} = \frac{N_s}{N_p} R_s \quad (2.9)$$

$$R_{sh-tot} = \frac{N_s}{N_p} R_{sh} \quad (2.10)$$

$$A_{tot} = N_s A \quad (2.11)$$

where "N_p" is the number of parallel cells and "N_s" is the number of series cells.

2.4. Photovoltaic System Connection Forms

There are mainly three types of PV system connection forms: stand-alone PV system, grid-tied PV system and hybrid systems (Xiao et al., 2007).

2.4.1. Stand-alone Photovoltaic Systems

For places that are particularly remote from a conventional power generation system, stand-alone PV systems have been considered a visible alternative (Salas et al., 2006). This system can be used for both domestic and non-domestic areas and completely independent from the grid. Non-Domestic applications can be illustrated by solar water pump system, traffic lights and space satellites. Also, building integrated PV systems are generally given as an example of domestic applications. The possible installation power range can be extended for both domestic and non-domestic applications from 100W to 15 kW (Kerekes et al., 2007). This power range information is experienced from commercial companies that deal with this area.

Stand-alone PV systems can only include load and PV module or may additionally comprise the battery for providing continuous energy. Stand-alone systems fundamentally contain PV panel, charge controller, batteries, and inverter (Fragaki and Markvart, 2008). Block diagram of a stand-alone PV system is showed in Figure 2.11.

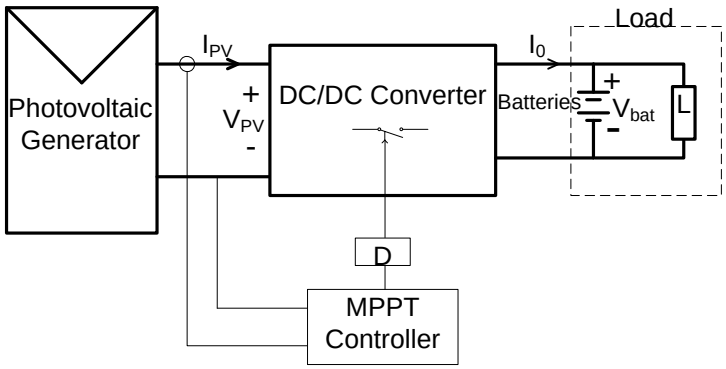

Figure 2.11. General block diagram of a stand-alone PV system with MPPT (Salas et al., 2006)

2.4.2. Grid Connected Photovoltaic Systems

Nowadays, the grid-connected PV systems are getting more popular over traditional stand-alone PV systems (Lalili et al., 2013). A grid connected PV system's output is conducted directly to the grid. The produced DC power converted

to AC power through a high quality inverter for feeding the grid. These types of PV systems contain either a single or a two stage power conditioning system, this affects the control strategies in order to achieve grid-code appliance (Nanou and Papathanassiou, 2014). In other words having DC-DC converter changes the control diagram, because without DC-DC converter MPPT controller must be integrated to inverter's controller. Grid connected PV systems, which demonstrated in Figure 2.12, are generally designed to generate huge amount of power, therefore reliable and efficient operation is the most important issue. Hence, power electronic inverter, converter, controller of them, protection and grid-code compatibility gaining more and more importance.

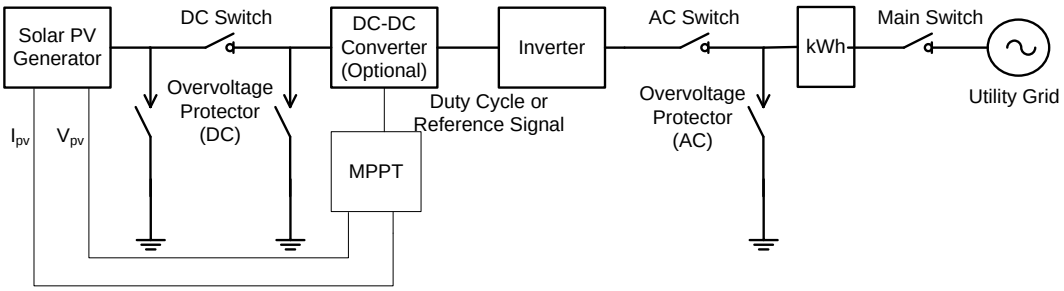

Figure 2.12. General block diagram of a grid connected PV system with MPPT

2.4.2.1. Grid Connection Standards and Codes

Before making a network connection of a PV system, it should be evaluated to show how it affects the network. To be synchronized with the network is a crucial problem. To design a power electronic inverter for grid-tied PV system, an overview of rules and regulations should be investigated in order to be allowed to connect to the grid. With these regulations a common point is created and reliable, safe and steady operation of the system is aimed (Evju, 2007; Sarıbulut, 2012). There are various grid codes, standards and related documents are available. By using them technical requirements for connection of National Electricity Transmission System is specified. These rules will however not be the same for all countries; they demonstrate small variations in the degree of limitations and in the definitions.

The standards from two of the major international standardization organizations listed below, an overlook of the most important demands and limitations can be found (Evju, 2007).

- Institute of Electrical and Electronics Engineers – IEEE
- International Electrotechnical Commission – IEC

In Turkey these regulations are demonstrated in ELECTRICITY MARKET GRID REGULATION (EMGR) which published in Official Gazette of the Republic of Turkey no. 25001 on 22/01/2003. Due to the connection of Turkey to the interconnected electrical system, given specifications in this regulation are mostly same with the European regulations. Technical criteria regarding transmission system performance, plant and equipment parameters are (EPŞY, 2015):

- Frequency: Rated frequency of the system is controlled by TEİAŞ around 50 Hertz (Hz) between 49.8-50.2 Hz range. The system must be disconnected in 0.2 sec. for low voltage connections and 0.5 sec. for high voltage connections when the operating frequency becomes less than 47 Hz or exceeds 51 Hz.
- Voltage fluctuations: Instantaneous changes of the voltage not allowed exceeding 1% of the operating voltage level. Larger voltage changes can be permitted up to 3% by TEİAŞ in extraordinary cases without affecting the transmission system or other consumers. In Table 2.1, the voltage distortion limit values are presented. In Table 2.2, the current distortion limits for general distribution systems are shown.
- Voltage and Current distortion limits: In Table 2.1, the voltage distortion limit values are presented. In Table 2.2, the current distortion limits for general distribution systems are demonstrated.

Table 2.1. Voltage distortion limits (Teke, 2011)

Bus Voltage at PCC	Individual Voltage Distortion (%)	Total Voltage Distortion THD(%)
69 kV and below	3.0	5
69 kV through 161 kV	1.5	2.5
161 kV and above	1	1.5
Note: High voltage systems can have up to 2.0 % THD where the cause is an HVDC terminal that will attenuate by the time it is tapped for a user.		

Table 2.2. Current distortion limits for general distribution systems (Teke, 2011)

Individual Harmonic Order (Odd Harmonics), h						
I_{sc}/I_L	Max. Harmonic Current Distortion for h					TDD
	h<11	11≤h<17	17≤h<23	23≤h<35	35≤h	
Below 20	4.0	2	1.5	0.6	0.3	5.0
Between 20-50	7.0	3.5	2.5	1.0	0.5	8.0
Between 50-100	10.0	4.5	4.0	1.5	0.7	12.0
Between 100-1000	12.0	5.5	5.0	2.0	1.0	15.0
Above 1000	15.0	7.0	6.0	2.5	1.4	20.0
Even harmonics are limited to 25% of the odd harmonics limit above						
Current distortions that result in dc offset, e.g., half wave converters, are not allowed						
All power generation equipment is limited to these values of current distortion, regardless of actual I_{sc}/I_L						
I_{sc}= Maximum short circuit current at PCC, I_L= Maximum demand load current (fundamental frequency component) at PCC.						

- Harmonic distortion: Harmonic distortion cannot exceed 5% for both the current and voltage as noted in IEC-61000-4-7.
- Vector shift: Relay trip setting must be adjusted to 6°…9° and the system must be disconnected in 0.2 sec. for both low voltage and high voltage applications.
- Injected DC current: The value of the injected DC current must be limited 0.5% of the rated current.

2.5. Summary

In this chapter, an overview of renewable energy and its types are investigated. The solar PV technologies, PV cell and module characteristics and PV system connection forms are reviewed. Mathematical model of PV cell is provided and it is modeled in a simulation program to make an evaluation for effects of atmospheric conditions on PV modules. The on-grid and off-grid PV systems are also discussed and their components are focused. Grid connection standards and codes for Turkey is discussed and provided.

3. PHOTOVOLTAIC CONVERTERS AND MPPT CONTROLLERS

3.1. DC-DC SWITCH MODE CONVERTERS

DC-DC converters share an important role with inverters for the PV applications. Especially for stand-alone and two stage grid-tied PV systems, these converters are essential part of the system. They can be used to adjust only voltage level by controlling the output voltage or they can be employed for the MPPT process through a control algorithm by using PV output parameters. To implement the MPPT process DC-DC converters are acts as a resistance regulator, according to position of the switch resistance at the input side is attempted to equalize resistance at the output side. It can be considered as Thevenin theorem, for obtaining maximum power $R_{out}=R_{in}$ condition must be supplied. This is clearly visible on the I/V graph of a PV panel as shown in Figure 3.1.

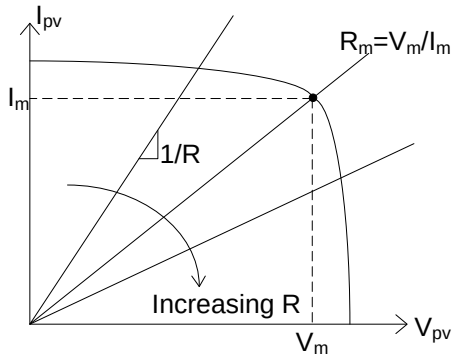

Figure 3.1. I/V graph of a PV panel

Value of R is changed continuously in order to bring the operating point to the maximum operating point. Intersection point moves along the I/V curve and try to find MPP.

Different types of DC-DC switch mode converters, which improved according to the desired purpose of usage, are available theoretically and practically. The common objective of these converters can be expressed to give the desired output value by operating with high efficiency. In the next subtitles, mostly used

converter types are separately investigated, their mathematical analyses and output current and voltage forms are presented.

3.1.1. Buck Converter

The Buck converter, which has been one of the basic types of the switch mode DC-DC converter, is widely used as a step-down converter. The circuit diagram of the buck converter is given in Figure 3.2. When we investigate the circuit diagram, it can be clearly seen that a Buck converter consists of two parts. The main goals for this type converter are reducing the voltage level and obtaining pure DC output from the circuit. For this purpose a DC chopper and an output LC filter to reduce the ripples are employed (Hart, 2011; Enrique et al., 2007). It can be operated under both continuous conduction mode (CCM) and discontinuous conduction mode (DCM). This can be specified by the circuit component selection of the designer. When inductor current does not decrease to zero, it operates on CCM, otherwise it operates on DCM.

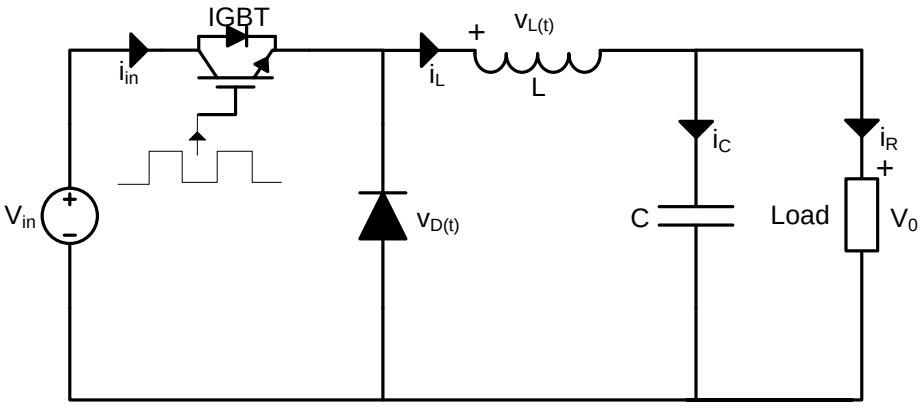

Figure 3.2. Circuit diagram of a Buck converter

Position of the switch determine the output voltage, in other words being on and off position of the switch over a period gives the relation between the input and output voltages. The average of the output voltage equals to zero.

$$V_0 = \frac{1}{T}\int_o^T v_0(t)dt = \frac{1}{T}\int_o^{DT} v_s(t)dt = V_s D \quad (3.1)$$

The relationship between output and input voltage:

$$(V_{in} - V_{out})t_{on} - V_{out}t_{off} = 0$$

$$\frac{V_{out}}{V_{in}} = \frac{t_{on}}{t_{on}+t_{off}} = D \quad (3.2)$$

3.1.2. Boost Converter

Boost converter is also one of the mostly used basic converter topology which has capability of step-up the voltage level. The circuit diagram of the boost converter is given in Figure 3.3. The conventional boost converter includes an ideal switch, energy storage inductor, diode and filtering capacitor. These components are employed for increasing the voltage level and reducing the ripples. Moreover, it has two operation mode named as CCM and DCM. Operation mode is related with the value of the energy storage inductor. The minimum combination of inductance and switching frequency should be adjusted for operation on CCM mode (Hart, 2011).

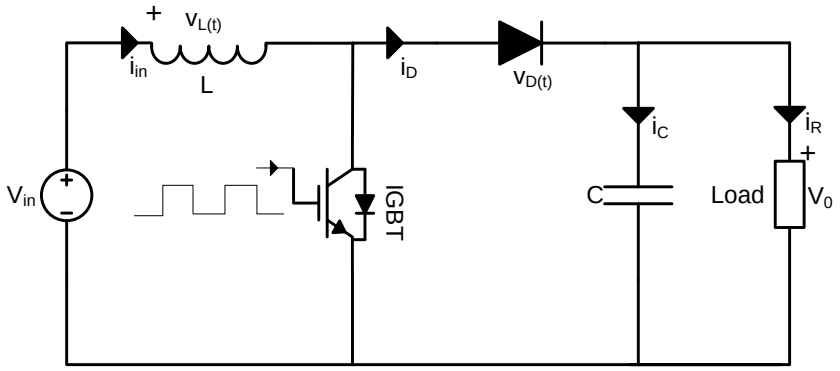

Figure 3.3. Circuit diagram of a Boost converter

When the circuit topology and operating principle of this converter examined, it can be clearly seen that for the time switch is on energy stored in the inductor and

the power supply is transferred to the load the, for the time is off storage inductor is charged, diode is reverse biased the capacitor provides the energy for the load (Enrique et al., 2007)

The average of the output voltage equals to zero and the relationship between output and input voltage (Hart, 2011):

$$(\Delta i_L)_{open} + (\Delta i_L)_{closed} = 0$$

$$V_s(D + 1 - D) - V_0(1 - D) = 0$$

$$V_0 = \frac{V_s}{1-D} \tag{3.3}$$

3.1.3. Buck-Boost Converter

Another basic switched-mode converter is the buck-boost converter shown in Figure 3.4. The output voltage of the buck-boost converter topology can be either used to perform stepping the voltage level up or down however; the polarity of the output voltage is opposite to that of the input.

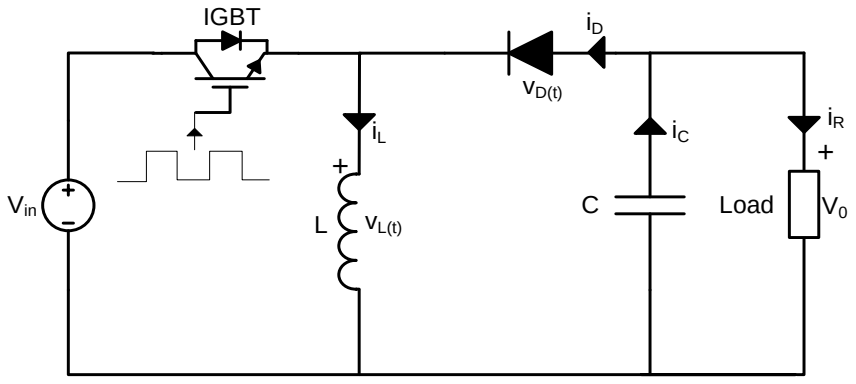

Figure 3.4. Circuit diagram of a Buck-Boost converter

The average of the output voltage equals to zero and the relationship between output and input voltage (Hart, 2011):

$$(\Delta i_L)_{open} + (\Delta i_L)_{closed} = 0$$

$$\frac{V_s DT}{L} - \frac{V_0(1-D)T}{L} = 0$$

$$V_0 = -V_s(\frac{D}{1-D}) \quad (3.4)$$

3.1.4. Interleaved Boost Converter

Interleaved boost converters can be defined as the parallel connection of the two or more boost converters. As it is known, especially for PV systems, high power applications recently attract more attention. Due to the increase in high power applications, division of power and control of it in small parts becomes more important (Lee et al., 2000). In addition, cost and size of the converter should be taken into account during the design process because these are other significant parameters.

In high-power applications, boost converters are often paralleled in an interleaved manner to increase the output current and reduce the input current ripple (Lee et al., 2000), higher efficiency is realized by sharing the output current into two or more branches, substantially reducing I^2R losses and decrease leakage inductance to achieve a lower switching loss (Tseng and Wang, 2013; Ramaprabha et al., 2013). Furthermore, the size and losses of the filtering section can be reduced, and the switching and conduction losses (Shin et al., 2005). One of the demerits is the rise in cost and the other one is that the voltage across the switch is very high during the resonance mode (Jung et al., 2011). However, this rise is not remarkable owing to lower rating components may be employed as the current is divided between the parallel branches (Ramaprabha et al., 2013).

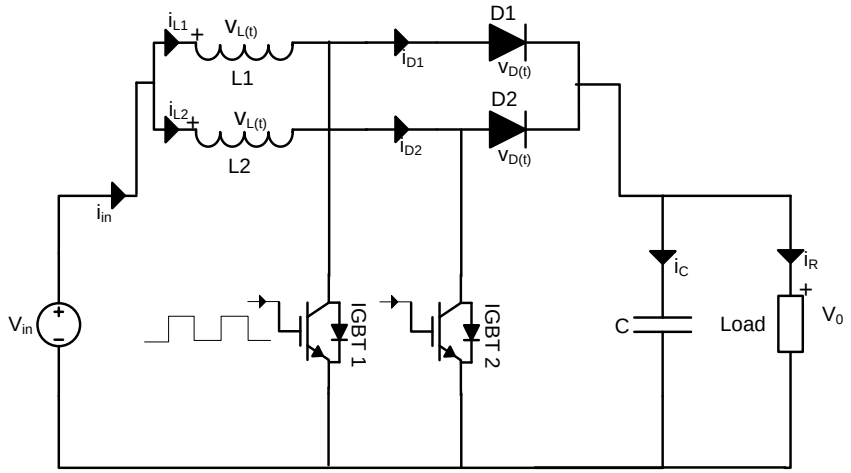

Figure 3.5. Circuit diagram of an Interleaved Boost converter (Lee et al., 2000)

When considering the PV applications, interleaved boost converters shown in Figure 3.5 are applied as power-factor-correction front ends. Efficiency is required for the power conditioning system (PCS), which transmits power from the PV array to the load (Jung et al., 2011). Firstly, reduced electromagnetic interference and reducing ripple in the input and output waveform provides effective control possibility to MPPT controller. Further, to split up the arrays into strings can ensure conservation against losses from partial shading. Because controlling in narrow frame demonstrates better results. Last but not least, speeding up the transient response by use of smaller inductance contributes to the steady-state and dynamic performance of the entire system (Veerachary et al., 2003).

Basic design of an interleaved DC-DC converter is given as following (TI, 2013);

$$D_{max} = \frac{V_{out}+V_d-V_{in(min)}}{V_{out}+V_d-V_{on}} \tag{3.5}$$

$$D_{min} = \frac{V_{out}+V_d-V_{in(max)}}{V_{out}+V_d-V_{on}} \tag{3.6}$$

$$L_{(crit)} = \frac{(V_{in(min)}-V_{on})D_{max}(1-D_{max})}{f_s I_{out}} \tag{3.7}$$

3.2. DC-AC Switch-Mode Inverters

Inverters are static power electronic converters that transfer power from dc power supply to ac load. According to the type of ac output waveform, they can be named as current source inverters (CSI) or voltage source inverters (VSI). CSIs have controlled ac output in current waveform which particularly used in special functional devices. On the other hand, VSIs have controlled ac output in voltage form and naturally behave as voltage source. VSIs are widely used in industrial applications like adjustable speed drivers, uninterruptible power supplies and energy conversion stages as in PV applications (Rashid, 2007). The ability to control the current output of the power converter both in magnitude and phase angle enables the power inverter to precisely control the fluxes of the electric motors (NREL, 2015). Hence, the capabilities to control output current are applicable to PV inverter applications (Muljadi et al., 2013).

Single-phase VSI can be found as half-bridge and full-bridge topologies and covers the low power range. Three phase VSIs cover medium to high power applications. In conventional grid connected VSIs a three-phase bridge circuit consisting of switching components that operates according to the control signal generated by control algorithm. The controlled variables can be amplitude, phase and frequency of the voltage (Rashid, 2007). The standard three-phase VSI topology is shown in Figure 3.6.

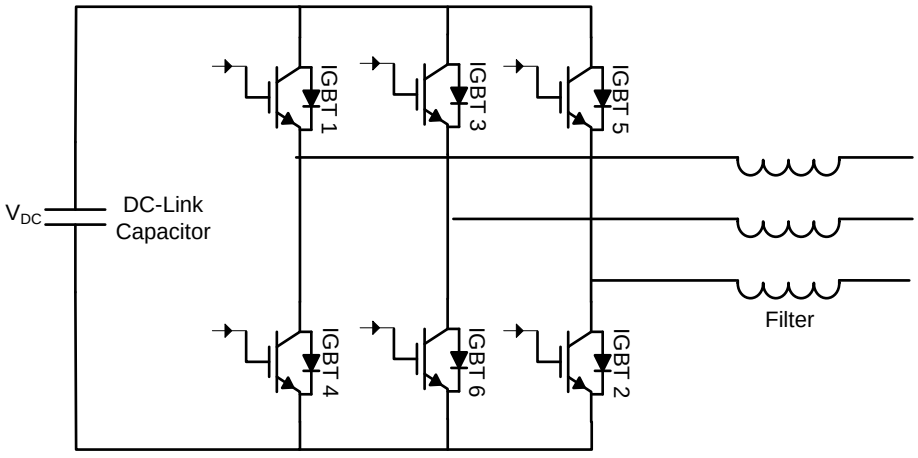

Figure 3.6. Three phase VSI

To obtain the three-phase AC current in three phases VSI, six gating signals need to be sent to the switches of the inverter. H1, H3, H5 are 3 phase symmetrical switching function with phase shift 120°. The switch S1 and S4 is turned on for 180°. The switches of any leg of the inverter cannot be switched simultaneously due to preserving the dc link voltage supply from being short circuited. Conduction states of the switches are given in Table 3.1.

Table 3.1. Conduction state of the switches (Rashid, 2007)

State	State#	V_{ab}	V_{bc}	V_{ca}
S1, S2 and S6 are on S4, S5 and S3 are off	1	V_{dc}	0	V_{dc}
S2, S3 and S1 are on S5, S6 and S4 are off	2	0	V_{dc}	V_{dc}
S3, S4 and S2 are on S6, S1 and S5 are off	3	V_{dc}	V_{dc}	0
S4, S5 and S3 are on S1, S2 and S6 are off	4	V_{dc}	0	V_{dc}
S5, S6 and S4 are on S2, S3 and S1 are off	5	0	V_{dc}	V_{dc}
S6, S1 and S5 are on S3, S4 and S2 are off	6	V_{dc}	V_{dc}	0
S1, S3 and S5 are on S4, S6 and S2 are off	7	0	0	0
S4, S6 and S2 are on S1, S3 and S5 are off	8	0	0	0

This thesis is based on the most commonly used topology named as the full bridge two level VSI; however it is also possible to employ more advanced multilevel inverters. By using this type of inverter, a pure sinusoidal current, low harmonic distortion and unity power factor can be obtained by implementing an effective controller.

3.3. Photovoltaic Array and Inverter Configurations

Depending upon the solar PV panel arranging, the system can be designed in different four general ways. The configuration of the PV panels and proper selection of inverter associated with it will directly have influence on cost and efficiency of the entire system. There are centralized inverters, string inverters, multistring inverters and module based inverter configurations available (Kjaer et al., 2005). Table 3.2 depicts comparison of different PV inverter configurations on several bases.

Table 3.2. Comparison of different PV inverter configurations

	Central Inverters	String Inverters	Multi-String Inverters	Module based Inverters
ADVANTAGES	High inverter efficiency.	Less overall loss.	Provide independent MPPT.	High MPPT capability.
	Simplicity.	A bit complex.	Wide input voltage range.	Elimination of DC-wiring.
	Low THD.	Design independency for different orientation.	High power output than string inverter.	Space efficient.
	Low cost.	Reduced version of central inverter.	More efficiency.	No need for active cooling.
	A single MPPT is used within the inverter.	High power yield under partial shading conditions.	Higher power level than a string inverter.	A panel becomes deactivate when an inverter disrupted.
	Especially for medium and large scale applications.	Fewer arrays are impacted with one inverter failure.	Having separate MPPT control for each string.	Design independency for different orientation.
DISADVANTAGES	Mismatch losses.	Higher DC watt unit cost.	Always needs two power conversion stages	Higher installation costs.
	Missing individual MPPT for each string.	Requires more distributed space to placing inverters.	Losses due to DC-DC converter.	High heat could reduce its life.
	Inefficiency under shading effects.	Safety hazard due to high voltage levels.	Requires more distributed space to placing inverters.	
	Different orientation of modules not allowed.			
	Conversion efficiency very low at low power range.			

3.3.1. Module Integrated Inverters

In module integrated inverter configuration, which demonstrated in Figure 3.7, one inverter is attached to per PV panel. Due to being proper to the low power applications, these inverters are small and can be integrated frame of the PV panel. In addition, these panels can be connected to the grid through the module integrated inverters. Advantages of this configuration, the mismatch losses between the PV modules is removed, DC cabling is almost removed, it is possible to optimize the converter to the PV module, and thus also allowing individual MPPT of each module (Evju, 2007). Moreover, minimizing of DC wiring prevents the risk of electric arc and firing. On the other hand the low power level per unit may reduce the overall efficiency. Also, for high power applications of PV systems, this type of inverter is not appropriate because of the high cost and workmanship. Furthermore, the inequality between inverter lifetime and panel lifetime is another handicap.

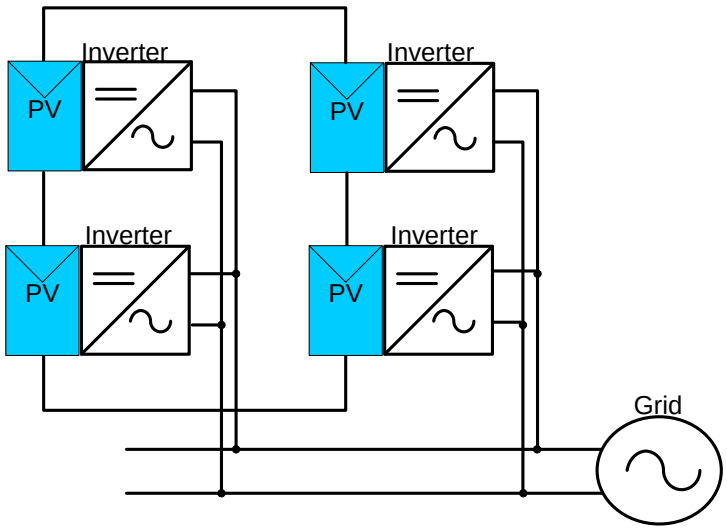

Figure 3.7. Module integrated inverter configuration (Evju, 2007)

3.3.2. String Inverters

String inverters shown in Figure 3.8, can be considered as a reduced version of centralized inverters (Evju, 2007). When we consider a medium power application (1-5 kW) of PV systems, which is installed on a roof and may be positioned on an

irregular area, the PV panels cannot be installed with the same orientation and be exposed to different shading conditions during the day (Schimpf and Norum, 2008). So this type of inverter is usable for such applications because only one string is attached to one inverter and thus the mismatch losses are reduced. Also allowing individual MPPT of each string is another advantage of string inverter. Consequently, this configuration increases the overall system efficiency when compared to the central inverter. However, a disadvantage compared to the centralized inverters is higher price per kW because of the rather low power level per unit (Evju, 2007; Schimpf and Norum, 2008).

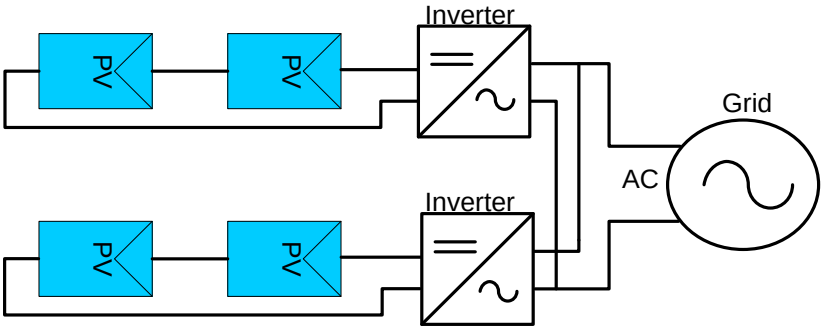

Figure 3.8. String inverter configuration (Evju, 2007)

3.3.3. Multi-String Inverters

Multi-String inverters can be assumed as a variation of the string inverter. Fundamentally, it is a string inverter, but it has one more inputs. Extra input ports of inverter ensure efficient control of the entire system by controlling of MPP in small strings of PV systems. Actually, the multi-string inverter configuration formed on more than one distinct and independent PV panel strings with their own MPPT connected to a unique inverter (Meza et al., 2006). Moreover, it can reach a higher power level than a string inverter and removes the higher price per kW handicap of string inverters against to centralized inverters. Also, a plant can be constructed with fewer components than the string converter, and this supplies profit in terms of cost and workmanship. Because of having two stage designs, input voltage range is very wide. Hence, it may benefits from the day light more than other inverters and this

increases power generation capability. Last but not least, multi-string inverters, which exhibited in Figure 3.9 allow freedom of design facility to designers (Schimpf and Norum, 2008).

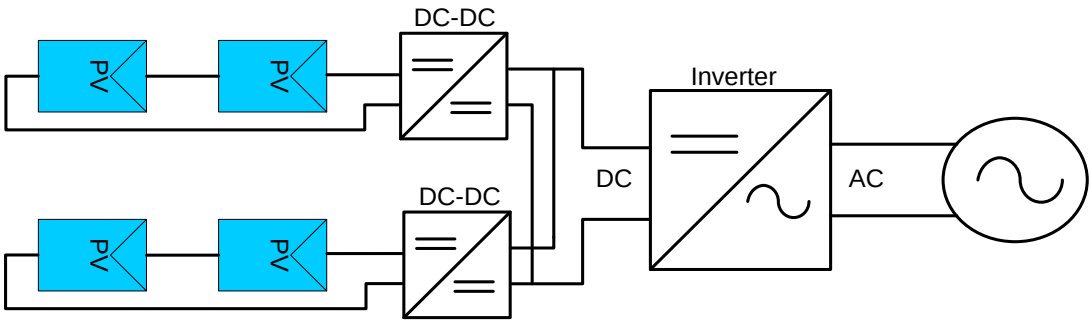

Figure 3.9. Multi-string inverter configuration (Evju, 2007)

3.3.4. Centralized Inverters

These inverters are defined as an old technology, and are based on the connection of a large number of PV modules to an inverter. The most crucial missing of these inverters are mismatching losses. They suffer from missing individual MPPT for strings, different orientation of modules and when a part of array exposed to different shading conditions during the day, entire of the system is affected by this condition. Centralized inverters are not capable of dealing with these states. Further, use of high-voltage DC-cables between the PV modules and the converter, losses in the string diodes make it inconvenient. Besides these disadvantages, having high inverter efficiency, simplicity and low cost make it popular. Centralized inverters, which demonstrated in Figure 3.10, are still enormously used in medium and high power PV system applications (Schimpf and Norum, 2008).

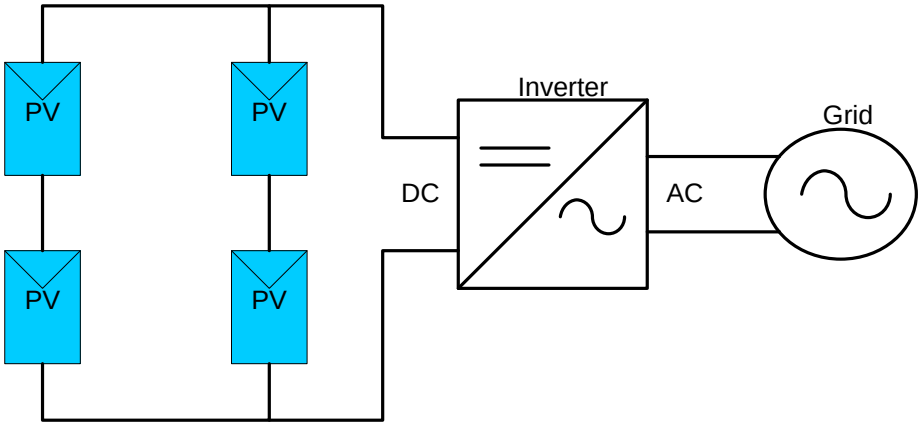

Figure 3.10. Central inverter configuration (Evju, 2007)

3.4. Maximum Power Point Tracking Controller and Algorithms

The most important performance criterion of a PV system can be stated as operating at the MPP regardless of the changing atmospheric conditions. The modest changes in the operating current and voltage of PV panel, which relying on the temperature and radiation, constitutes visible variations in the output power of the panel. In order to mitigate these variations and force the system to study on MPP, a control block is needed to track the MPP. Therefore, MPPT techniques are used to control DC-DC converters or inverters for the sake of obtaining maximum output power from a PV system throughout the ever-changing daily conditions. The DC converter is continuously controlled to operate the panel at its MPP despite possible variations in the environmental conditions by employing the switching components having a high switching frequency.

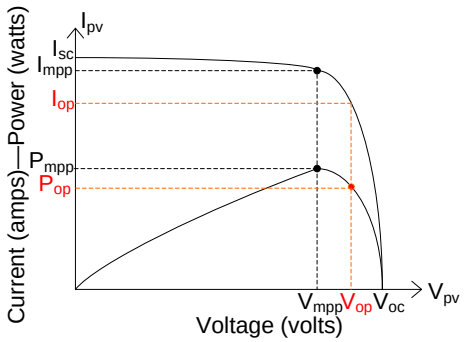

Figure 3.11. I/V and P/V characteristic curve of a PV panel

As seen in Figure 3.11, when the I/V characteristic curve and P/V curve of a PV panel is investigated, it is quite clear to see that the MPP is a unique point. Furthermore, this is equivalent to just one specific value of current and voltage. Especially the increase or decrease of the current value of the panel will dramatically affect the output power. That's why the main purpose of this controller is to keep the panel's operating point at its MPP. These controller approaches have been effectively implemented in both standalone and grid-tied PV systems. Most of them provide significant efficiency gains with the help of well-developed controller algorithms

Nowadays, various MPPT techniques have been carefully studied. These techniques can include iterative methods, soft computing methods, numerical methods or optimization methods. In summary, these techniques can be grouped under three sub-headings named as online methods, offline methods and hybrid methods (Reisi et al, 2013) as illustrated in Table 3.3.

Table 3.3. Classification of MPPT Techniques

Offline MPPT Techniques	**Online MPPT Techniques**	**Hybrid MPPT Techniques**
Short-Circuit Current MPPT Technique	Perturb and Observation MPPT Technique	Perturb and Observation & Artificial Neural Network Based MPPT Technique
Open-Circuit Voltage MPPT Technique	Incremental Conductance MPPT Technique	
Look-up Table MPPT Technique	Parasitic Capacitance MPPT Technique	Open-Circuit Voltage & Artificial Neural Network Based MPPT Technique
Numerical Calculation Based MPPT Technique	Voltage or Current Feedback MPPT Technique	
Curve Fitting Based MPPT Technique	Power Feedback MPPT Technique	Genetic Algorithm Optimized & Fuzzy Based MPPT Technique
Fuzzy Logic Based MPPT Technique	Sliding Mode Based MPPT Technique	
Artificial Neural Network Based MPPT Technique	Current Sweep MPPT Technique	
Evolutionary Algorithms Based MPPT Technique	Ripple Correlation Control MPPT Technique	
	Forced Oscillation MPPT Technique	
	Differentiation Based MPPT Technique	

To evaluate an MPPT technique, there are several attempts to consider such as control variable, circuitry, cost, complexity level, tracking speed, application type and stability (Subudhi and Pradhan, 2013) as shown in Table 3.4.

Table 3.4. Comparison of investigated MPPT Techniques (Esram and Chapman, 2007; Subudhi and Pradhan, 2013)

MPPT Technique	Control Variable	PV Array Dependent	Convergence Speed	Complexity Level	Periodic Tuning	Analog or Digital
P&O MPPT Technique	V, I	No	Low-Medium	Low	No	Both
INC MPPT Technique	V, I	No	Low-Medium	Medium	No	Digital
ANN MPPT Technique	G, T	Yes	Fast	High	Yes	Digital
Hybrid MPPT Technique	V, I, G, T	Yes	Fast	High	Yes	Digital

A deeply investigation of mostly used MPPT techniques is given in following sections.

3.4.1. Perturb and Observe MPPT Technique

Perturb and Observe (P&O) is an iterative online MPPT technique, which uses the voltage of the PV module for perturbation. It is widely used and simplest MPPT technique. This method sometimes called Hill climbing method, the main difference is P&O used PV panel voltage as a control variable while in Hill climbing method the duty cycle is used as control variable (Enrique et al., 2010; Boico and Lehman, 2012; Esram and Chapman, 2007; Subudhi and Pradhan, 2013).

In conventional P&O method, the small but constant perturbations are applied to reference voltage of the PV panel, then this reference voltage is subtracted from operating voltage and defined error is passed through a PI. The output of PI is compared with the carrier signal throughout a comparator and PWM signal is

created. Assume that an increment is applied to the voltage of the PV panel, and the output power is measured. If the output power of the panel increases, then the voltage is incremented in the same direction. If the output power decreases, the direction is completely reversed. The goal is determined as forcing the operating voltage towards V_{mpp} thereby operating voltage oscillates between positive increments and negative increments and output voltage oscillates around V_{mpp} associated with this situation (Salas et al., 2006; Sullivan and Powers, 1993; Subudhi and Pradhan, 2013; Bhatnagar and Nema, 2013). This loop can be clearly seen in flowchart of P&O algorithm which demonstrated in Figure 3.12.

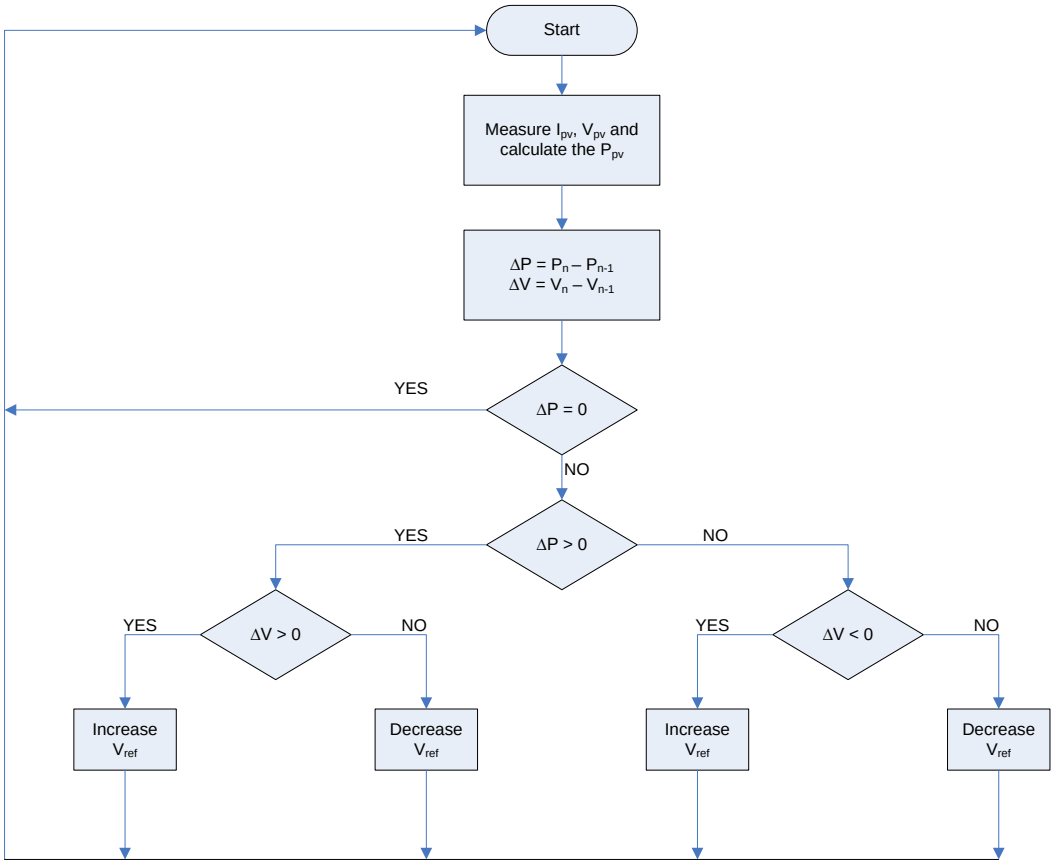

Figure 3.12. Flowchart of P&O algorithm

The P&O MPPT technique has some drawbacks that dramatically affect the output power of the PV system. One of them is perturbation size, this limits the convergence speed and determines the amplitude of oscillations around the V_{mpp}. It

cannot be stably positioned on V_{mpp} (Veerachary, 2008; Salas et al., 2006). To mitigate this situation adaptive perturbation size algorithms had been proposed in the literature (Femia et al., 2007; Abdelselam et al., 2011).

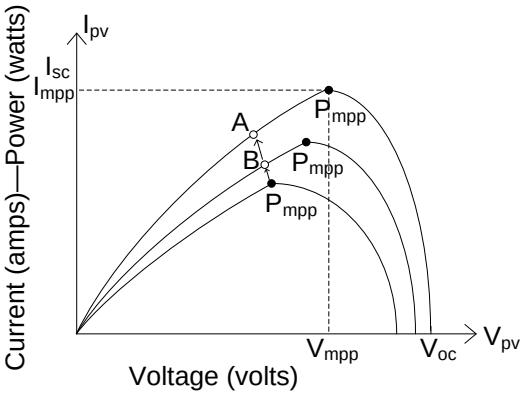

Figure 3.13. Example of erratic behavior of P&O algorithm under variable atmospheric conditions (Eltawil and Zhao, 2013)

Other one is, the algorithm lack of specifying the correct perturbation direction under rapidly changing atmospheric conditions as shown in Figure 3.13 and the operating point diverges from the V_{mpp}. However, being simple, not requiring PV panel characteristic attributes and easy implementation can be expressed as advantages (Bhatnagar and Nema, 2013; Enrique et al., 2010).

3.4.2. Incremental Conductance MPPT Technique

This technique is fundamentally based on the fact that the derivative of the PV panel output with its voltage as given in Equation 3.8 (Safari and Mekhilef, 2011).

$$\frac{dP}{dV} = 0$$

$$\frac{d(IV)}{dV} = I + V\frac{dI}{dV} \cong I + V\frac{\Delta I}{\Delta V} \tag{3.8}$$

Equation 3.8 can be explained as below;

$\frac{\Delta I}{\Delta V} = -\frac{I}{V}$, at MPP

$\frac{\Delta I}{\Delta V} > -\frac{I}{V}$, left of MPP

$\frac{\Delta I}{\Delta V} < -\frac{I}{V}$, right of MPP

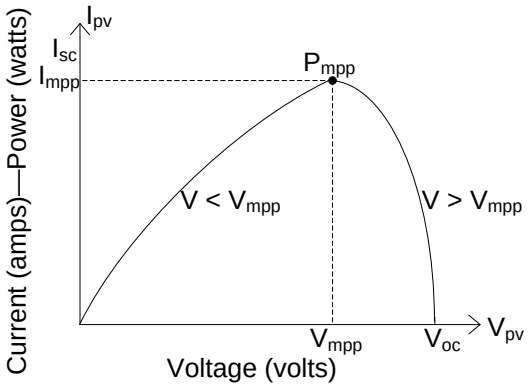

Figure 3.14. State of operating voltage of PV panel

One of the most crucial problems of P&O algorithm, oscillation of operating voltage around MPP, is mitigated by the Incremental Conductance method (INC). As mentioned before when operating voltage reaches the MPP where $\frac{dP}{dV} = 0$, this realized by the algorithm and the increase in voltage is stopped (Bhatnagar and Nema, 2013). The operation of PV panel is maintained at this point unless a change occurs at atmospheric conditions as seen in Figure 3.15 (Esram and Chapman, 2007; Hussein et al. 1995).

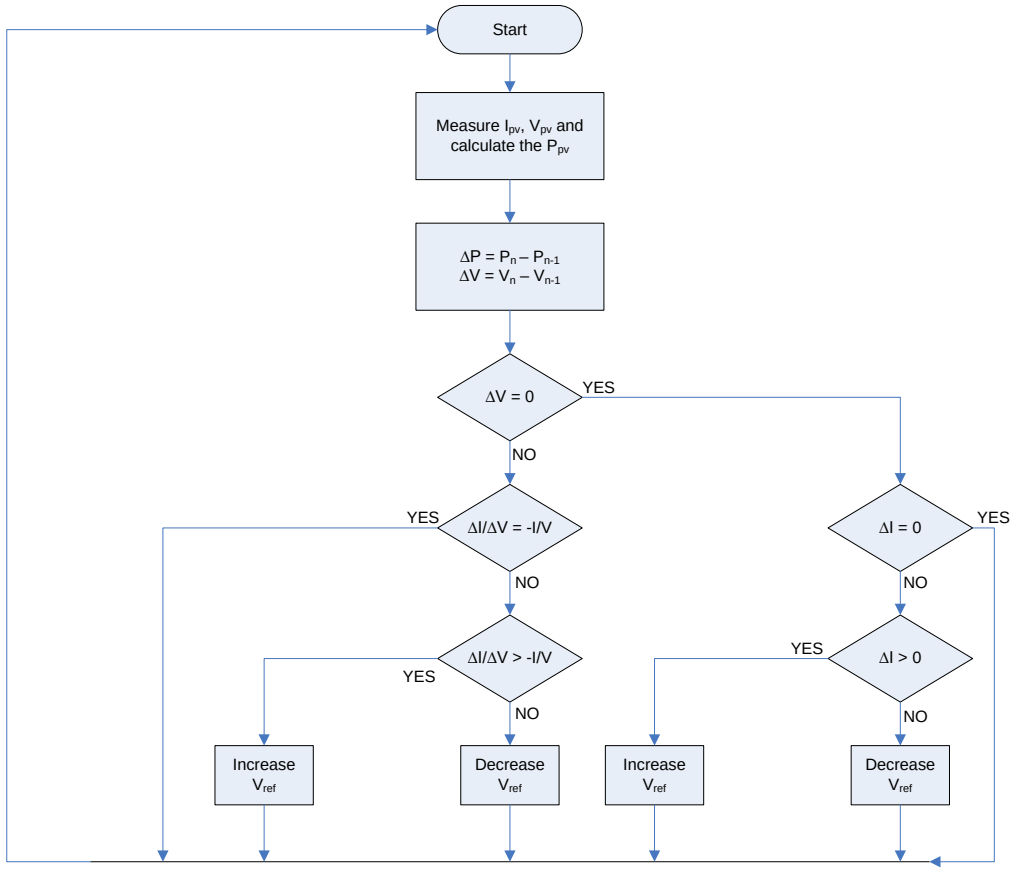

Figure 3.15. Flowchart of INC algorithm

As the P&O algorithm, specifying the rate of increment size is an important issue. Because, convergence speed is mainly rely on this parameter (Hussein et al. 1995; Eltawil and Zhao, 2013). This situation is handled by using variable step-size INC algorithm. According to the position of the operating voltage the step size is adjusted (Mei et al., 2011; Bennett et al., 2013).

INC method has many advantageous compared to P&O method in terms of tracking speed, tracking accuracy and efficiency. Furthermore, under partial shading conditions, INC method supplies more efficient results. On the other hand, INC MPPT method is more complex and in practical applications operation of the algorithm adversely affected by noise and errors on the measured control values (Safari and Mekhilef, 2011).

3.4.3. Artificial Neural Network Based MPPT Technique

Artificial neural networks (ANNs) are intelligent systems that are remarkably employed to solve sophisticated problems in many different areas such as pattern recognition, identification, classification and control systems (Hasni et al., 2012). ANN structure is based on our understanding of biological nervous system (Lippmann, 1987). Neurons are the basic structural unit of nervous system and receive inputs from other sources, combine them in some way, perform a generally nonlinear operation on the result, and then give the final result (Kung, 1993). ANN models fundamentally comprises of multiple connected neurons and nodes. The neurons have five basic components namely input, weight-bias, threshold, summing junction and output as illustrated in Figure 3.16.

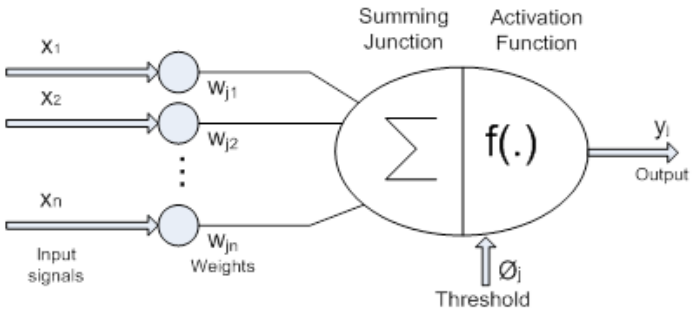

Figure 3.16. Basic structure of an artificial neuron

ANNs, which used for non-linear problems, commonly have three layers. These layers are named as input layer, hidden layer and output layer, respectively as shown in Figure 3.17.

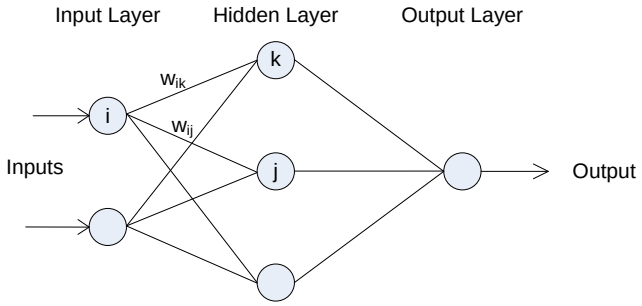

Figure 3.17. Illustration of a neural network

Number of inputs, number of neurons in each layer and initial values of weights and biases are completely user-dependent.

Nowadays, ANNs are widely employed in MPPT applications. Also they supply reasonable results in terms of performance and efficiency of the system. Especially, against partial shading conditions, the major problem of PV systems, provides better results compared to conventional algorithms (Liu et al., 2013; Mellit and Kalogirou, 2014; Salah and Ouali, 2011). The input parameters of network can be PV parameters like voltage and current or atmospheric variables such as temperature and irradiance. The output can be reference voltage or duty cycle which used to adjust the PWM signal of DC-DC converter to operate at MPP (Esram and Chapman, 2007).

Accuracy of the network mainly rely on the number of neurons in hidden layer, the learning algorithm, training data set and combination of input parameters. Also the network must be trained repeatedly to obtain the best model. Because the initial values of weights and biases are determined randomly, and one train is not enough to decide convenient network.

The merits of ANN are improving efficiency for both uniform irradiance and partial shading conditions. However, PV panels have different characteristics, so an ANN model cannot be used for every kind of PV panels. Also characteristics of panels are change with time and ANN become useless. To overcome this problem adaptive ANN methods are proposed in the literature (Mellit et al., 2007).

3.4.4. Hybrid MPPT Technique

Many researchers have introduced different MPPT techniques for tracking the MPP as mentioned in previous sections. These techniques have some merits and demerits relative to each other. If it is meticulously considered, these demerits can be converted to merits by combining different MPPT techniques.

A hybrid method that employs fractional open-circuit voltage (FOCV) and P&O techniques is proposed by Murtaza et al. This technique is equipped with duty cycle optimization method (Murtaza et al., 2014). A current-based sliding mode

MPPT algorithm is presented by Bianconi et al. to optimize the P&O (Bianconi et al., 2013). Another hybrid method, which uses offline calculation of the open circuit voltage and P&O technique is proposed by Moradi and Reisi (Moradi and Reisi, 2011; Tafticht et al., 2007). A MPPT technique that based on analytical equations of solar cell and P&O method is proposed by Moradi et al (Moradi et al., 2013).

Especially for partially shading conditions, which constitutes local MPPs and confusing the algorithm's operation can be exceeded by using hybrid methods. Moreover, convergence speed of the MPPT techniques can be improved remarkably. On the other hand, usage of hybrid techniques may cause erratic behaviors and unstable operation of the system. Also it makes the system much more complex and cost of the system may be dramatically increased. Number of controlled variables can be another parameter which can be taken into account for the evaluation of the developed MPPT technique.

3.5. Control of Grid Connected Three Phase Inverter

The capabilities to control output current are applicable to PV inverter applications, with the capability to restrict the over current during short circuit and adjust the power factor or reactive power or voltage very precisely (Muljadi et al., 2013). PV inverter can achieve current that alterable in its magnitude and phase angle. A change to be made in the magnitude of the current in phase with the voltage will affect the real power output only, changing the phase angle of the current will change both the real and reactive power output of the inverter (NREL, 2015). For the purpose of integrating a PV system to the utility grid, it is essential to convert DC output power to three phase AC power. A simple active power (P) and reactive power (Q) regulation method is one of the inverter control method, which can provide acceptable three phase AC output power (Muljadi et al., 2013; Rajapakse and Muthumuni, 2009).

3.5.1. Simple P and Q Regulation Inverter Control Method

It can be clearly said that unity power factor and pushing active power to the grid can be achieved by controlling active and reactive power flow of the system. P control can be implemented by controlling the DC-link voltage. To control DC-link voltage, a PI controller can be used. A reference voltage value is specified and compared with the actual voltage on the DC-link capacitor, and then the error signal is passed throughout a PI controller as extinguished in Figure 3.18. Output of the PI controller can be used to adjust phase angle of sinusoidal signal that employed in firing pulse generator (Kalbat, 2013).

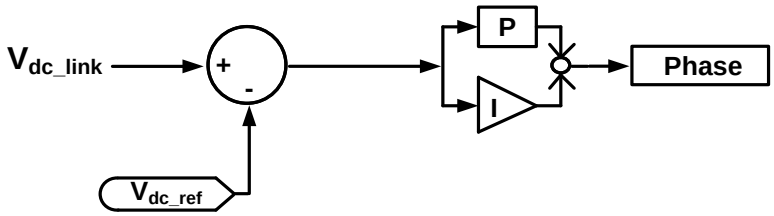

Figure 3.18. DC link voltage controller

The second PI controller is employed to set the reactive power flow. It is important to force the inverter to operate at unity power factor. This is necessary for supplying sinusoidal voltage and current which are in phase at the output of inverter. Output of this PI controller can be used to adjust magnitude of sinusoidal signal that employed in firing pulse generator.

3.6. Summary

In this chapter, PV converter types and MPPT controllers are discussed, and their importance are mentioned by explaining their merits and demerits. Interleaved boost converter's operation is discussed in details. Moreover, different conventional MPPT methods are investigated and their advantages and disadvantages are highlighted. Also, inverter configurations are discussed and information is provided about their respective superiority to each other.

4. DESIGN OF PROPOSED PHOTOVOLTAIC SYSTEM

4.1. Photovoltaic Module Verification

In order to study the embedded power system applications, generalized PV module and array model are quite essential. In this thesis, a generalized five parameters model of a PV panel is reviewed by employing an equivalent single diode model and performed with PSCAD/EMTDC software environment by employing a number of pre-defined constants with FORTRAN coding. The simulated model only uses the data provided by the manufacturer with equations given in previous section to extract the cell I–V characteristics curve for any operating condition.

Sun Power E19\240 solar panel output characteristics have been simulated and examined by taking into account the effect of operating temperature and irradiance on the I/V and P/V curves. Furthermore, a model is constructed to study the effect of partial shading on the PV array. To approve the validity of the model, the presented experimental results under STC in datasheet, which is demonstrated in Figure 4.1, is compared with the simulation results.

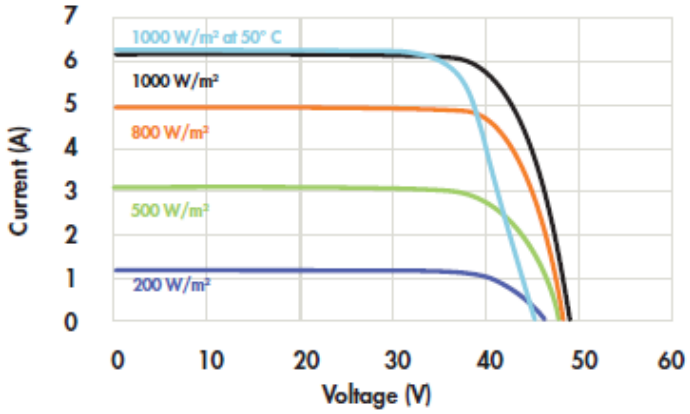

Figure 4.1. I/V characteristics of simulated PV Panel with dependence on irradiance and module temperature (SUNPOWER E19/240 Solar Panel)

The used mathematical model has more favorable features than the physical model, since it is easy to control diode quality factor, band gap energy and temperature coefficient by varying those (Said et al., 2012). The considered model

can be used to extract a cell characteristic or a module characteristic. Also the given model is applicable to different modules by changing the electrical data provided by the manufacturer such as open circuit voltage, short circuit current, voltage and current at maximum power point, number of parallel and series cells and reference temperature.

The most important point to obtain the closest simulated model of a real system, values of serial and parallel resistance must be accurately defined. The definition method consisting of serial and parallel resistance is fundamentally based on trial and error. The error rate is obtained by comparing the simulation results and experimental results provided by the datasheet of the PV module.

The power circuit used to extract I/V and P/V characteristics is given in Figure 4.2.

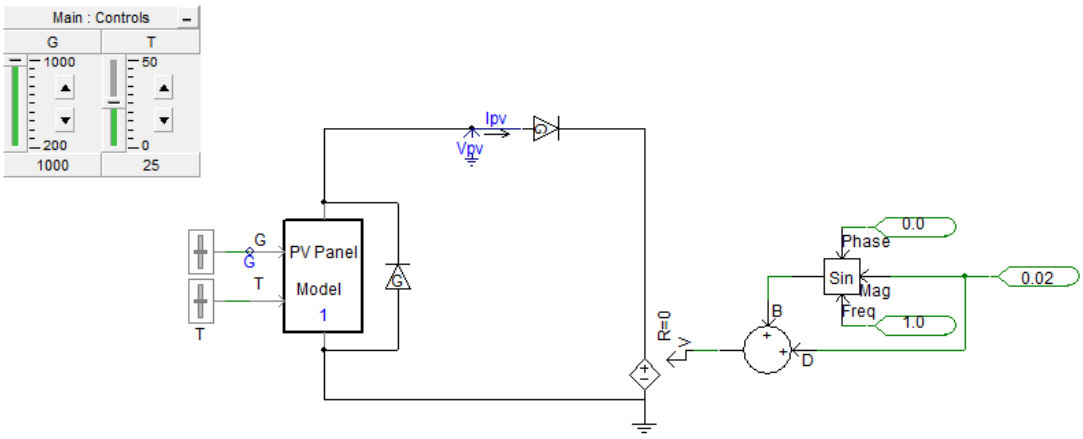

Figure 4.2. The power circuit used for characterization of modeled PV panel

The waveforms of open circuit voltage and short circuit current of the PV panel under different atmospheric conditions are given in Figure 4.3, Figure 4.4, Figure 4.5, and Figure 4.6, respectively.

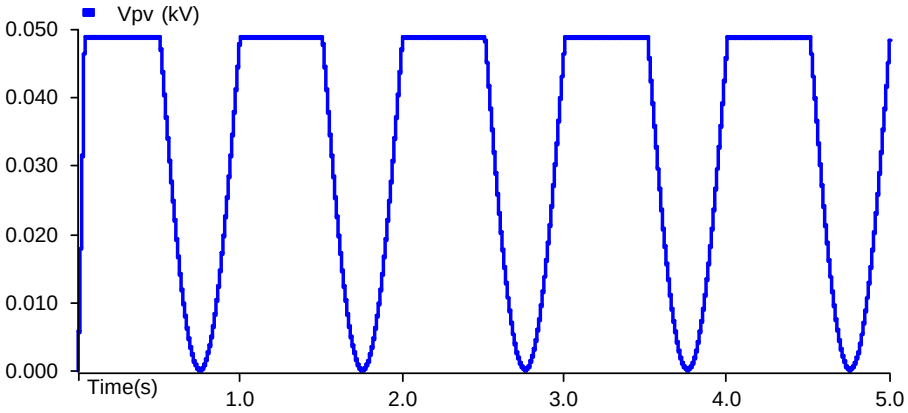

Figure 4.3. Open circuit voltage of the modeled PV panel at 1000 W/m^2 irradiance

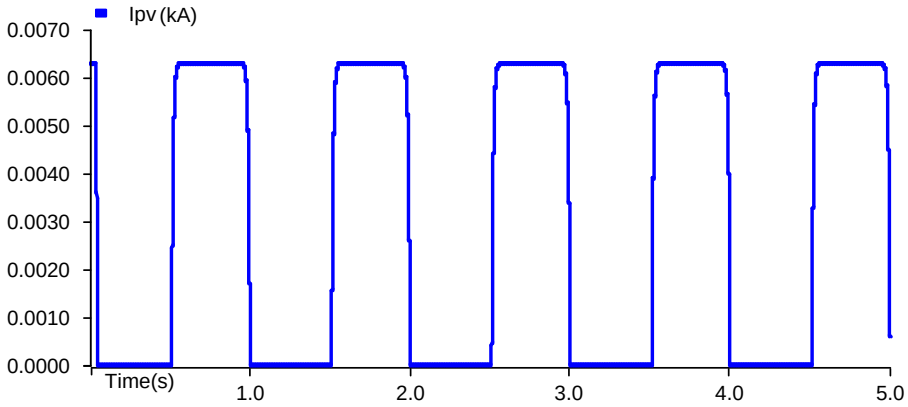

Figure 4.4. Short circuit current of the modeled PV panel at 1000 W/m^2 irradiance

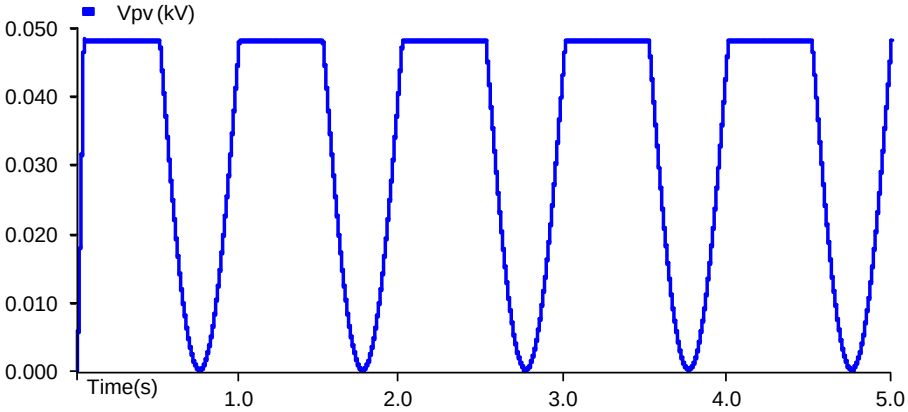

Figure 4.5. Open circuit voltage of the modeled PV panel at 800 W/m^2 irradiance

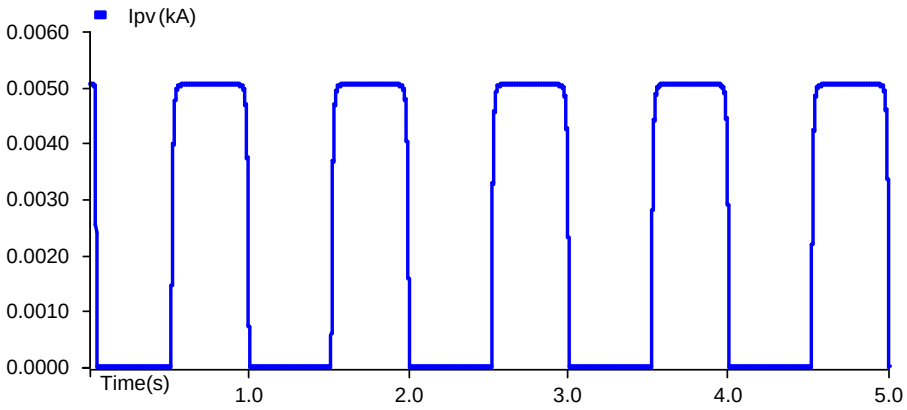

Figure 4.6. Short circuit current of the modeled PV panel at 800 W/m^2 irradiance

I/V characteristics of the modeled PV panel at 1000 W/m^2 irradiance and at 800 W/m^2 irradiance are demonstrated in Figure 4.7 and Figure 4.8, respectively.

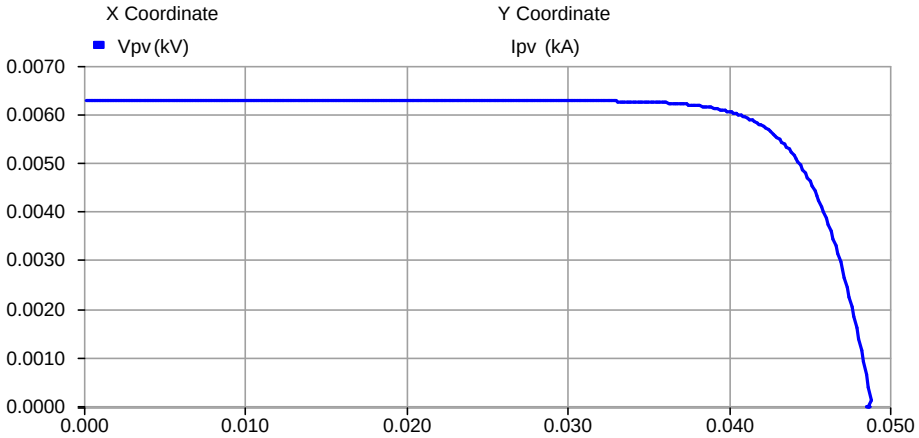

Figure 4.7. I/V characteristic of the modeled PV panel at 1000 W/m^2 irradiance

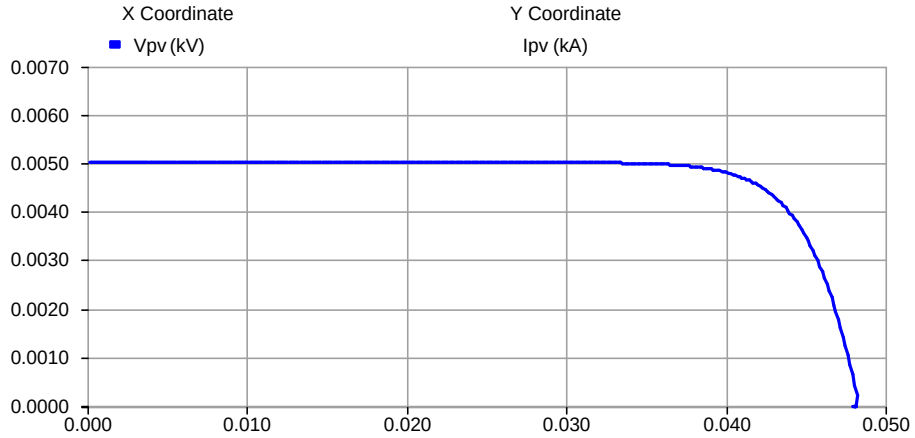

Figure 4.8. I/V characteristic of the modeled PV panel at 800 W/m^2 irradiance

The extracted panel characteristics results are presented for 1000 W/m^2 and 800 W/m^2 irradiance values. With the experimental results provided in datasheet, it is easy to compare the results for validation of the developed model.

Finally, the I/V and P/V characteristics of the constructed PV array, which includes 6 PV panel in parallel and 9 in series, is provided in Figure 4.9. Moreover, characteristics of the constructed PV strings are demonstrated in Table 4.1.

Table 4.1. Characteristics of the constructed PV strings

Number of series connected panels in a string	9
Number of parallel connected panels in a string	6
Output voltage rating at MPP under STC	364.5V
Output current rating at MPP under STC	35.58A
Maximum power output under STC	13.1kW

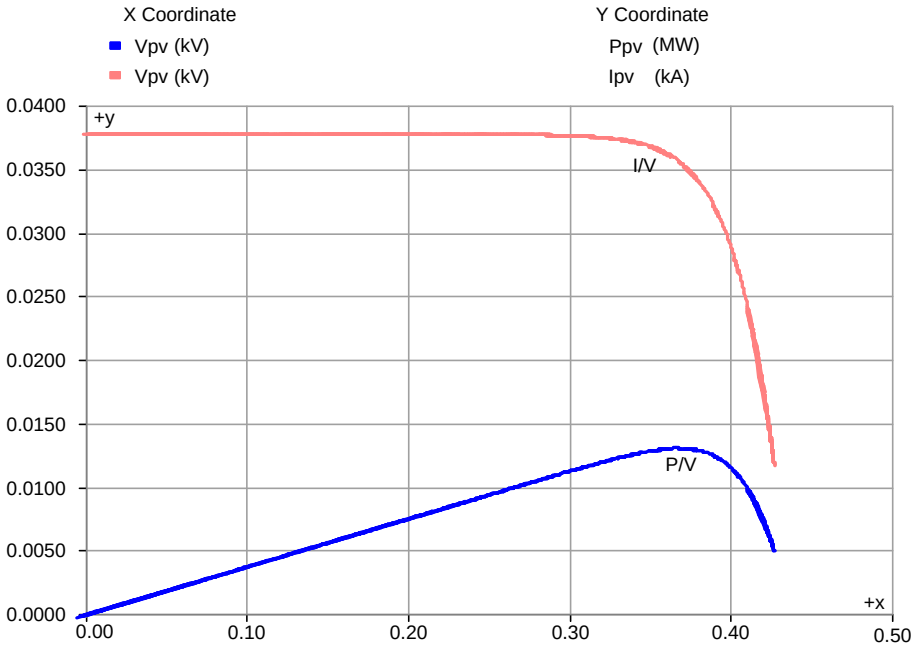

Figure 4.9. I/V and P/V curves of the constructed PV array

The employed power circuit for investigation of the effect of the partial shading is presented in Figure 4.10. The effect of partial shading on the I/V and P/V characteristic under different shading patterns and configurations are shown in Figure 4.11 and 4.12, respectively. The output of a PV module can be reduced dramatically in case of having even a small shaded area on the PV module. This

phenomenon can be extended for arrays which consist of strings of modules, when even a panel is shaded; it affects the performance of the entire string. External by-pass diodes, purposely added by the manufacturer or the system designer, improve performance of the PV panels. These diodes are added in parallel with modules or blocks of cells within a module to mitigate the impact of shading (Masters, 2013).

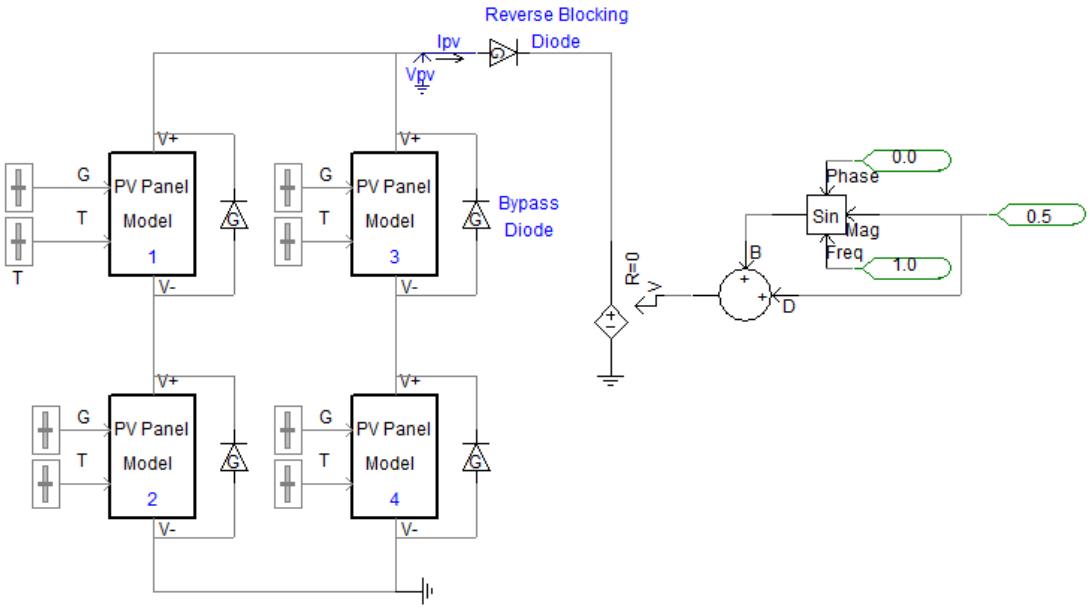

Figure 4.10. The power circuit used for characterization of the PV system under partial shading conditions

Two different cases are examined and the results are described below.

Case 1: When the irradiance value of 3rd PV panel reduced to 400 W/m^2,

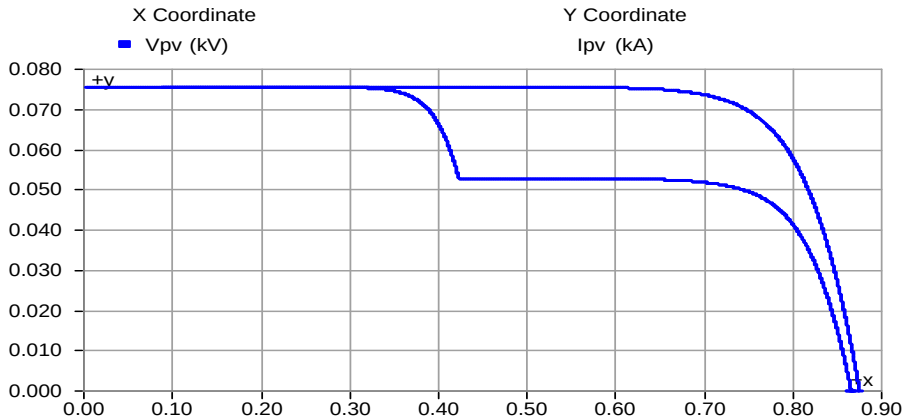

Figure 4.11. I/V characteristic of the modeled PV system under partial shading conditions

Case 2: When the irradiance value of 3rd PV panel reduced to 400 W/m^2 and then 2nd PV panel reduced to 200 W/m^2,

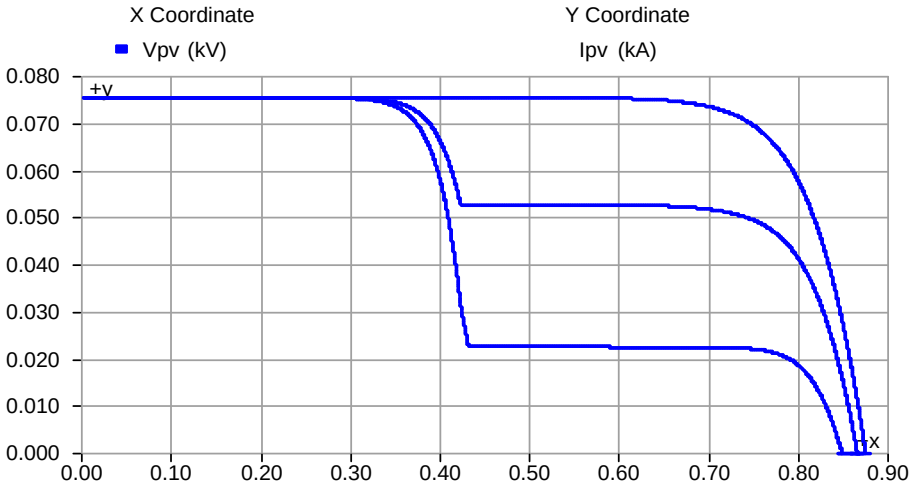

Figure 4.12. I/V characteristic of the modeled PV system under partial shading conditions

4.2. Design of the Interleaved Boost Converter

To ensure reaching the maximum operating point of the PV panels, an interleaved boost converter is employed. This structure is considered as two independent DC-DC converters, which operate independently from each other. Each converter has its own MPPT controller and switched with 180° phase shift relative to each other. Substantially, each branch can control an amount of power up to 13kW and permissible amount of current specified as 35A. The main goal is defined as obtaining higher efficiency by dividing the output current into two branches which reduces the I^2R losses, decreases leakage inductance to attain a lower switching loss, reduces electromagnetic interference and ripples in the input and output waveform. Two parallel switches are used for solving the heating problem of the switches.

The interleaved boost converter design fundamentally consists of the selection of the inductors, the input and output capacitors, the power switches and the output diodes (TI, 2013). It is considerably important to select proper inductor and capacitor. Because the ripples in the input and output waveform affect the controller performance and consequently overall efficiency of the system. Also these ripples

directly have influence on the lifespan of the converter components. The limit values of the ripples on the current and voltage defined as 10% and 1%, respectively. Switching frequency of the DC-DC converter is specified as 20 kHz. First step of the design can be determining the maximum value of the input power (P_{max}) to attain the maximum inductor current duty cycle (D) (TI, 2013).

$$I_{out-max} = \frac{P_{max}}{V_{out}} \tag{4.1}$$

$$R_{load} = \frac{V_{out}}{I_{out-max}} \tag{4.2}$$

$$D_{max} = \frac{V_{out}-V_{in-min}}{V_{out}} \tag{4.3}$$

$$D_{min} = \frac{V_{out}-V_{in-max}}{V_{out}} \tag{4.4}$$

$$L_{boost} \geq \frac{V_{in-min}D_{max}}{f_s \Delta I} \tag{4.5}$$

Employing the above equations yields the limit value of inductor (L_{boost}) as 2.335mH. The parameters of the Equation (4.5) are determined as $V_{in-min} = 340V$, $D_{max} = 0.514$ and $\Delta I = 3.742$.

$$L_{boost} \geq \frac{V_{out}D(1-D)}{f_s \Delta I} \tag{4.6}$$

$$C_{in} \geq \frac{I_{out-max}D^2}{0.02(1-D)f_s V_{in}} \tag{4.7}$$

According to the above equation, which is used for confirming the value of L_{boost}, desired output voltage (V_{out}) is 700V, V_{in} at P_{max} is 365V, P_{max} is 13kW. Depending on these data, D is found as 0.479, the value of inductor (L_{boost}) is calculated as 2.334mH. This value is the minimum limit value for the inductor

operating at CCM. Value of C_{in} is basically dependent on the output voltage of the PV panel, in other words the input voltage of the DC-DC converter. Therefore, it can be adjusted by analyzing PV output voltage characteristics.

The partial view of inductor current and output power of the converter is illustrated in Figure 4.13 and Figure 4.14, respectively.

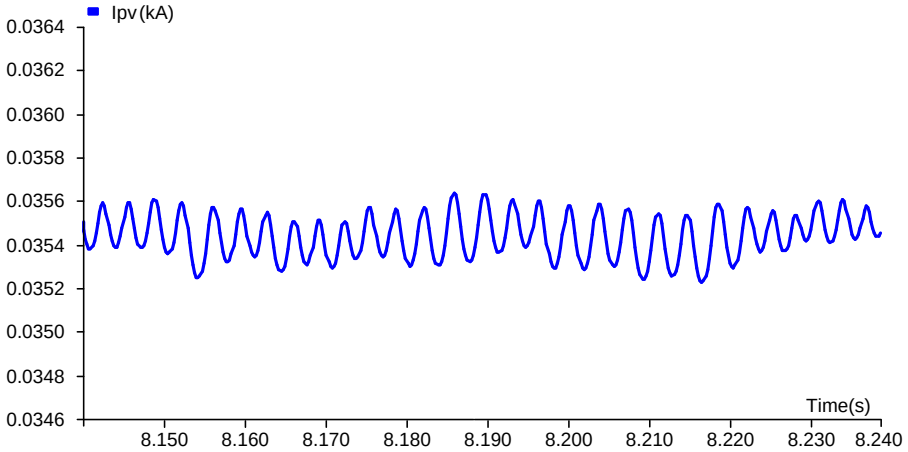

Figure 4.13. Inductor current of a branch of an interleaved boost converter

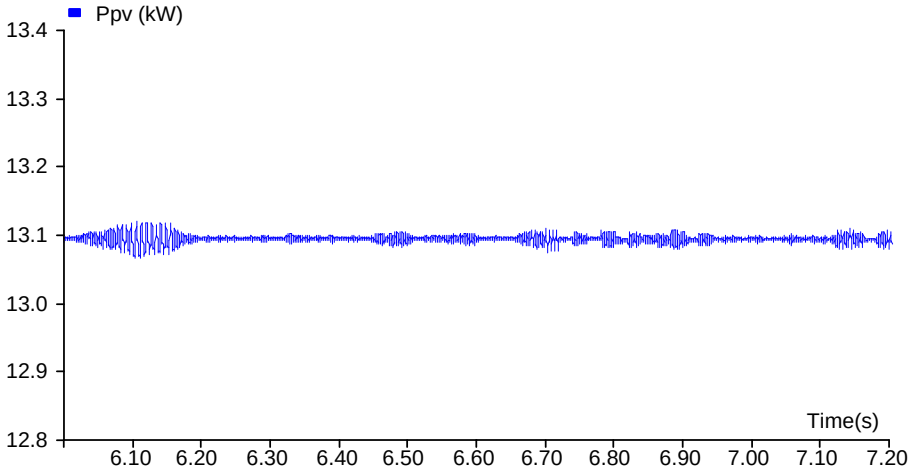

Figure 4.14. Output power of a branch of an interleaved boost converter

To generate switching signal for the interleaved DC-DC converter, output of MPPT block is subtracted from measured PV output voltage and then the outcome is fed into a PI controller. Finally, the result is compared with a carrier signal by using a comparator as shown in Figure 4.15.

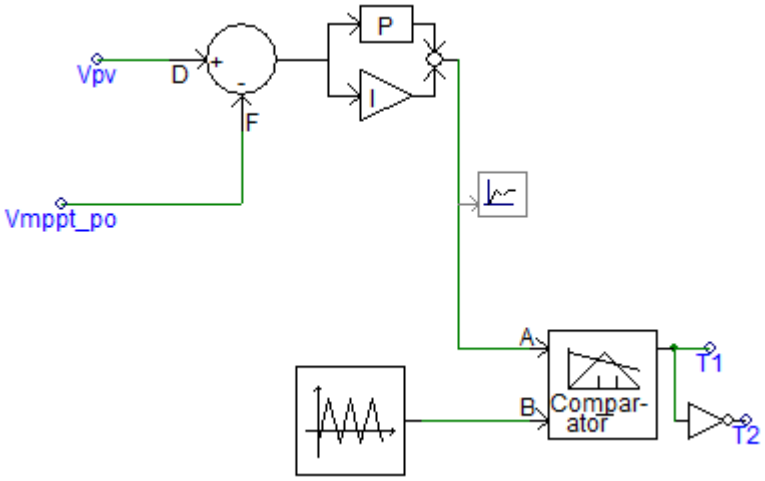

Figure 4.15. Generating the switching signal for Interleaved DC-DC converter

4.3. Design of the Proposed and Conventional MPPT Block

In this thesis, two conventional MPPT techniques and a novel ANN based hybrid MPPT algorithm is presented by employing EMTDC/PSCAD software environment by using a number of pre-defined constants with FORTRAN coding. The modeled blocks are shown below in Figure 4.16.

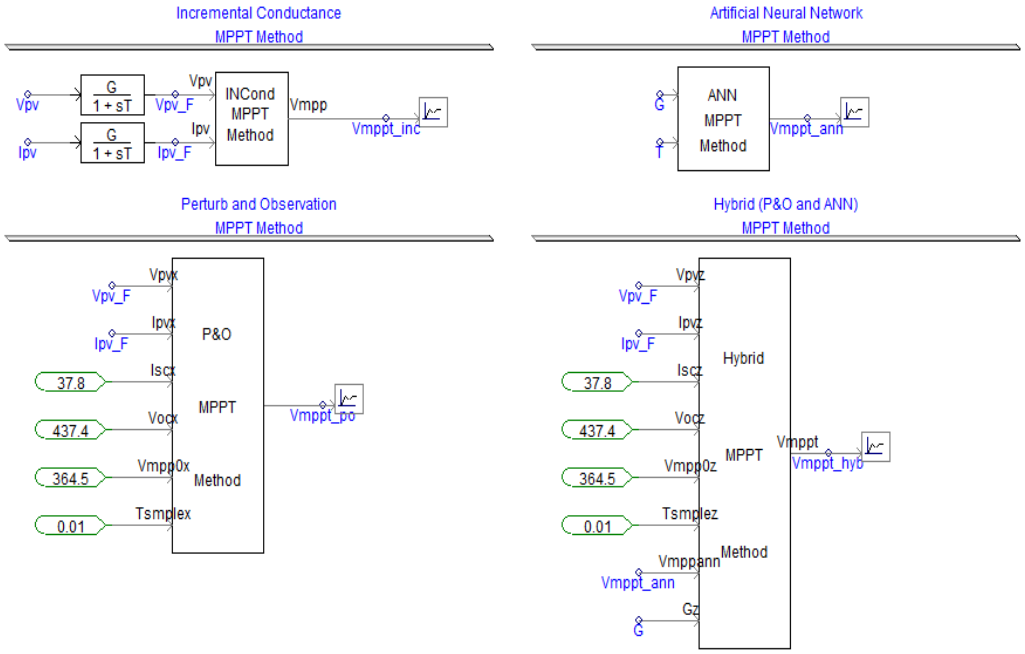

Figure 4.16. The modeled MPPT blocks

A signal generator is designed to compare performance of the MPPT techniques. This generator gives 1000 W/m^2 irradiance for 5 seconds, then decreases 950 W/m^2, 850 W/m^2, 700 W/m^2, 600 W/m^2 and finally increases 700 W/m^2, 800 W/m^2, and 1000 W/m^2. Each irradiance level is applied for 1 second as shown in Figure 4.17.

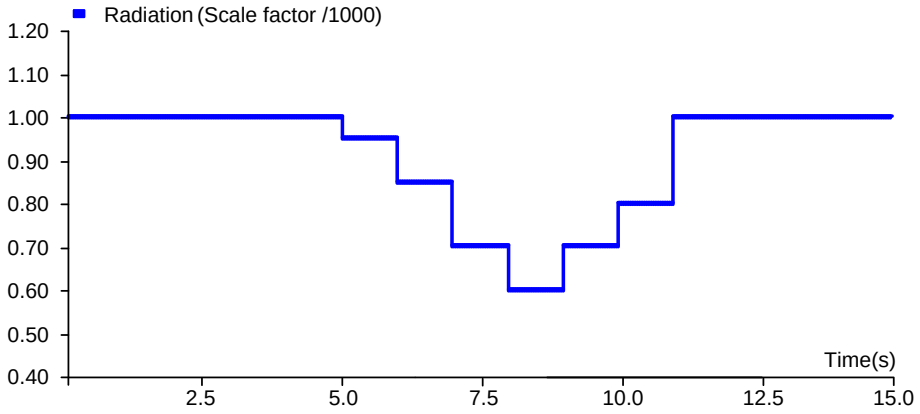

Figure 4.17. Output of the signal generator as irradiance level

4.3.1. Perturb and Observation MPPT Technique

Perturb and Observe (P&O) is an iterative online MPPT technique, which uses the voltage of the PV module for the perturbation as discussed in section 3.4.1. P&O MPPT technique is exhibited in PSCAD/EMTDC software environment by using a number of pre-defined constants with FORTRAN coding. The output is connected to the boost converter to achieve the MPPT. To evaluate the P&O MPPT technique, a number of test procedures are implemented; merits and demerits of the method are explained and shown in figures. Figure 4.18 illustrates voltage perturbation of the P&O algorithm under variable irradiance.

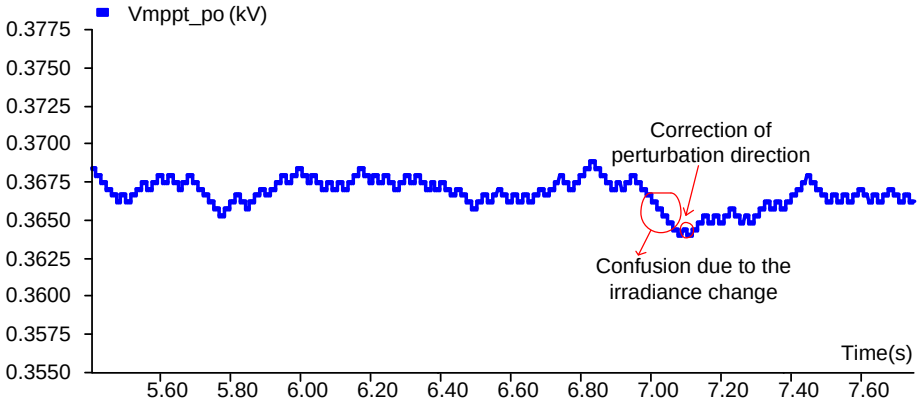

Figure 4.18. Voltage perturbation of the P&O algorithm under variable irradiance

Figure 4.19 shows PV output voltage and MPPT voltage, when irradiance is decreased from 1000 W/m^2 to 400 W/m^2.

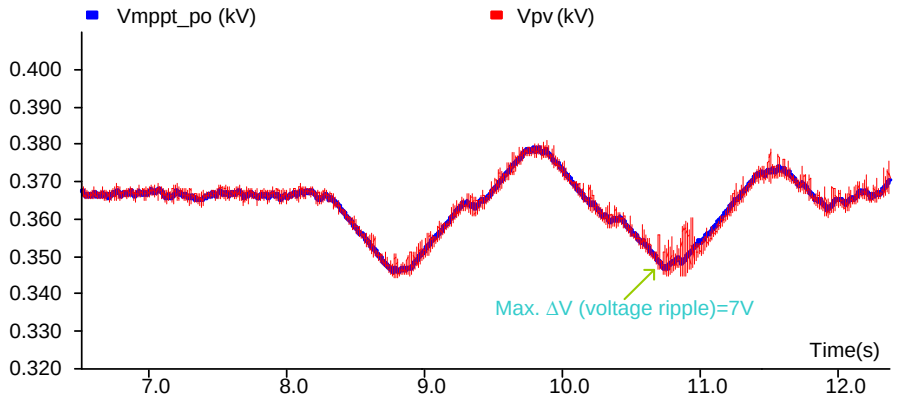

Figure 4.19. PV output voltage and MPPT voltage change when irradiance is varied

As can be seen in Figure 4.20, the PV output voltage follows the MPPT voltage, but it has some drawbacks such as being unable to track the MPPT voltage when a sudden change occur in irradiance. It remains under the generated MPPT voltage, cannot quickly restore itself and also suffers from high oscillations.

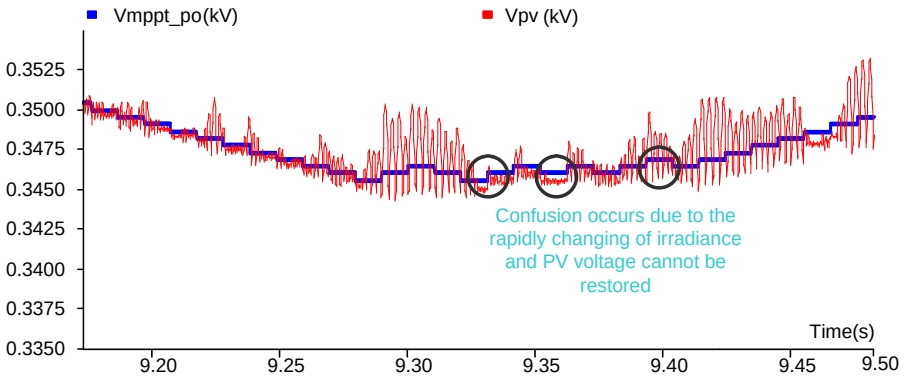

Figure 4.20. MPPT voltage and PV voltage behavior under rapidly changed irradiance

P&O algorithm suffers from oscillations around V_{mpp}, restoring itself after the fluctuations in atmospheric conditions and determination of accurate tracking direction as seen in Figures.

The power output of a branch of the interleaved boost converter under rapidly changed irradiance exhibited in Figure 4.21.

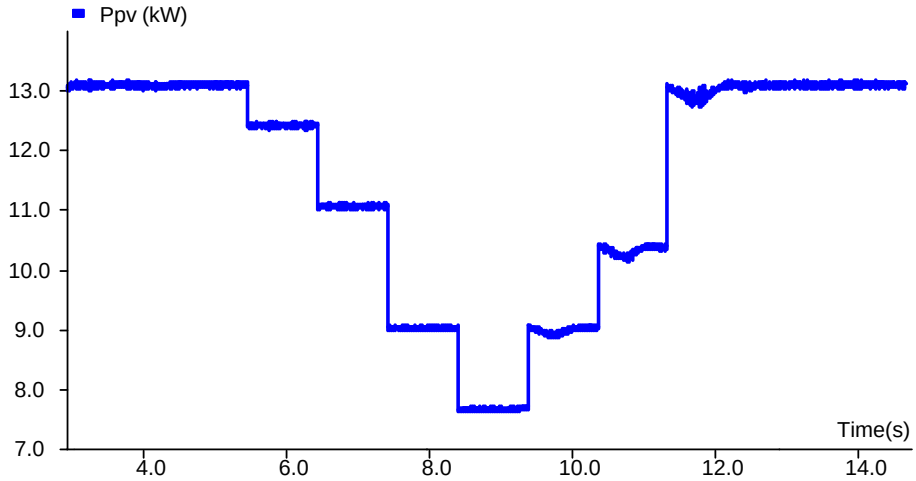

Figure 4.21. The effect of rapidly changed irradiance on the power output of PV array

The effect of rapidly changed irradiance on the I/V and P/V characteristics of PV array is presented in Figure 4.22.

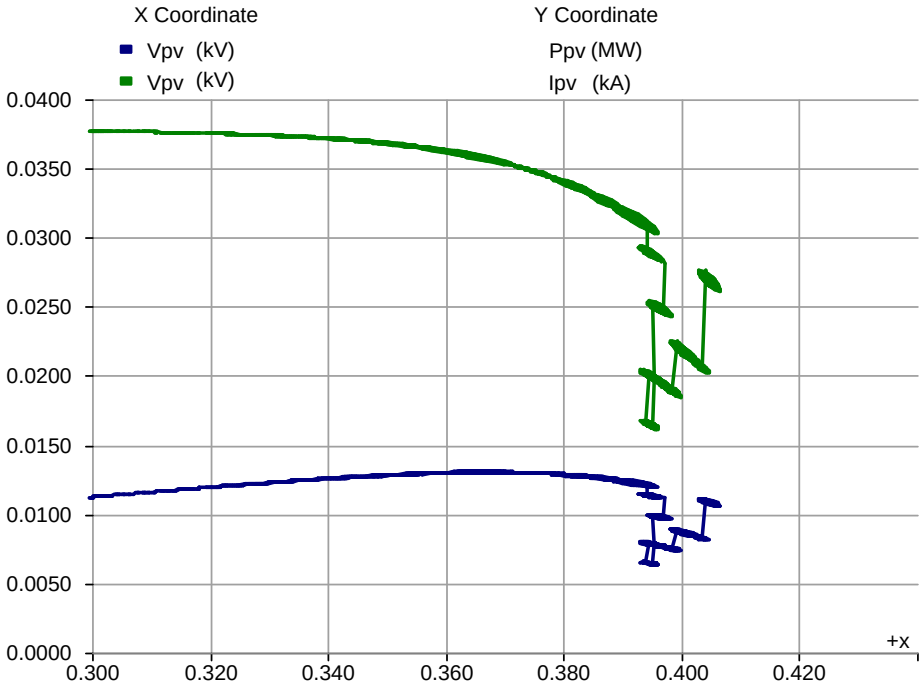

Figure 4.22. The effect of rapidly changed irradiance on the I/V and P/V characteristics of PV array

4.3.2. Incremental Conductance MPPT Technique

INC is another iterative online MPPT technique, which developed for eliminate the deficiencies of P&O algorithm. INC method far more superior compared to P&O method in terms of tracking speed, tracking accuracy and overall system efficiency. However, this method is more complex and more sensitive against the noises and errors on the measured control values, because it operates with the logic of derivative. INC MPPT technique is exhibited in PSCAD/EMTDC software environment by using a number of pre-defined constants with FORTRAN coding.

To investigate the INC MPPT technique some test procedures are implemented, advantages and disadvantages of the algorithm are explained and demonstrated in figures.

Figure 4.23 shows voltage perturbation of the INC algorithm under variable irradiance.

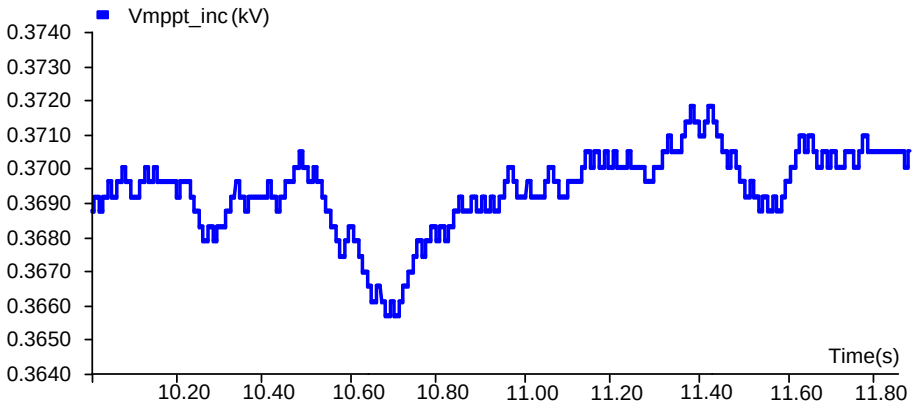

Figure 4.23. The voltage perturbation of the INC algorithm under variable irradiance

Figure 4.24 shows PV output voltage and MPPT voltage, when the irradiance level is rapidly increased and decreased.

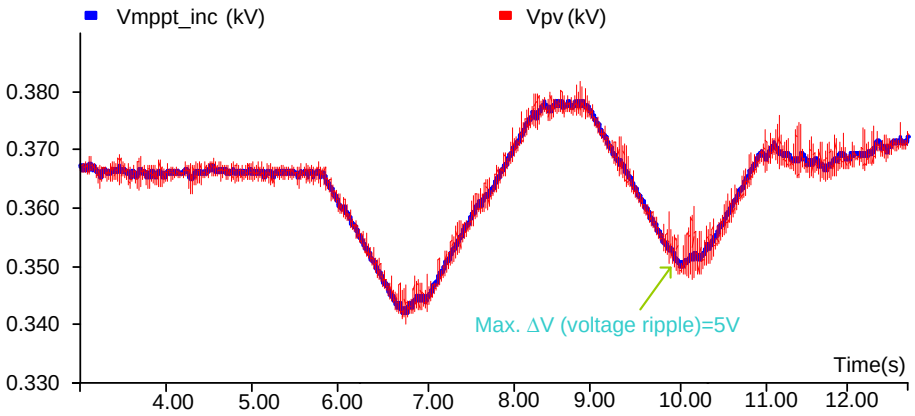

Figure 4.24. PV output voltage and MPPT voltage change related to irradiance level

As seen in Figure 4.25, the PV output voltage tracks the MPPT voltage without any significant spike or tracking fault.

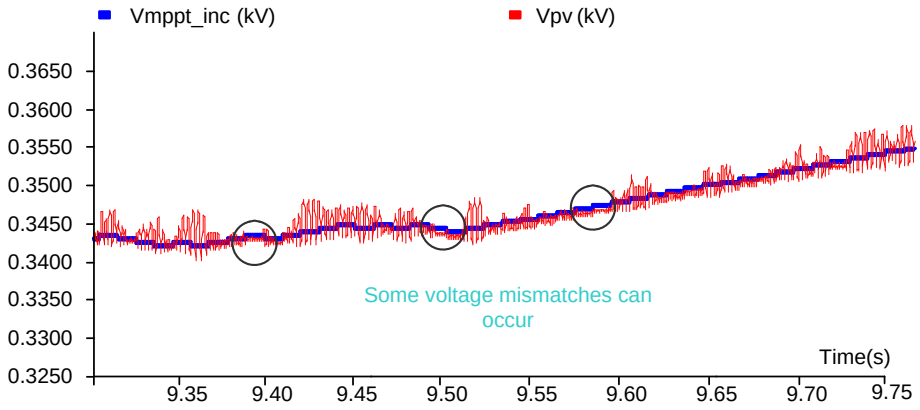

Figure 4.25. MPPT voltage and PV voltage behavior under rapidly changed irradiance

The effect of rapidly changed irradiance on the power output of PV array is demonstrated in Figure 4.26.

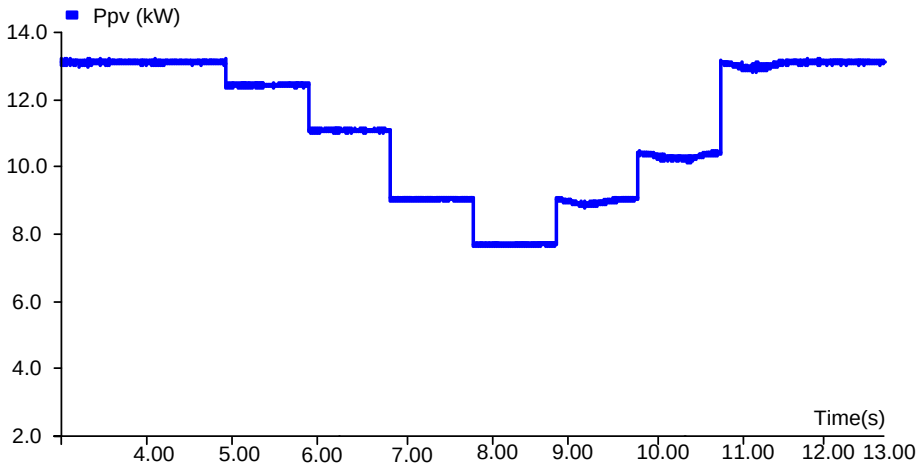

Figure 4.26. The effect of rapidly changed irradiance on the power output of PV array

The effect of rapidly changed irradiance on the I/V and P/V characteristics of PV array is demonstrated in Figure 4.27. It is obviously seen in this Figure INC method is more powerful than P&O algorithm in terms of determination of accurate tracking direction under rapidly changing irradiance level.

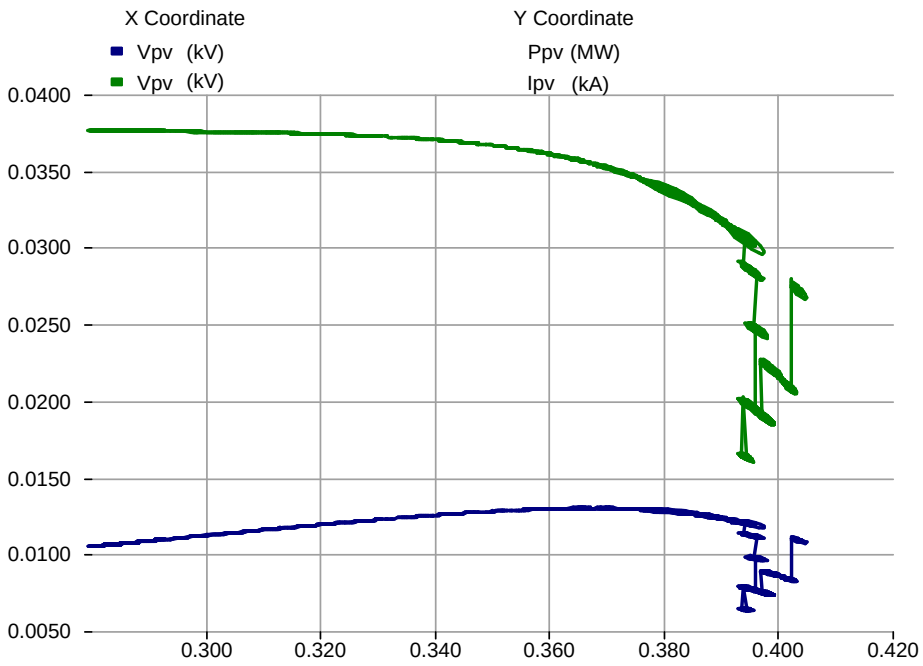

Figure 4.27. The effect of rapidly changed irradiance on the I/V and P/V characteristics of PV array

4.3.3. Proposed Artificial Neural Network Based MPPT Technique

In this thesis, ANN is implemented using MATLAB m-file. The proposed ANN has two inputs, which are named as solar irradiance and temperature and one output which is the maximum power point voltage. The network is trained using the 'MATLAB nnet tool box' as shown in Figure 4.28. To create accurate neural network model usage of MATLAB is quite easier and more effective than using PSCAD. In this thesis, MATLAB is only used for determination of weights and biases, in other words it is only employed for training stage. After specifying weights and biases, these values are transferred to PSCAD and application of ANN is implemented by using FORTRAN codes. Mathematical calculations like normalization of the input data that sensed in real time, processing of normalized data in hidden and output layer and denormalization of network's output are realized in PSCAD/EMTDC.

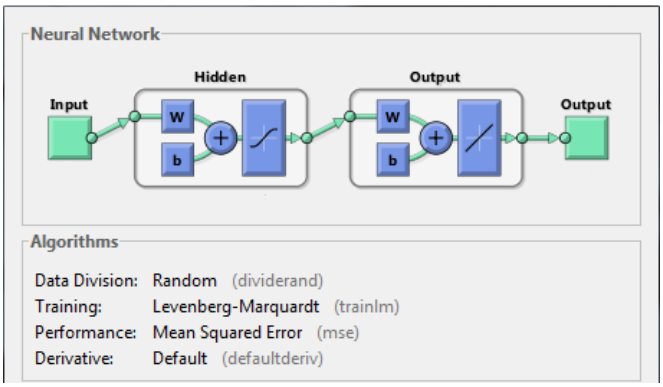

Figure 4.28. MATLAB neural network tool box

The first step of developing the ANN model is the selection of the input variables and the second step is the determination of the number of hidden neurons. These steps are employed with different learning algorithms and the number of hidden layers. The input and target data is adjusted in the range from -1 to 1 for normalization. The system is selected as 2x96 input matrix with 1x96 output matrix. The input/target datasets are divided randomly into three subsets: training; validation; and testing datasets. 70% of dataset is used for training, 15% of dataset is used for testing and 15% of dataset is used for validation. The numbers of hidden neurons are varied from 3 to 10 for obtaining best model. A network with few hidden neurons will have limited learning capabilities, while an excess of hidden neurons will lead to over fitting or generalization loss.

Some of the system parameters are given as; the number of epoch is 100, specified number of iterations (net.trainParam.max_fail) for preventing over fitting is 50, learning algorithms are LM and SCG algorithm, transfer functions are tansig and purelin. On the other hand ‘over fitting’ is obstructed by the usage of early stopping techniques. When the error on validation set increases for a defined number of iterations, the training process is finished automatically. The model was run about 50 times to obtain the best results. The reason of several attempts, weights and biases are chosen randomly and this affects the accuracy of the model. Design procedure is given in Figure 4.29.

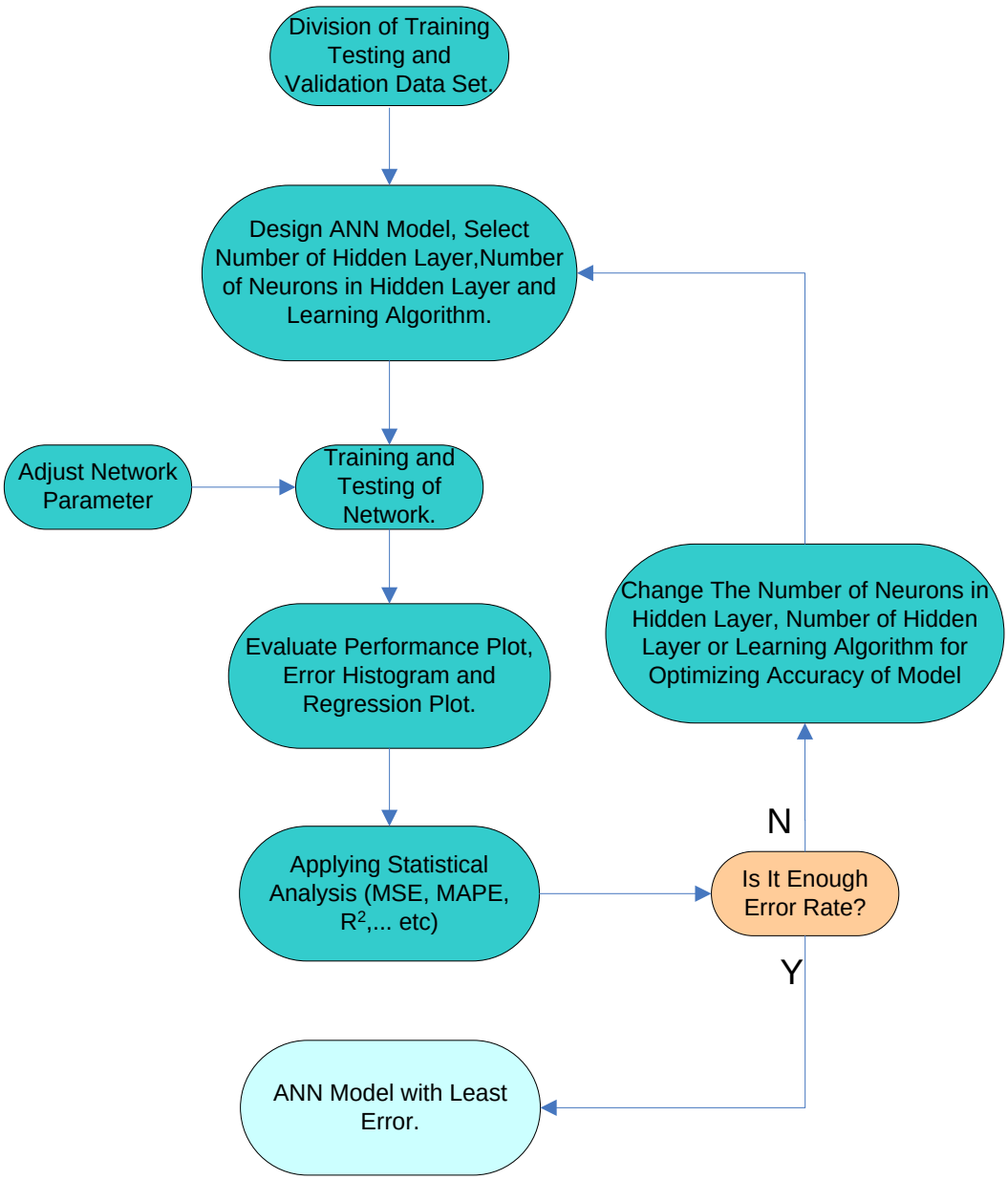

Figure 4.29. Training procedure of proposed ANN based MPPT algorithm

Performance and regression plots are illustrated in Figure 4.30 and 4.31, respectively. The results reveal that MSE (Mean Squared Error) becomes minimum and no significant over fitting at epoch 16, regression plot shows network output and targets are almost close because very good fit occurs along 45° line.

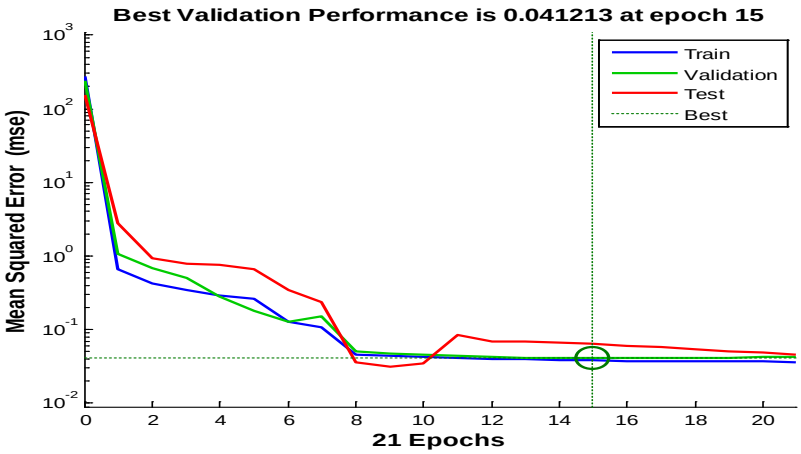

Figure 4.30. Performance plot of network

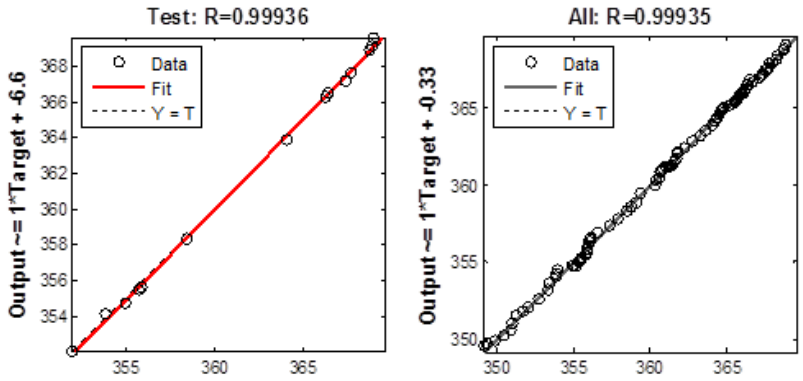

Figure 4.31. Regression plot of network for all and test

ANN is an offline soft computing MPPT technique, which is developed to eliminate the deficiencies of conventional algorithms. The proposed method has much superiority compared to conventional MPPT techniques in terms of tracking speed, tracking accuracy, oscillations and overall system efficiency. However, this method is more complex and its accuracy highly relies on PV panel characteristics.

As illustrated in Figure 4.32, numbers of oscillations are reduced according to mostly used MPPT techniques P&O and INC. Furthermore, the following of accurate tracking direction is achieved by the proposed ANN based MPPT technique.

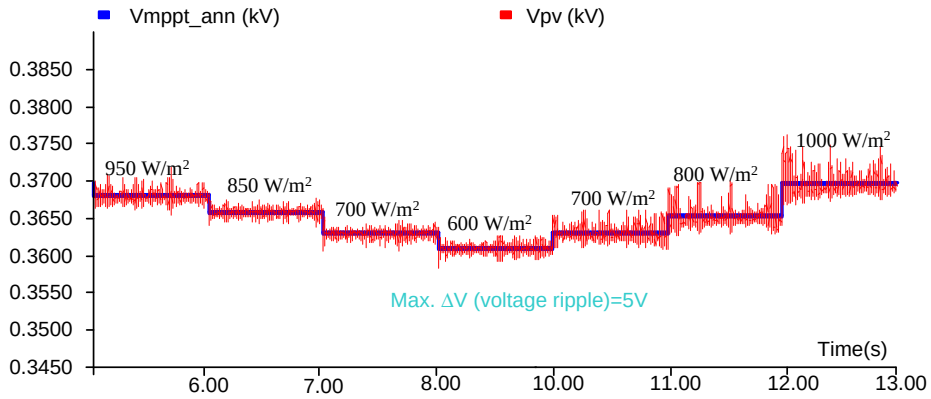

Figure 4.32. MPPT voltage and PV voltage behavior under rapidly changed irradiance

The effect of rapidly changed irradiance on the power output of PV array is demonstrated in Figure 4.33. It is quite clear that the power flow is improved by using the proposed algorithm when compared to INC and P&O algorithms. Hence, the overall system efficiency is increased by employing proposed MPPT algorithm.

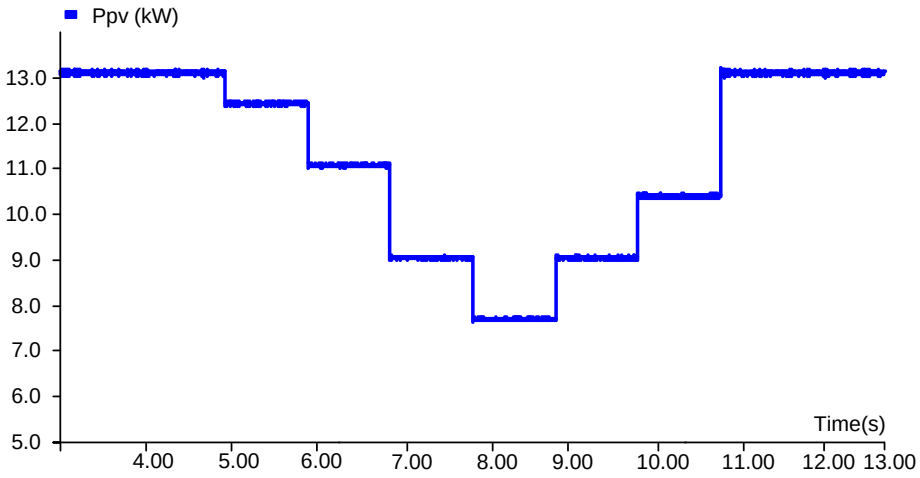

Figure 4.33. PV output power under different irradiance level by using ANN based MPPT algorithm

The effect of rapidly changed irradiance on the I/V and P/V characteristics of PV array, when ANN based MPPT technique is applied, is demonstrated in Figure 4.34. It can be clearly seen that the operation voltage mainly located around the MPP voltage. This situation affects the number of oscillation and tracking accuracy.

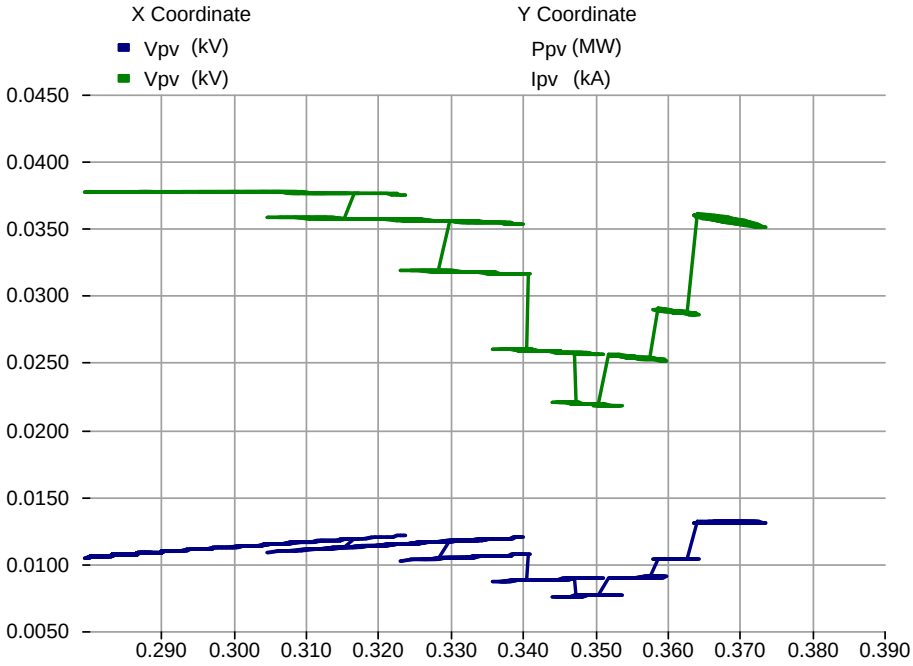

Figure 4.34. The effect of rapidly changed irradiance on the I/V and P/V characteristics of PV array

4.3.4. Proposed Hybrid MPPT Technique: Combination of P&O and ANN

This method is developed to eliminate deficiencies of conventional algorithms, and to create an efficient solution against the partially shading conditions. This method is focused on the irradiance level; solar radiation is measured at multiple points. These measurement results are processed and when the average irradiance change exceeds specified value, MPP reference voltage is provided by the ANN based MPPT technique. It is planned to overcome the slowness of convergence speed and the amplitude of oscillations. Design procedure of the proposed Hybrid MPPT technique is given in Figure 4.35.

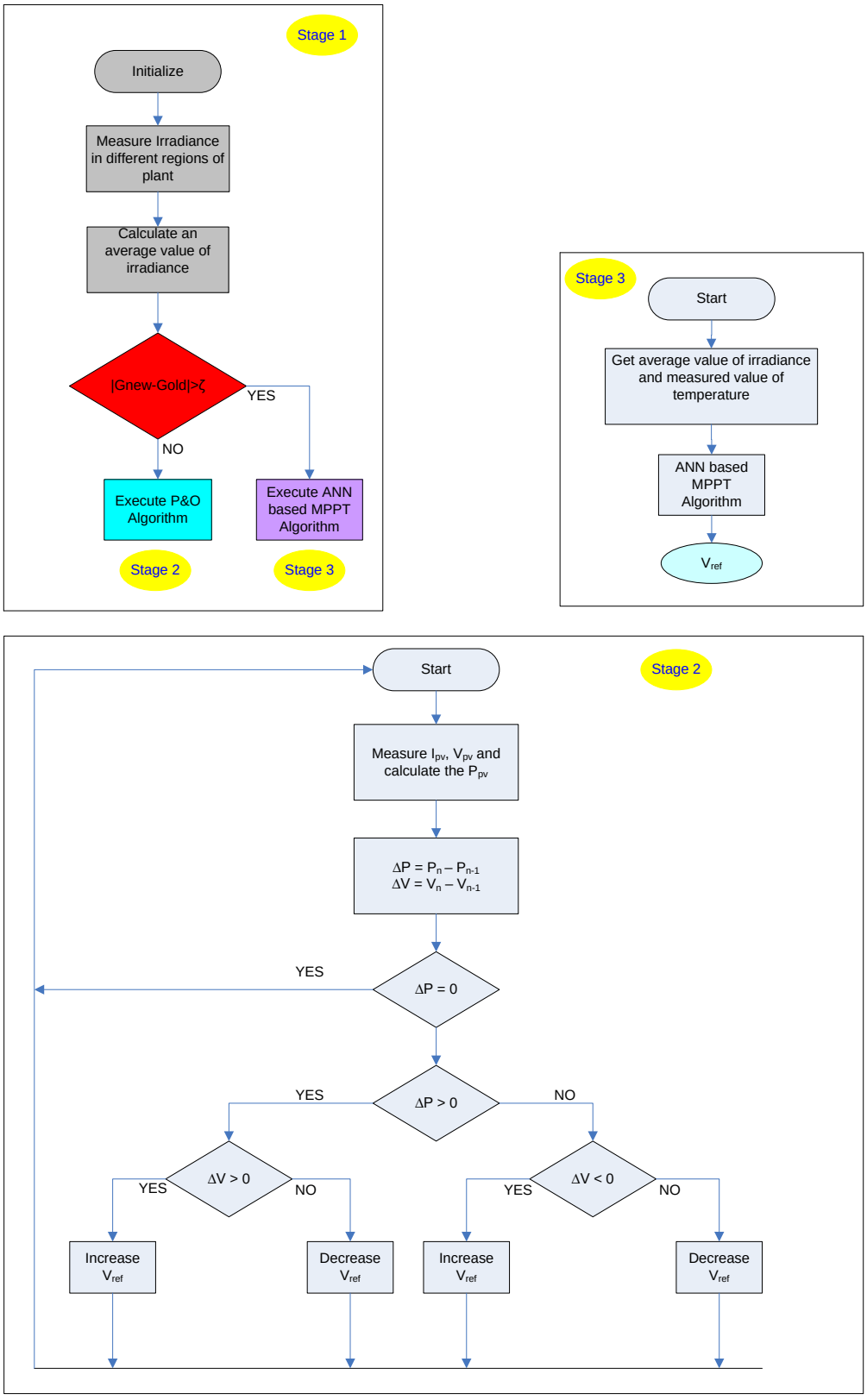

Figure 4.35. Design procedure of the proposed Hybrid MPPT technique

Also reference voltage changes and voltage perturbation related with the proposed hybrid MPPT technique is demonstrated in Figure 4.36

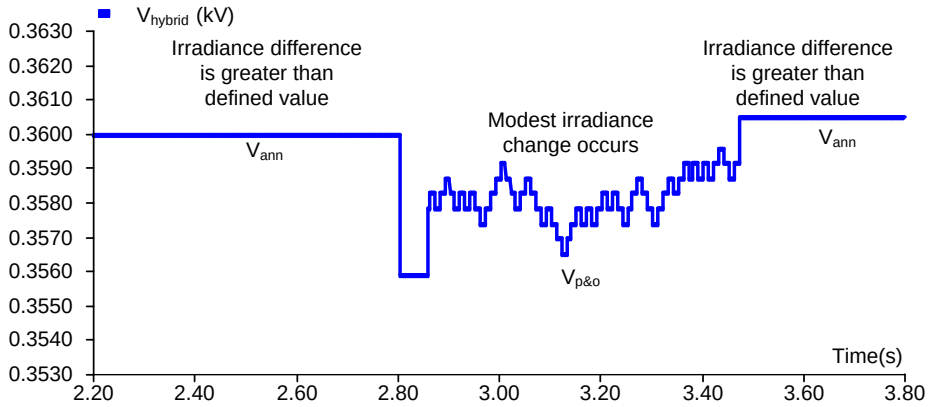

Figure 4.36. Reference voltage changes with the proposed hybrid MPPT technique

However, it makes the system much more complex and cost of the system may be dramatically increased. Number of controlled variables can be another parameter which can be taken into account for the evaluation of the developed MPPT technique.

The number and layout of the sensors are very important. Because the sensors used for measuring the solar irradiance level are too expensive. Therefore, definition of a proper layout with minimum number of sensors is an important issue. It is suggested that the alignment of the sensors should not be on same axis like east-west or north-south. When the cloud transition occurs the average change of the irradiance become zero and the system cannot realize this transition. The strings used in this thesis for a branch of interleaved DC-DC converter is demonstrated in Figure 4.37.

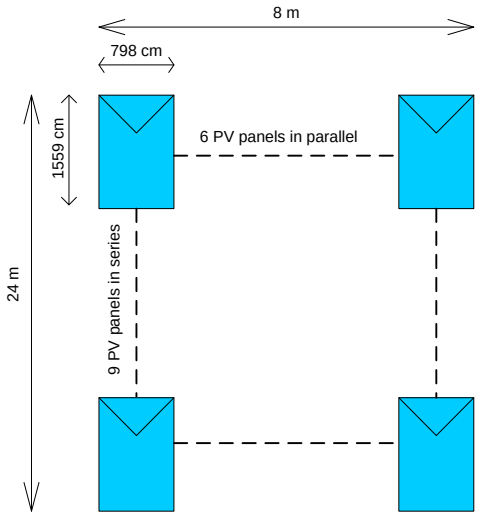

Figure 4.37. A string, which connected to a branch of converter

In this string PV panels are divided into two parts and sensors are located as illustrated in Figure 4.38. It is planned to cover all possible changes in atmospheric conditions in terms of shading. Sensors are located at the point where the three medians of the triangle intersect. It was placed in the center of gravity, in other words. With this location plan the most efficient point is defined and the covered area is divided into equal areas.

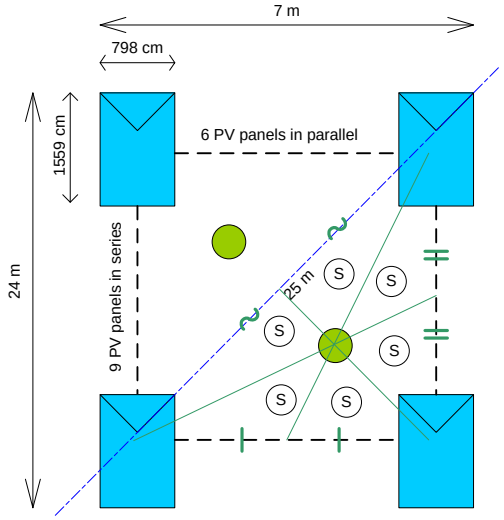

Figure 4.38. The suggested layout of irradiation measurement sensors

With the proposed Hybrid MPPT method, it will be easy to follow sudden voltage changes due to the irradiance change. Hence, this method can eliminate deficiencies like slowness of convergence speed and the number of oscillations. Also it will contribute to follow small changes with the help of iterative method. Furthermore, it can be exploited from superiority of the ANN based MPPT method in partial shading conditions.

4.4. Design of the Voltage Source Inverter

The inverter circuits are used for converting DC voltage to AC voltage. Switching devices with anti-paralleling diodes having turn-off capability are employed in the inverter circuits. A VSI is energized by a capacitor named as DC-Link capacitor at the input. An interface filter is used for obtaining an available waveform at the output side of VSI and the connection in parallel to the distribution line as illustrated in Figure 3.6.

The VSI that employed in PV systems provides a sinusoidal current waveform. This current can be injected to the grid after filtered. To obtain the three-phase AC current in three phases VSI, six gating signals need to be sent to the switches of the inverter. H1, H3, H5 are 3 phase symmetrical switching function with phase shift 120°. The switch S1 and S4 is turned on for 180°. The switches of any leg of the inverter cannot be switched simultaneously due to preserving the dc link voltage supply from being short circuited. It can be concluded that the desired waveform is obtained by accurately controlling the switches in the inverter.

One of the most important design stages is choosing an appropriate DC-link capacitor value. A DC-link capacitor provides constant DC-link voltage to the inverter and controlling the DC voltage on the capacitor ensures to control active power flow to the grid. Moreover, it reduces the voltage ripple across the PV terminals.

The selection of reference capacitor voltage (V_{dcref}) and capacitance of the DC-link capacitor C_{DC} can be extracted by using (4.8) and (4.9),

$$V_{dcref} = \frac{2\sqrt{2}\,V_{LL}}{\sqrt{3}m_a} \tag{4.8}$$

where V_{dcref} is the reference capacitor voltage, V_{LL} is line to line grid voltage, m_a is the modulation index, C_{dc} is the DC capacitor value. Reference DC voltage is accepted as 700V using Equation (4.8) when m_a=1 and $V_{LL} = 400V$.

$$C_{dc} = \frac{3S_n nT}{(1.8V_m)^2 - (1.4V_m)^2} \tag{4.9}$$

where V_m is peak value of grid voltage, S_n is apparent power of system, T is system time period, n is the cycle that starts working the controller. DC capacitor value is calculated as 44 mF using (4.9) when $V_m = 326.6V$, $S_n = 200kVA$, $n = 0.5$ and $T = 0.02\ s$. The DC link capacitor value is selected as 40mF.

4.5. Design of the Voltage Source Inverter Controller

The ability to control the current output of the power converter both in magnitude and phase angle enables the power inverter to control active and reactive power flow control. In this thesis for providing the active power control, DC-link voltage is controlled by a PI controller. A reference DC-link voltage is specified and the system is forced to operating at this voltage value. To generate proper phase angle for reference sine wave used in firing pulse generator, reference DC-link voltage is subtracted from measured DC voltage on DC-link capacitor and then the outcome is passed through a PI controller. Output of PI controller is employed as phase angle of reference sine wave. Phase angle variation under variable irradiance level is illustrated in Figure 4.39.

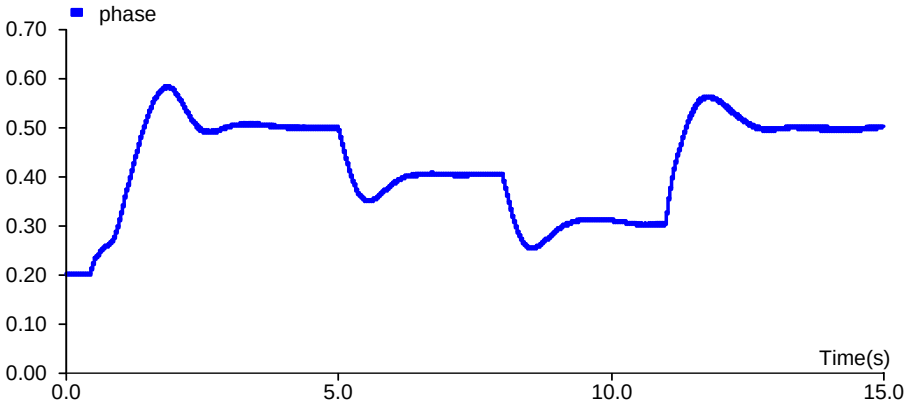

Figure 4.39. Output of DC-link controller under variable irradiance level

Fluctuations on the DC-link capacitor is illustrated in Figure 4.40

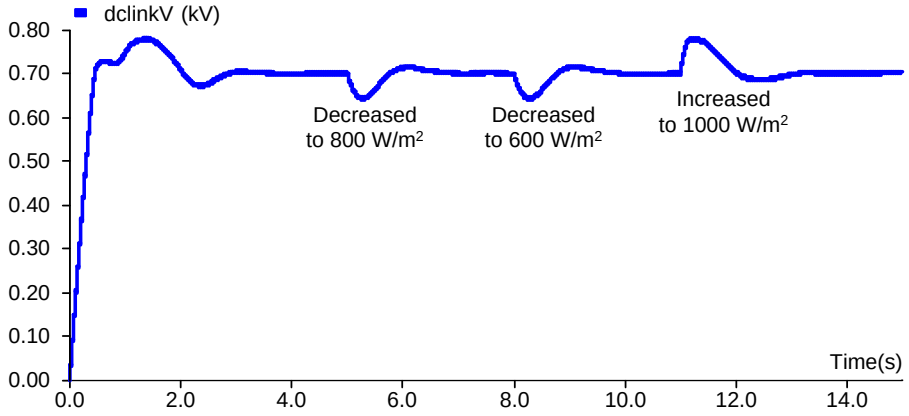

Figure 4.40. Fluctuations of the DC-link voltage.

By using same way, reactive power control is implemented by using a PI controller. Reference reactive power value is assumed to be zero. To generate proper magnitude for reference sine wave employed in firing pulse generator, reference reactive power value is subtracted from measured reactive power injected to the grid and then the outcome is passed through a PI controller. Output of PI controller is employed as magnitude of reference sine wave. Magnitude variation under variable irradiance level is shown in Figure 4.41.

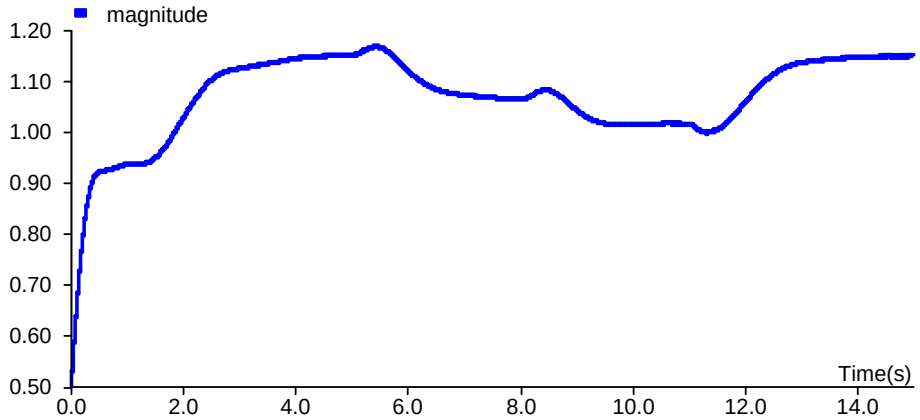

Figure 4.41. Output of reactive power controller under variable irradiance level

Compensated reactive power output is demonstrated in Figure 4.42.

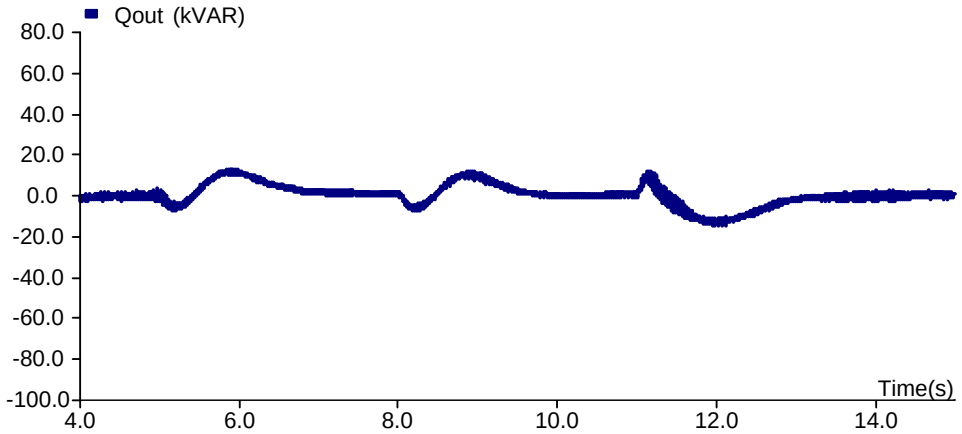

Figure 4.42. Variation of the output reactive power

Variation of injected current under variable irradiance level is shown in Figure 4.43.

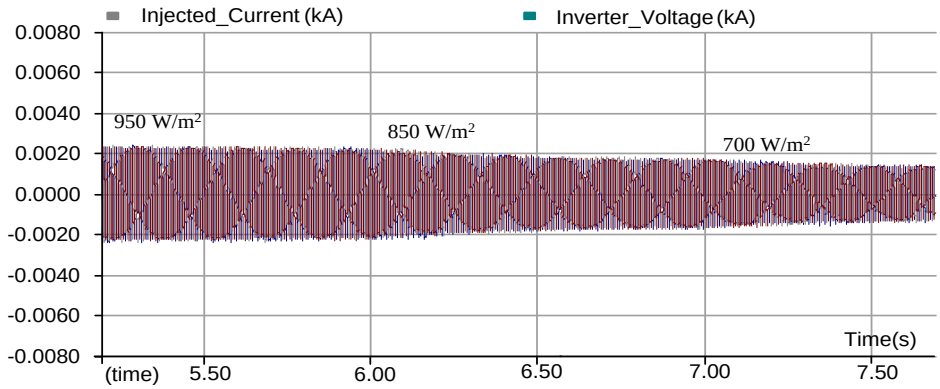

Figure 4.43. Overview of injected current under variable irradiance level

Effect of rapidly changing irradiance level on the injected current is exhibited in Figure 4.44.

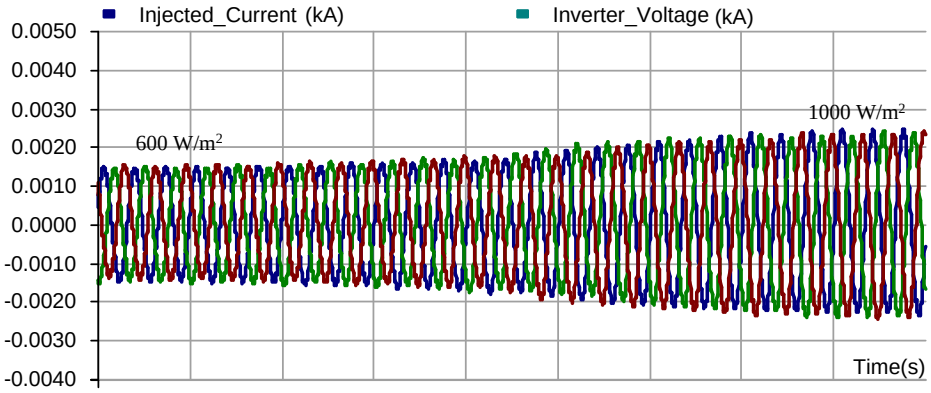

Figure 4.44. Effect of rapidly changing irradiance level on the injected current

4.6. Design of the Inverter Output Filter

4.6.1. L Filter

To operate under variable irradiance level, an AC filtering stage is required to further smoothen the output and limit the voltage drop in the AC side of the inverter (Rahman and Varma, 2011).

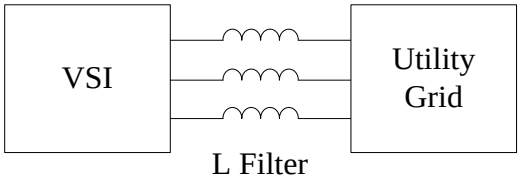

Figure 4.45. Circuit diagram of L filter

Peak ripple current is a criterion to design the inductor. For calculating the ripple current, maximum current generation capacity is considered and the effect of inductor resistance is considered to be negligible. Depending on these circumstances, the inverter reference voltage is equal to the supply voltage. Thus the required smoothing inductance is given by (Chaoui et al., 2008):

$$L_f = \frac{V_g}{6 f_{sw} \Delta_{ph(p-p)max}} \tag{4.10}$$

where $\Delta_{ph(p-p)max}$ = 15% of peak compensation current, V_{dc} is the supply voltage of inverter (DC link voltage) and f_{sw} is the switching frequency. The smoothing inductance is calculated as 2.34mH using (4.10) when V_{dc} = 700V, $\Delta_{ph(p-p)max}$= 20A and f_{sw} = 2.5kHz. To improve the smoothing inductance performance in simulation study, the inductance is selected as 2.2mH.

4.7. Summary

In this chapter, design of the overall system is presented. Selection of circuit components for each part of the system is given with mathematical equations and calculations. The important selection criteria are highlighted. The PV model is verified by using the manufacturer data sheet. The conventional and proposed MPPT techniques are simulated and discussed. A deeply comparison is made between these techniques, disabilities of conventional methods are revealed and improvements with proposed methods are explained. The circuit diagram of the modeled PV system is shown in Figure 4.46.

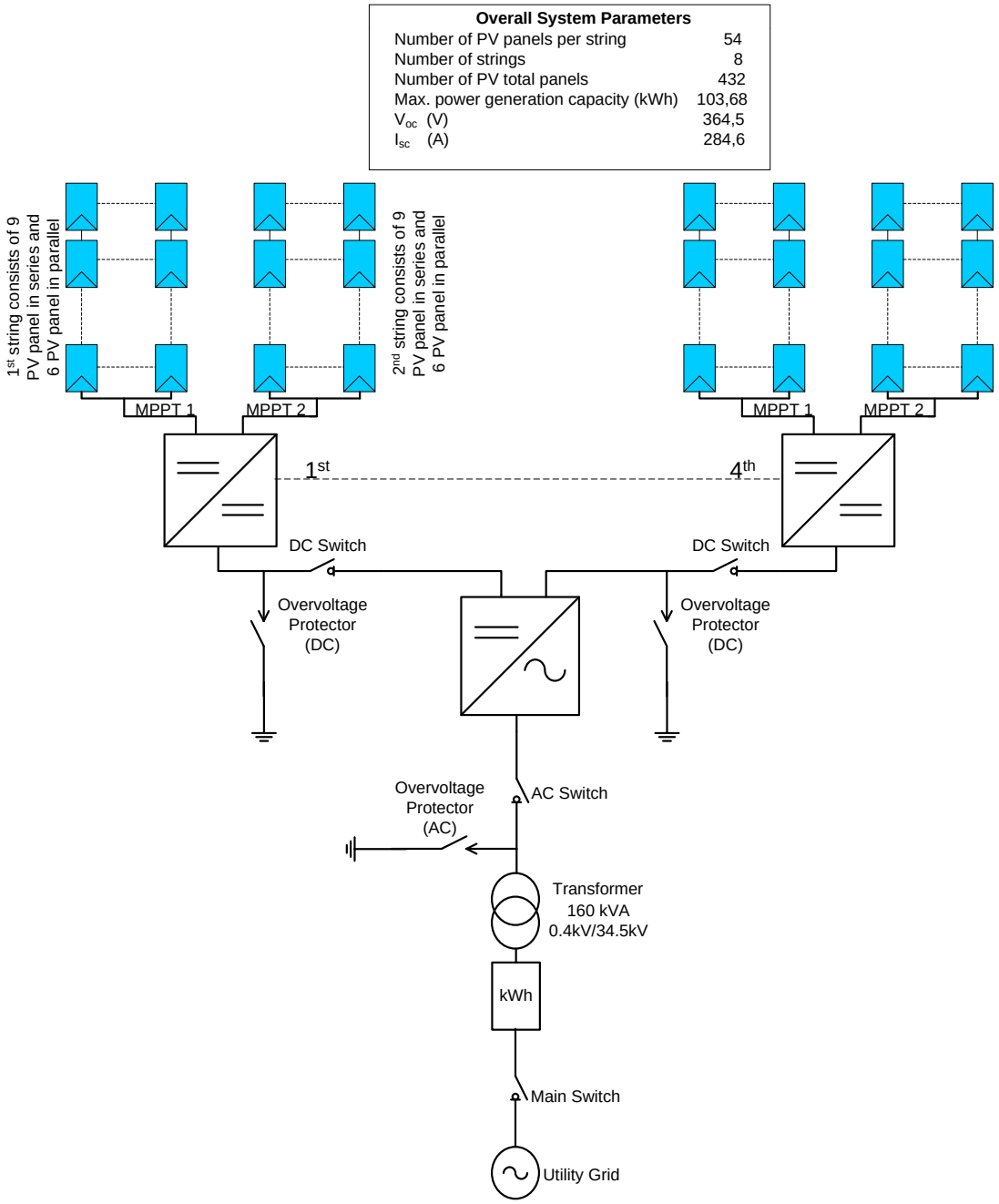

Figure 4.46. The circuit diagram of the modeled PV system

5. CASE STUDIES AND SIMULATION RESULTS

5.1. Test System

In this section, all the simulations for the whole system, most commonly used conventional MPPT techniques, proposed ANN and ANN based hybrid MPPT techniques are demonstrated and investigated. The simulation of the system is realized with predefined PSCAD blocks and FORTRAN coding based user defined blocks. To simulate the whole system, the modeled PV arrays are subjected to 1000W/m^2, 800W/m^2, 600W/m^2 and 700W/m^2 of solar irradiance, respectively. A signal generator is presented as an irradiance source. With the help of this signal source, the value of irradiance is instantaneously changed and performances of the MPPT techniques are easily specified.

The each test PV string consists of 9 modules in series and 6 modules in parallel. Different levels of insolation and temperature are applied to panels and the strings are allocated into several parts which receives different insolation level for creating different partial shading conditions. The goal of the simulation study is to verify the dynamic and steady state response of the conventional and proposed MPPT techniques under rapidly changed irradiance level and partially shading conditions. The modeled system has been tested with different conventional and proposed MPPT techniques and without MPPT controller under different atmospheric conditions. System test parameters are listed in Tables 5.1 - 5.3.

Table 5.1. PSCAD/EMTDC simulation parameters

PSCAD/EMTDC Parameters	
Solution time step	20 μs
Channel plot step	100 μs
Duration of simulation run	15 s

Table 5.2. System parameters

System Parameters	
Voltage source (V_{mpp})	330V-370V
Fundamental frequency	50 Hz
Impedance of feeder	R=0.134 Ω, X=1.067mH (for 1km)
Linear load	P=100kW Q=10kVAR
DC link voltage	700V
DC link capacitor	40 mF
Switching frequency	Converter 20 kHz---Inverter 2.5 kHz
L filter	L_i=2.2 mH
L boost	L_b=2.5 mH
C boost	C_{in}=1mF

Table 5.3. Control system parameters

DC Link PI Controller Parameters	
Proportional gain	0.5
Integral time constant	1.2 s
Reactive Power PI Controller Parameters	
Proportional gain	0.2
Integral time constant	0.1 s
Converter PI Controller Parameters	
Proportional gain	1.2
Integral time constant	0.5 s

The power circuit diagram of grid connected two stage PV system on PSCAD/EMTDC employed in this thesis is shown in Figure 5.1.

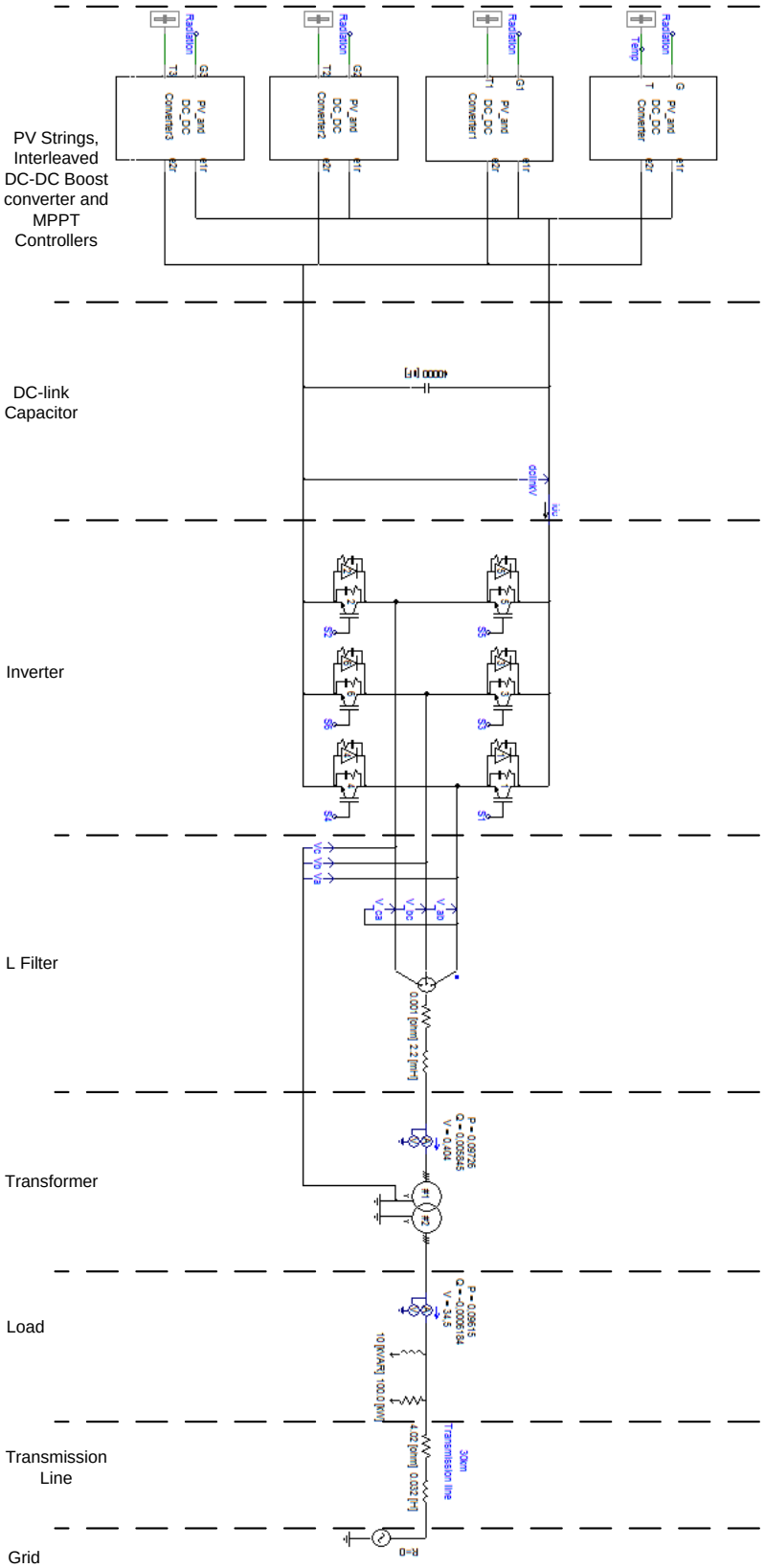

Figure 5.1. PSCAD/EMTDC model of grid connected two stage PV system

5.2. Photovoltaic System without MPPT

The simulation is run at t=0s to 15s. The output power of the one PV string varies from 13kW to 7.5kW due to the change of irradiance. First the system is operated at certain reference voltage (V_{ref}), which achieves the maximum output power at STC (25°C and 1000W/m^2) and then the atmospheric conditions (temperature and irradiance) are changed with the help of signal generator. Figure 5.2 provides that the power output after the conditions have changed is not the maximum power as the PV array voltage remains at certain value of voltage. This value is not the voltage required to achieve the maximum power in that case.

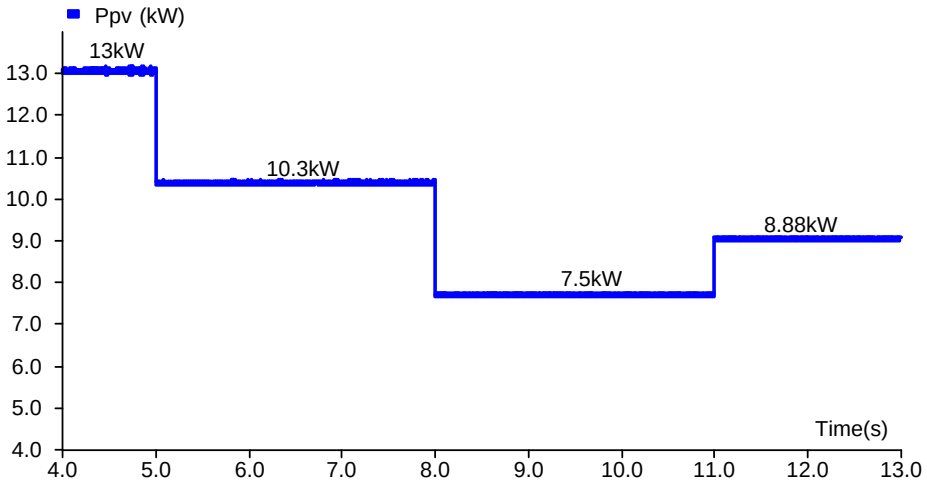

Figure 5.2. The output power of the PV array without MPPT

It is clear that when atmospheric conditions change, the reference voltage of the DC-DC converter should also be changed to compensate the difference in the voltage and to track the MPP. Although major changes are performed in radiation, Figure 5.3 shows that the V_{MPP} remains constant. Hence, maximum power cannot be extracted from the PV panels.

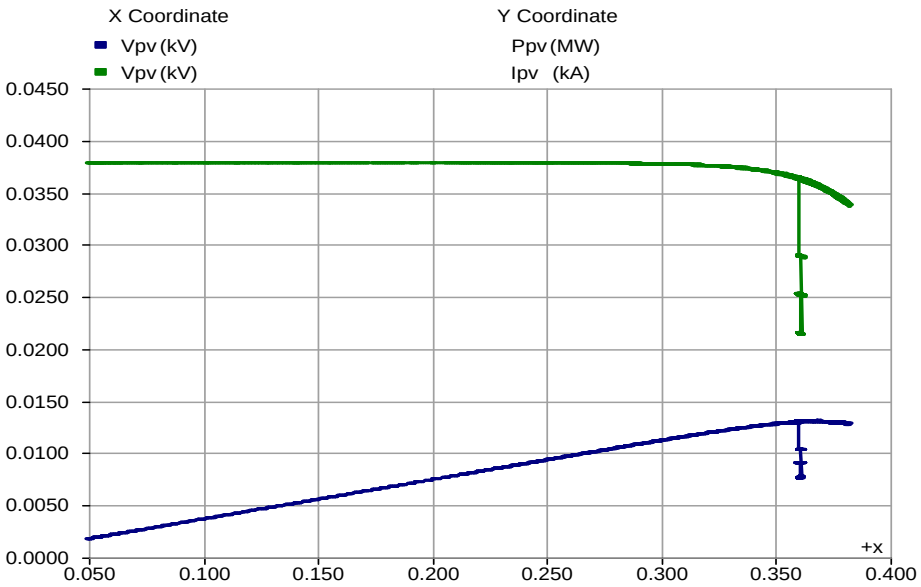

Figure 5.3. I/V and P/V characteristic of PV string with INC MPPT technique

The DC link voltage is almost kept constant at 700V with the help of DC link voltage controller as illustrated in Figure 5.4.

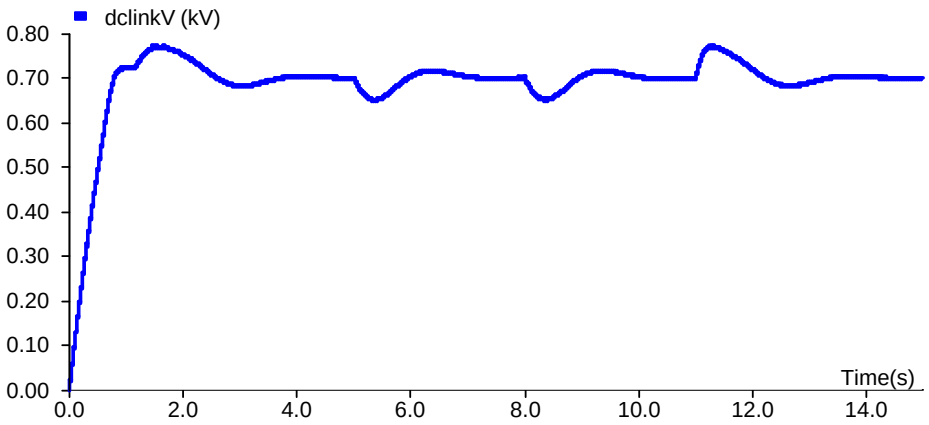

Figure 5.4. The DC link voltage of the system under variable atmospheric conditions

The injected reactive and active power to the grid is demonstrated in Figure 5.5 and Figure 5.6, respectively. As seen in Figure 5.5, the amount of injected reactive power is successfully controlled by the controller of the inverter and the system is operated at unity power factor.

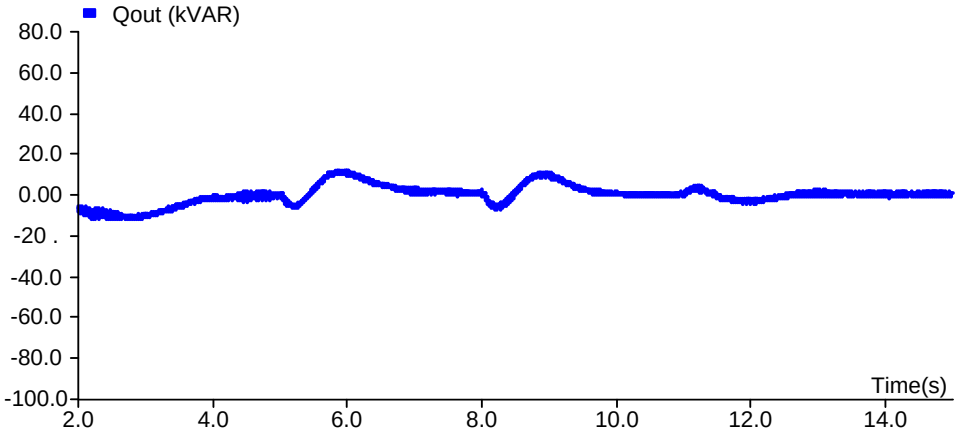

Figure 5.5. Reactive power output of the system without MPPT

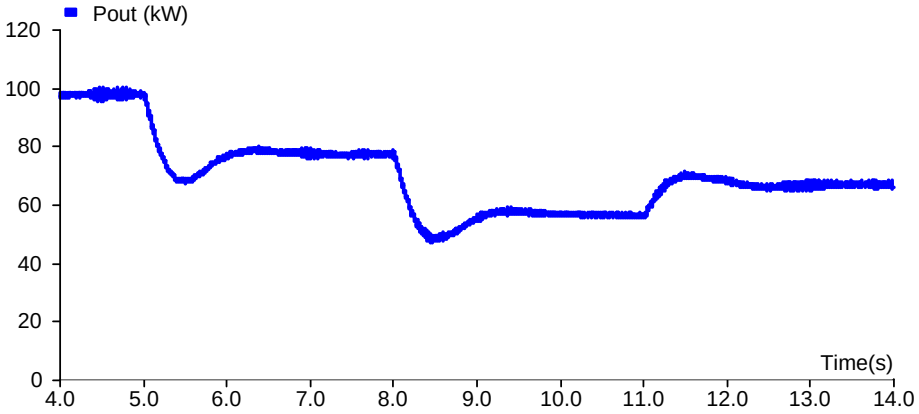

Figure 5.6. Active power output of the system without MPPT

To show the system is operating at unity power factor, output voltage and current of the inverter is overlapped in Figure 5.7.

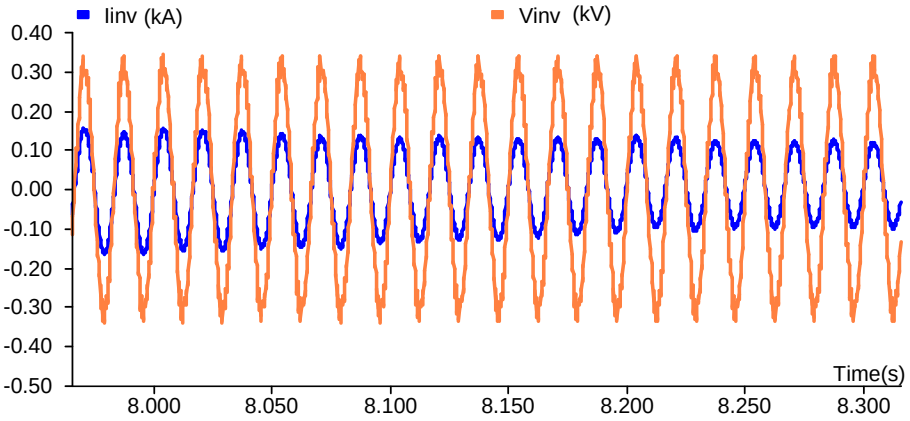

Figure 5.7. Inverter operation at unity power factor

THD value of the injected current is decreased below 5% with the help of L filter as shown in Figure 5.8.

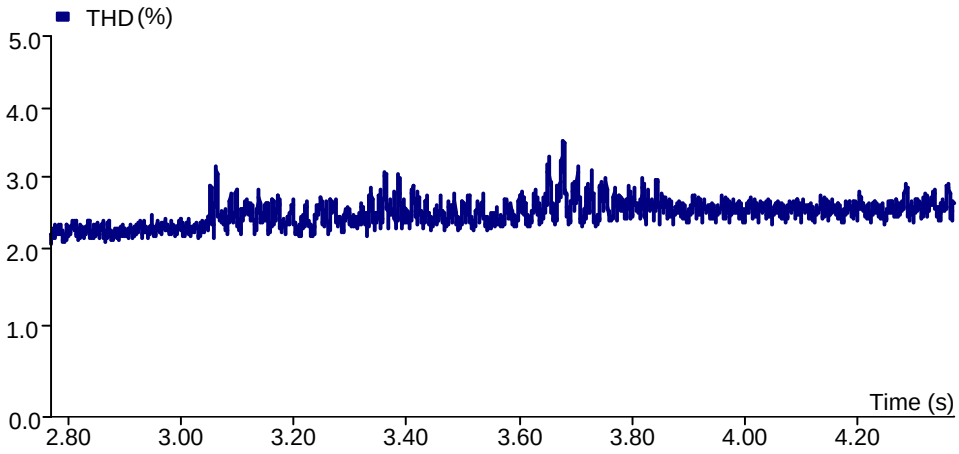

Figure 5.8. THD value of the injected grid current

The fluctuation of the inverter output current with the change of the irradiance is showed in Figure 5.9 (a) and (b).

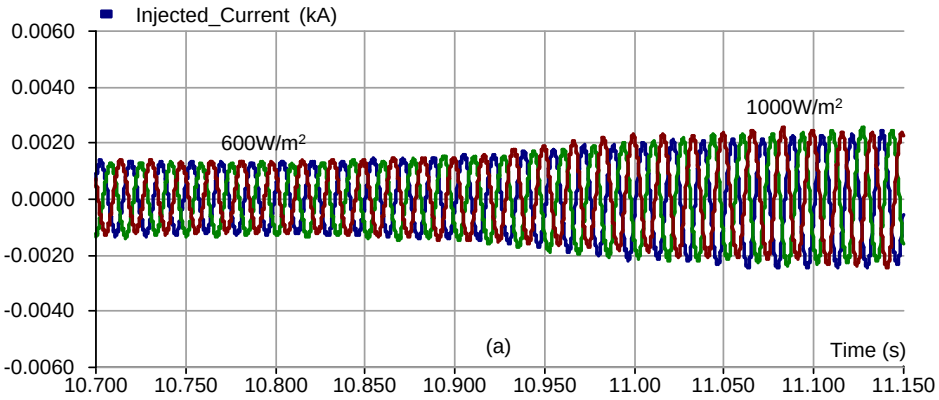

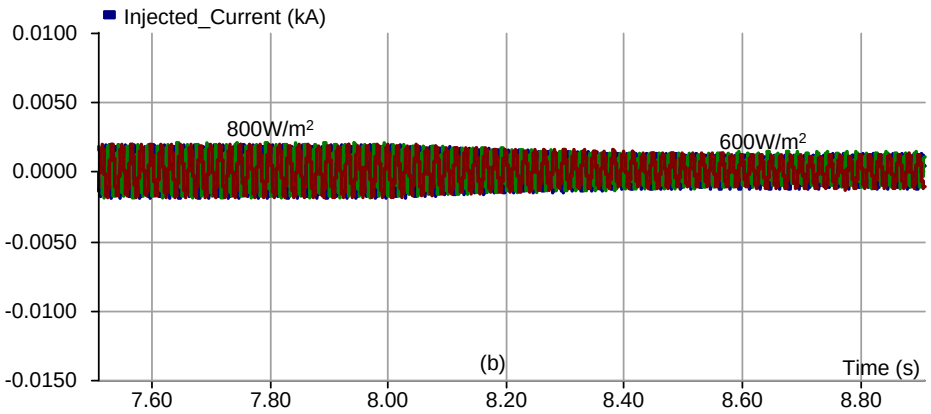

Figure 5.9. The fluctuation of the inverter output current with the irradiance change (a) from 600W/m^2 to 1000W/m^2 (b) 800W/m^2 to 600 W/m^2

Grid synchronization is provided by using output of the reactive power and DC-link voltage controller, which employed as modulation index and phase angle directly in firing pulse generation block. To demonstrate the grid synchronization output voltage of the inverter and the grid voltage is overlapped in Figure 5.10.

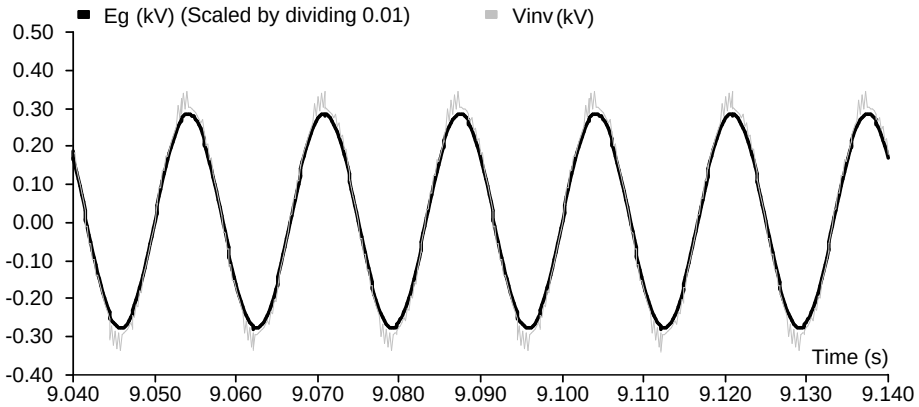

Figure 5.10. Grid synchronization of the system

5.3. Photovoltaic System with Perturb and Observation Technique

The simulation is run at t=0s to 15s. The output power of the PV string varies from 13.08kW to 7.6kW as a result of the variation of the irradiance. The system is operated at reference voltage (V_{ref}), which is obtained from the P&O algorithm to achieve the maximum output power. Figure 5.11 provides power output after the conditions have changed. When the irradiance value is suddenly increased, an instant

fluctuation occurs in output power. The main reason of this situation can be explained as this MPPT technique lacks of specifying the accurate perturbation side of the MPPT voltage when a sudden change occurs in irradiance. It remains under the generated MPPT voltage, cannot quickly restore itself and also suffers from high oscillations.

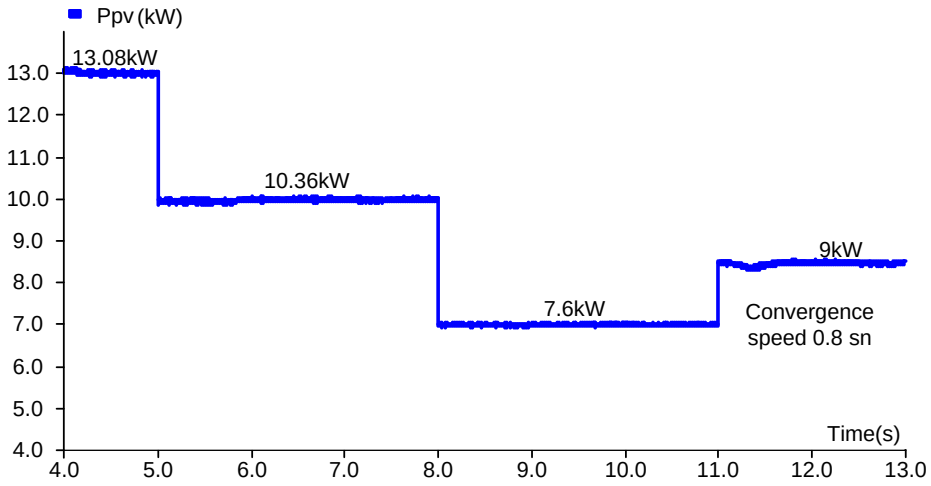

Figure 5.11. The output power of the PV array with P&O MPPT technique

The effect of rapidly changed irradiance on the I/V and P/V characteristics of PV array is demonstrated in Figure 5.12. V_{MPP} is changed with the variation of the irradiation by the P&O algorithm. P&O MPPT technique works well under constant irradiance but has more difficulty under rapid irradiance change as it needs more time to track the V_{MPP} of new irradiance.

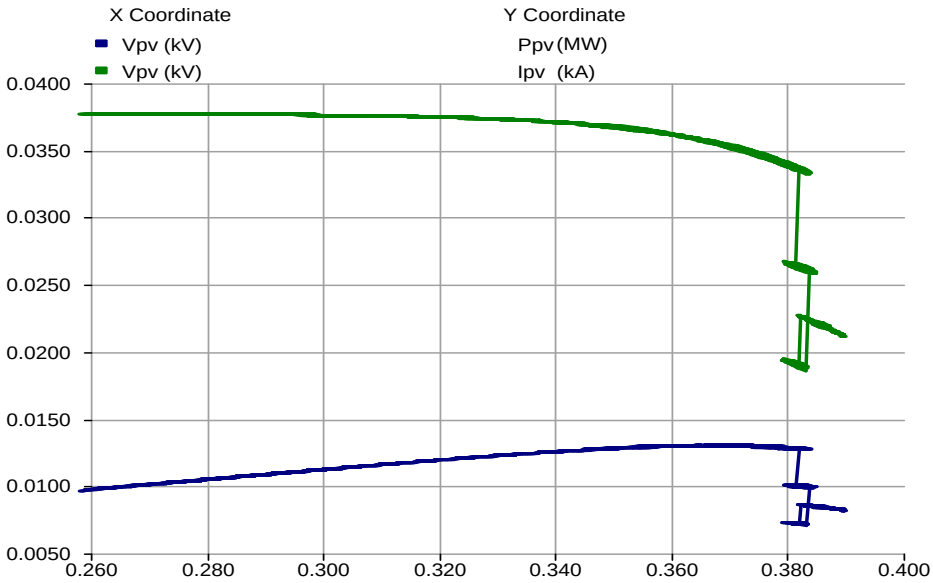

Figure 5.12. I/V and P/V characteristic of PV string with P&O MPPT technique

The DC link voltage is kept constant at 700V as illustrated in Figure 5.13.

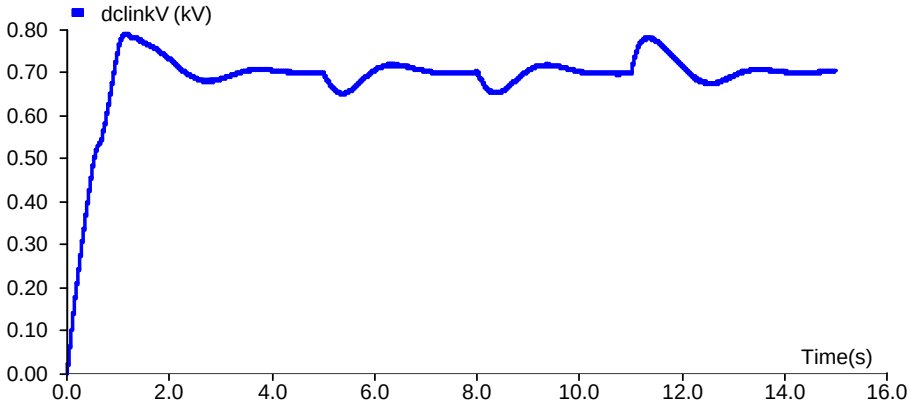

Figure 5.13. The DC link voltage of the system under variable atmospheric conditions

The injected reactive and active power to the grid is demonstrated in Figure 5.14 and Figure 5.15, respectively. As seen in Figure 5.14, the amount of injected reactive power is successfully controlled by the controller. It almost forces the system to move reactive power injection to a value near zero.

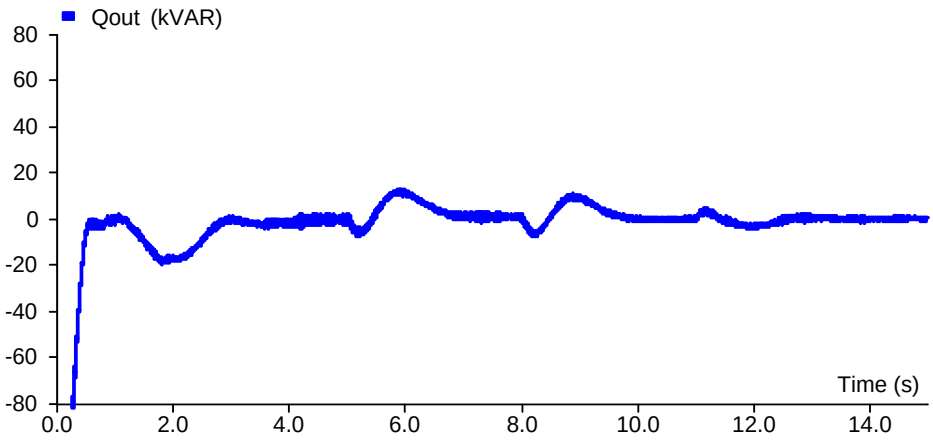

Figure 5.14. Reactive power output of the system with P&O MPPT technique

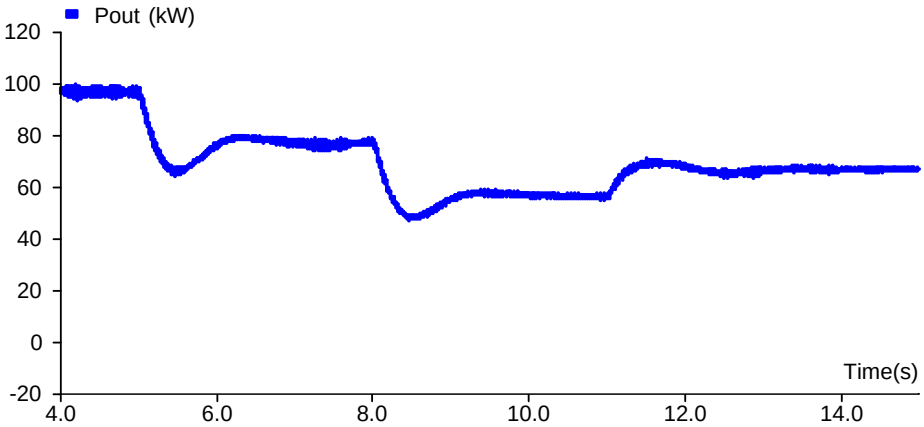

Figure 5.15. Active power output of the system with P&O MPPT technique

To prove the system is operating at unity power factor, output voltage and current of the inverter is overlapped as shown in Figure 5.16.

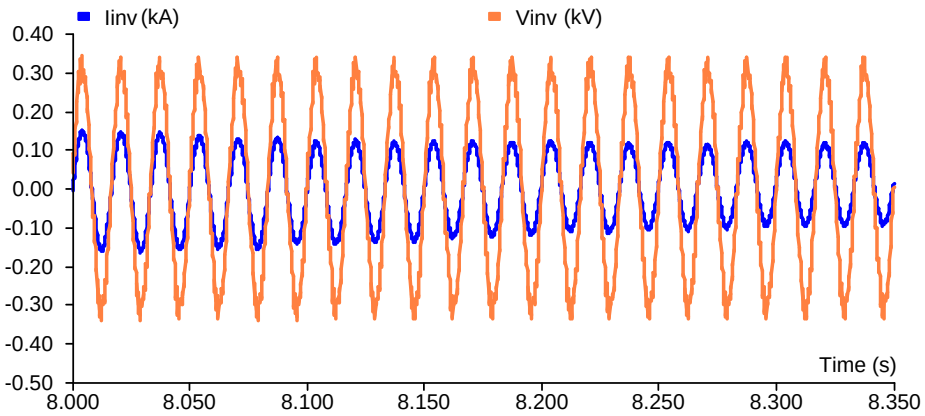

Figure 5.16. Inverter operation at unity power factor

THD value of the injected current is decreased below 5% by usage of L filter as shown in Figure 5.17.

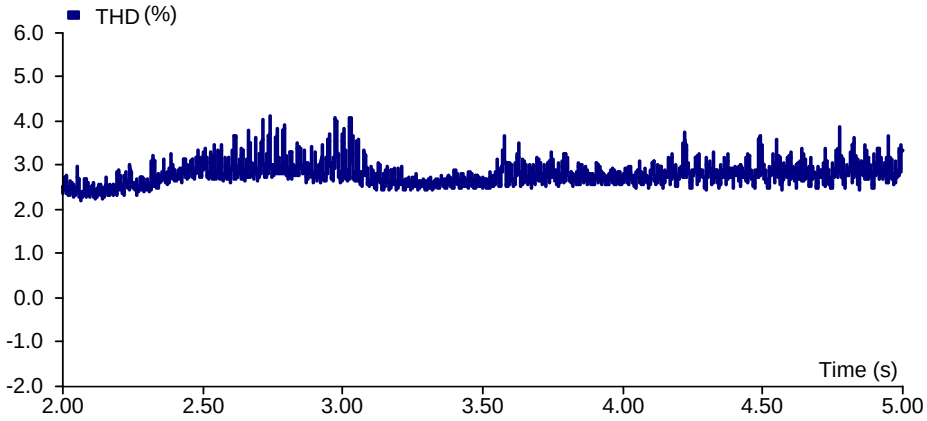

Figure 5.17. THD value of the injected grid current with P&O MPPT technique

The fluctuation of the inverter output current with the change of the irradiance is showed in Figure 5.18 (a) and (b).

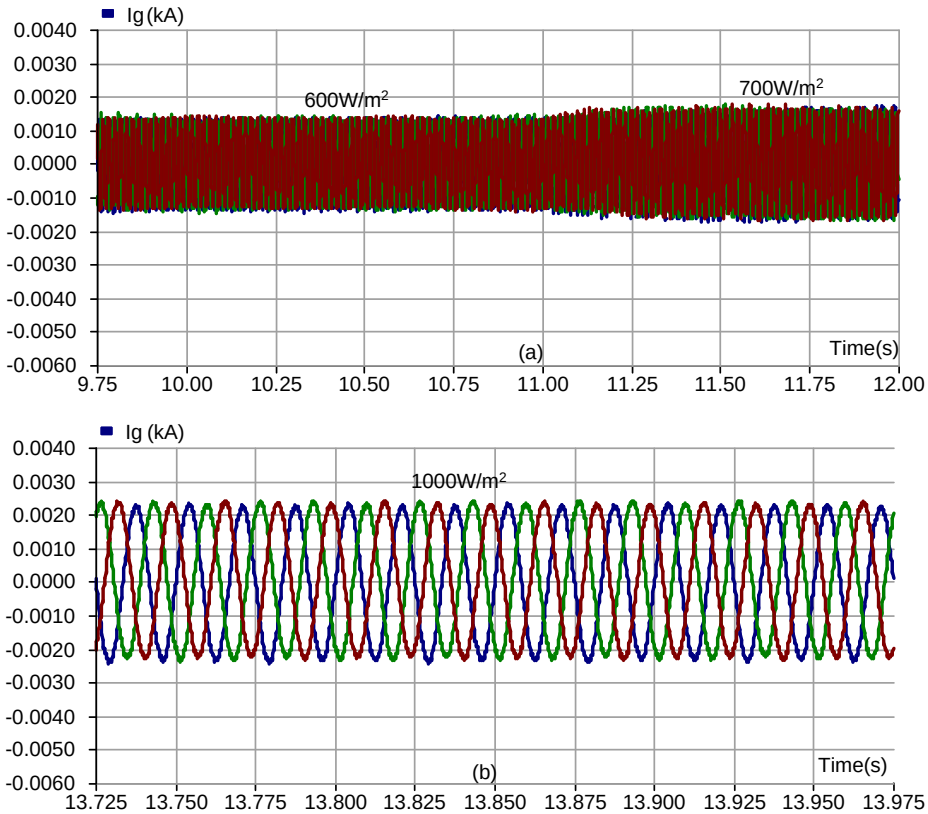

Figure 5.18. The fluctuation of the inverter output current with the irradiance change (a) from 600W/m^2 to 700W/m^2 (b) 1000 W/m^2

To demonstrate the grid synchronization output voltage of the inverter and the grid voltage is overlapped in Figure 5.19.

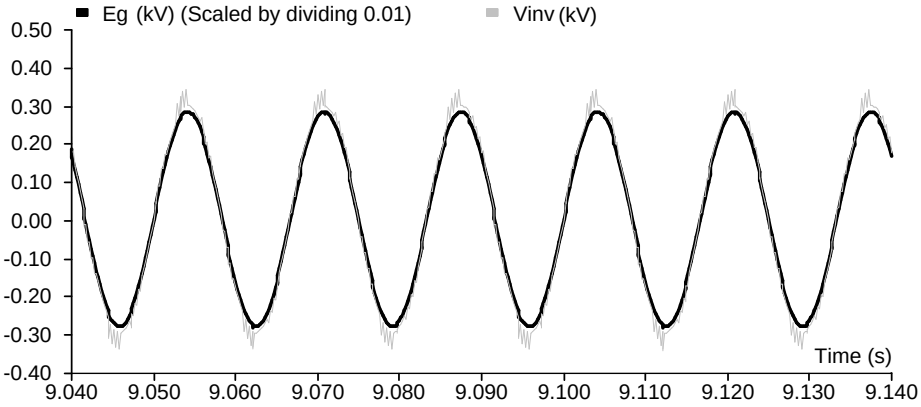

Figure 5.19. Grid synchronization of the system with P&O MPPT technique

5.4. Photovoltaic System with Incremental Conductance Technique

For the same conditions, the system is operated again with the INC algorithm. The output power of the PV string varies from 13.1kW to 7.65kW because of the change of the irradiance. The system is operated at reference voltage (V_{ref}), which is specified by the INC algorithm to generate convenient switching signal and achieve the maximum output power. Figure 5.20 shows the output power after the atmospheric conditions have changed. INC algorithm yields much more energy beside the P&O algorithm. With reference voltage perturbation related to $\frac{dP}{dV}$, faster recovery and accurate perturbation side of the V_{MPP} is achieved. In addition, INC MPPT technique is less confused by noise, system dynamics and change in atmospheric conditions compared to the P&O MPPT technique. Moreover, INC method far more superior compared to P&O method in terms of tracking speed and tracking direction accuracy.

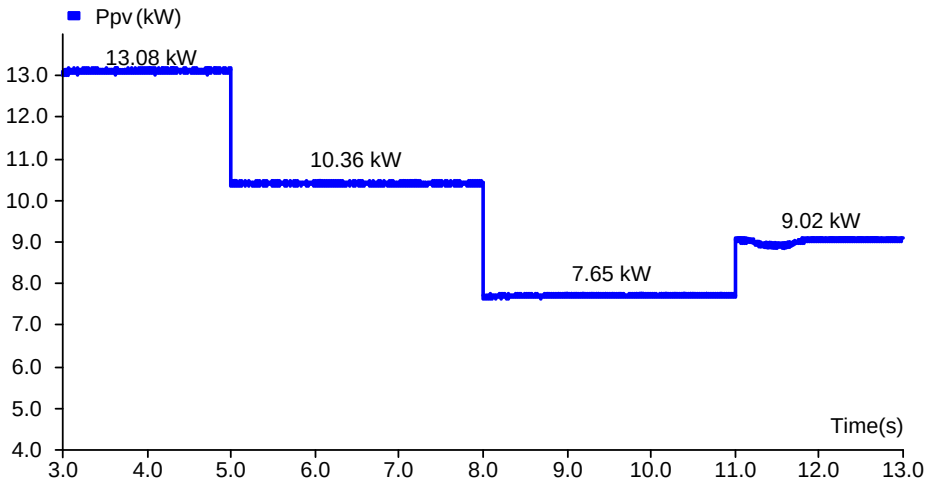

Figure 5.20. The output power of the PV array with INC MPPT technique

The effect of rapidly changed irradiance on the I/V and P/V characteristics of PV array is demonstrated in Figure 5.21. V_{MPPT} is changed with the variation of the irradiation by the INC algorithm. INC MPPT technique works well under both constant and variable irradiance compared to P&O MPPT technique.

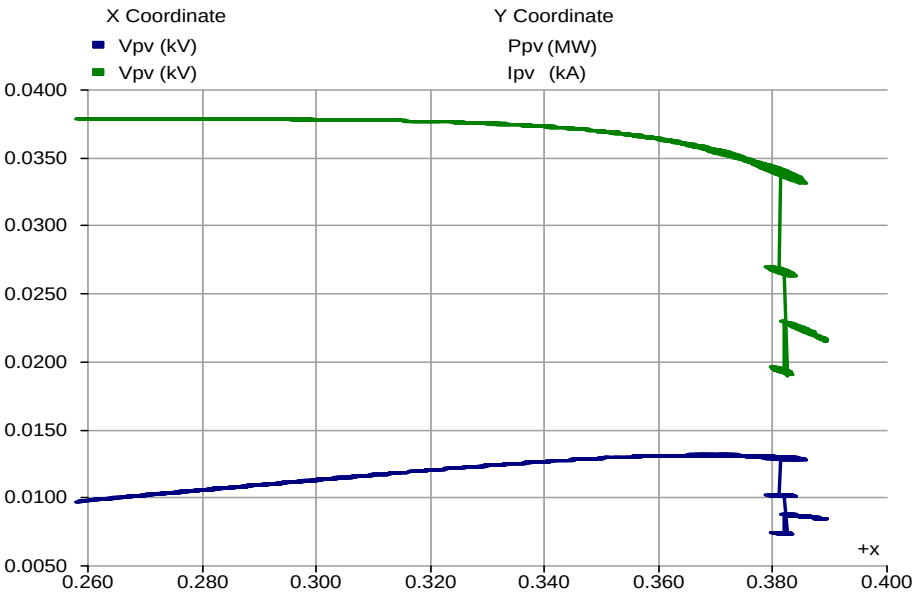

Figure 5.21. I/V and P/V characteristic of PV string with INC MPPT technique

Despite the radiation changes, the DC link voltage is almost kept at 700V as demonstrated in Figure 5.22.

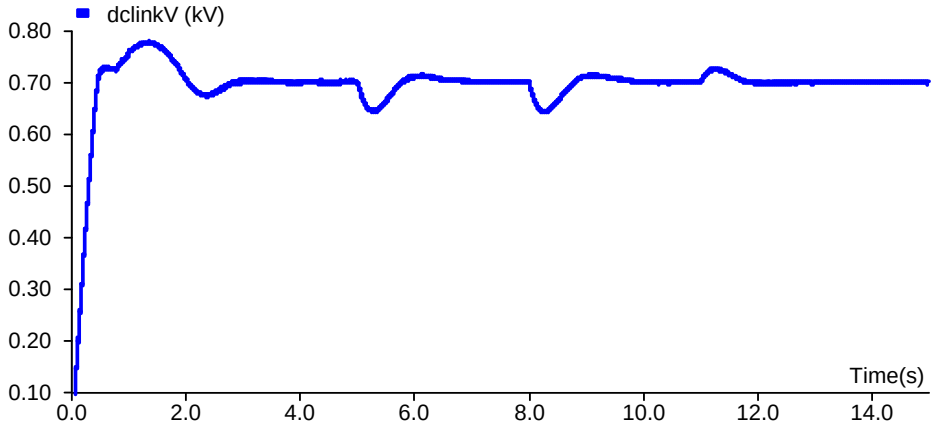

Figure 5.22. The DC link voltage of the system under variable atmospheric conditions

The injected reactive and active power to the grid is illustrated in Figure 5.23 and Figure 5.24, respectively.

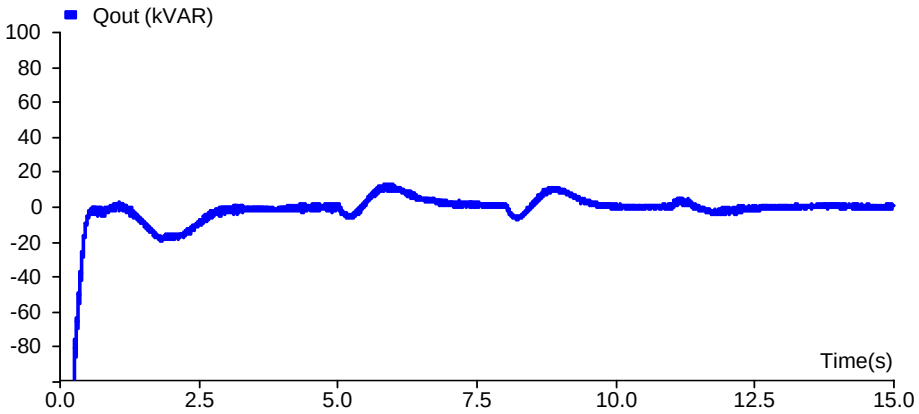

Figure 5.23. Reactive power output of the system with INC MPPT technique

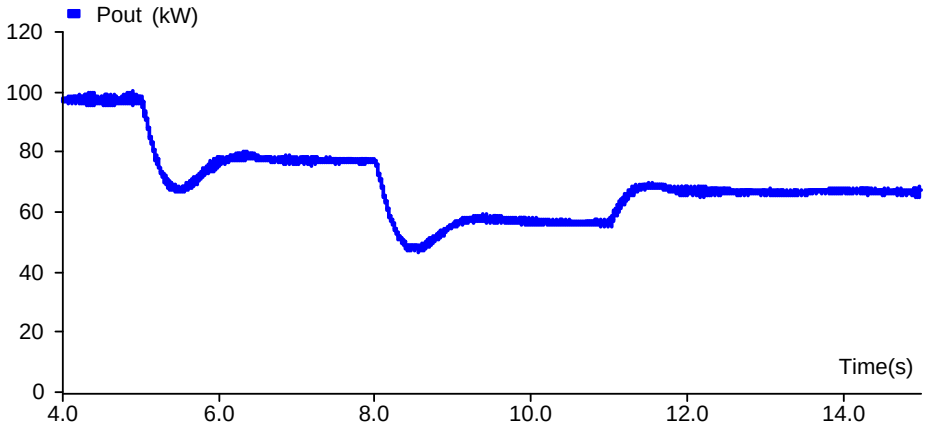

Figure 5.24. Active power output of the system with INC MPPT technique

As seen from Figure 5.25. the inverter operates at unity power factor and irradiation changes are successfully compensated by the controller.

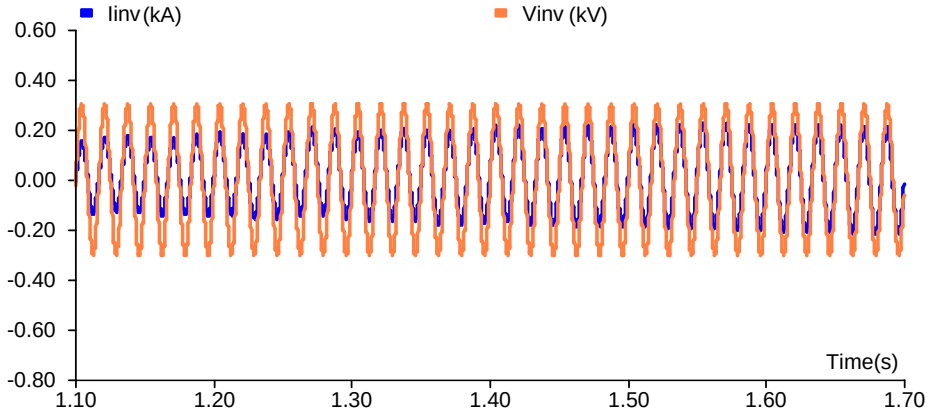

Figure 5.25. Inverter operation at unity power factor

THD value of the injected current is decreased below 5% as shown in Figure 5.26.

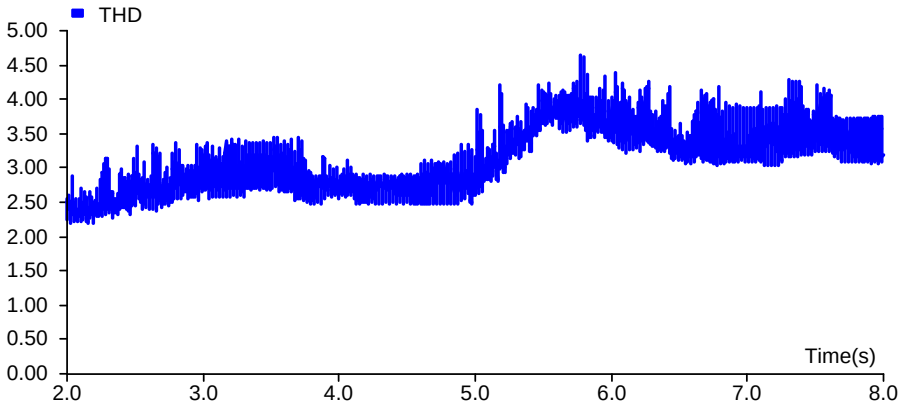

Figure 5.26. THD value of the injected grid current with INC MPPT technique

The fluctuation of the inverter output current with the change of the irradiance is showed in Figure 5.27 (a) and (b).

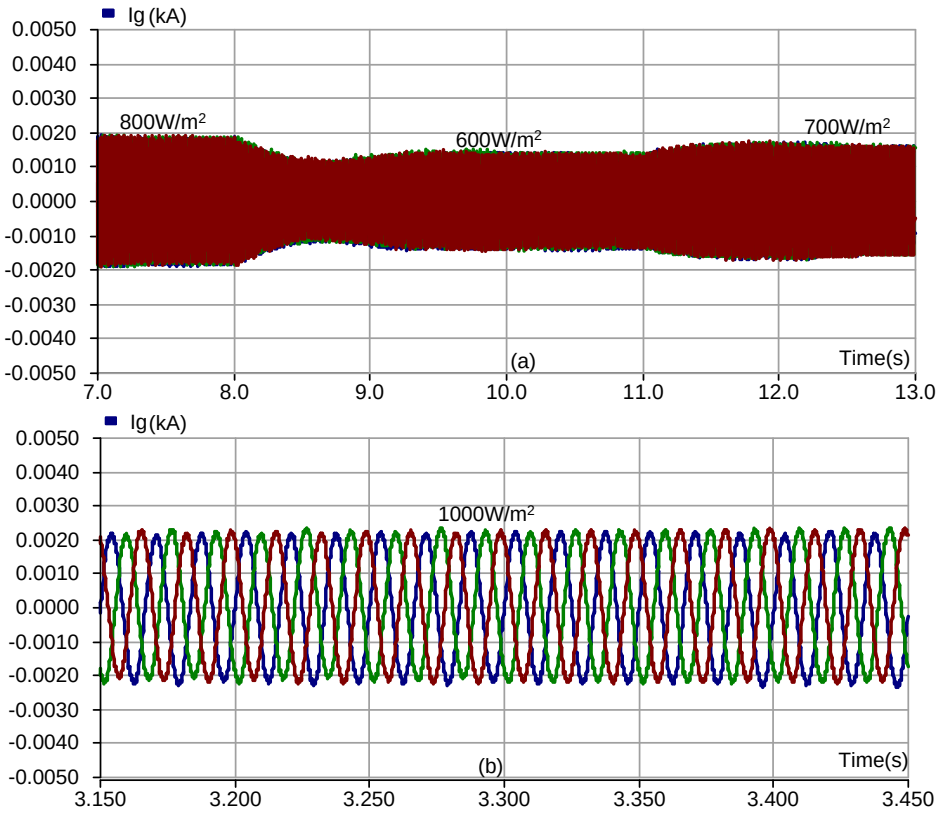

Figure 5.27. The fluctuation of the inverter output current with the irradiance change (a) from 800W/m^2 to 600W/m^2 and then 700W/m^2 (b) 1000W/m^2

Grid synchronization of the system is shown in Figure5.28.

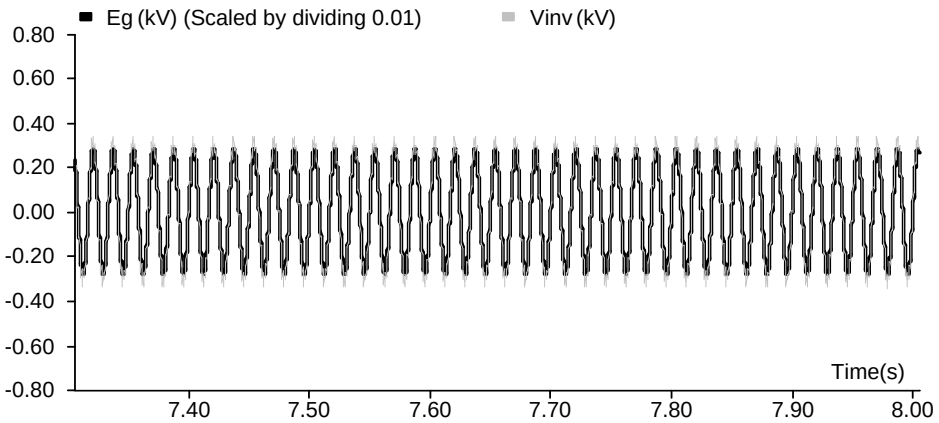

Figure 5.28. Grid synchronization of the system with INC MPPT technique

5.5. Photovoltaic System with Proposed ANN based MPPT Technique

The simulation is run at t=0s to 15s. The output power of the PV string varies from 13.1kW to 7.68kW due to the change of irradiance. The system is operated at reference voltage (V_{ref}), which is generated by the presented ANN algorithm to achieve the maximum output power. Figure 5.29 demonstrates the output power variations due to the atmospheric conditions are reduced by the proposed algorithm. In addition, deficiencies of the conventional MPPT techniques like determining correct perturbation direction when a sudden change occurs in irradiance, restoring the reference voltage, number of oscillations and convergence speed are improved. It can be concluded that the results realized by this MPPT technique are more efficient than those obtained with the conventional MPPT techniques.

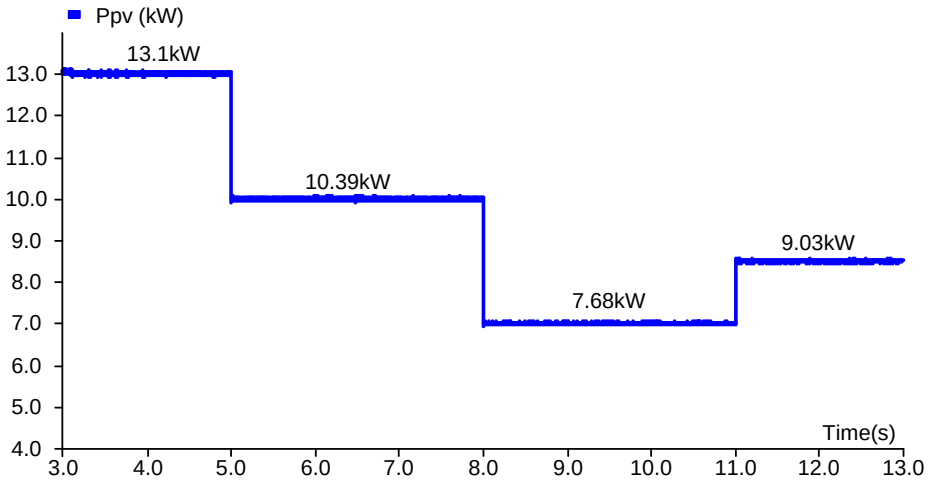

Figure 5.29. The output power of the PV array with ANN based MPPT technique

The effect of rapidly changed irradiance on the I/V and P/V characteristics of PV array is demonstrated in Figure 5.30. V_{MPPT} is changed with the variation of the irradiation by the proposed ANN algorithm. It can be clearly seen that the convergence speed and tracking accuracy is considerably improved. The presented ANN MPPT technique works well under both constant and variable irradiance compared to P&O and INC MPPT technique.

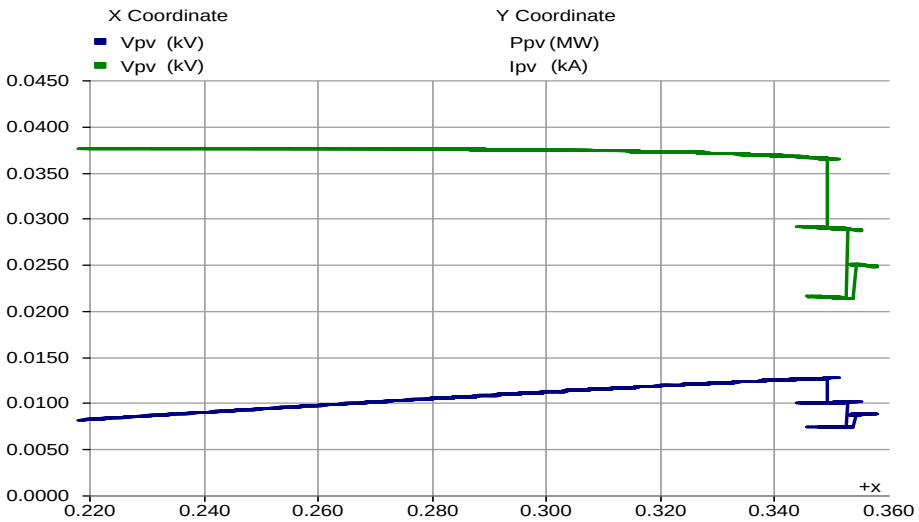

Figure 5.30. I/V and P/V characteristic of PV string with ANN based MPPT technique

The DC link voltage is kept constant at 700V as demonstrated in Figure 5.31.

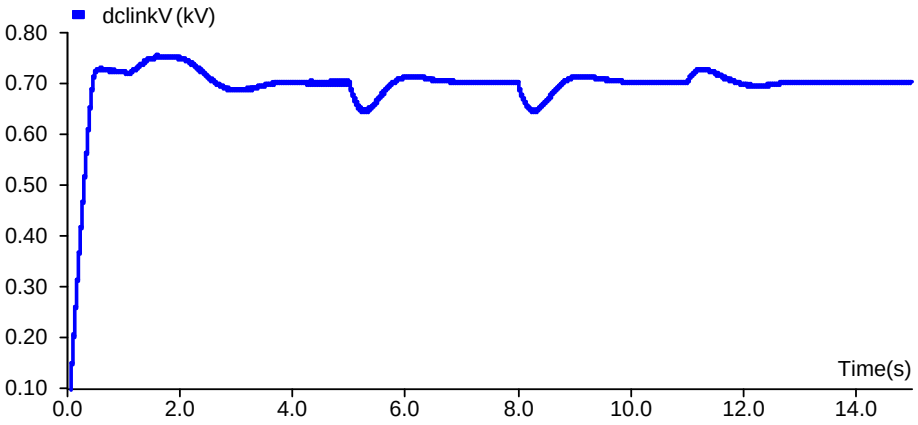

Figure 5.31. The DC link voltage of the system under variable atmospheric conditions

The injected reactive and active power to the grid is demonstrated in Figure 5.32 and Figure 5.33, respectively. As seen in Figure 5.32 the amount of injected reactive power is successfully controlled by the controller of the inverter and the system is operated at unity power factor.

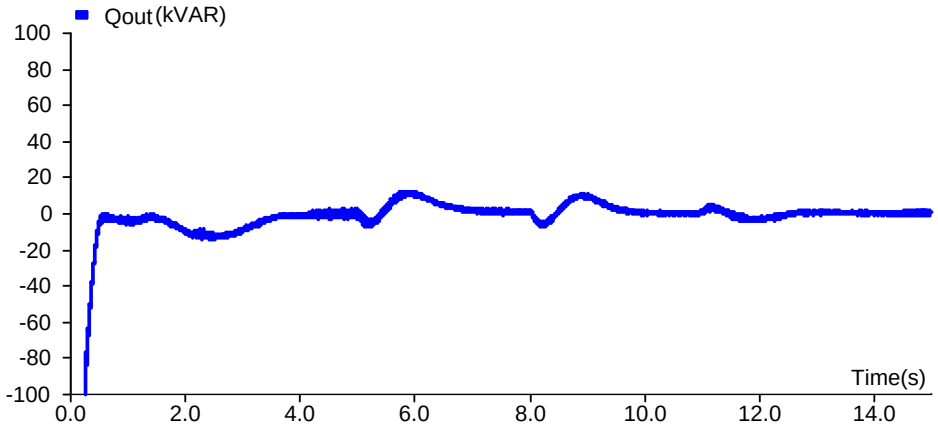

Figure 5.32. Reactive power output of the system with ANN based MPPT technique

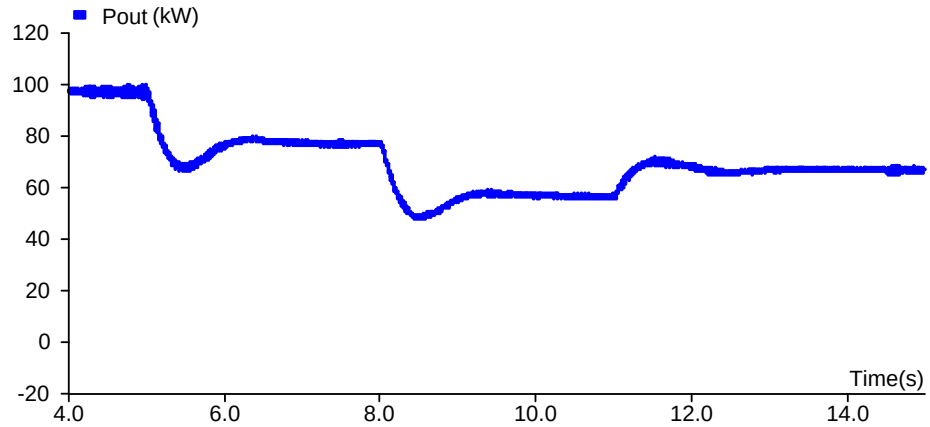

Figure 5.33. Active power output of the system with ANN based MPPT technique

To show the system is operating at unity power factor output voltage and current of the inverter is overlapped in Figure 5.34.

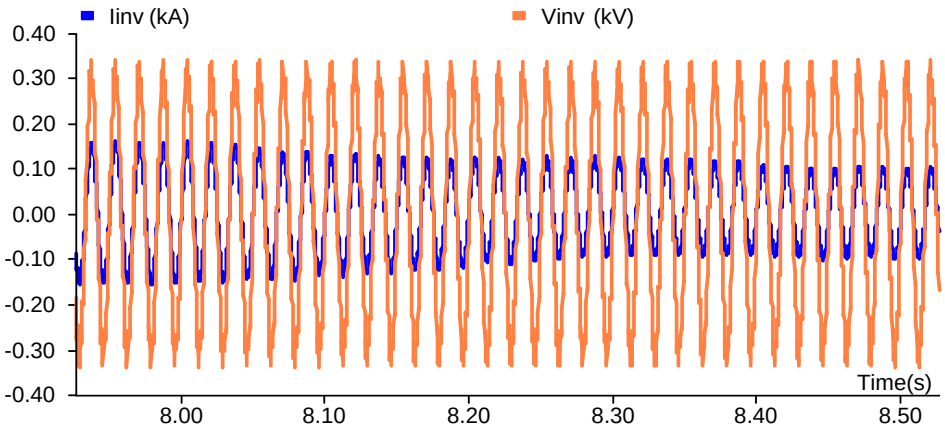

Figure 5.34. Inverter operation at unity power factor

THD value of the injected current is decreased below 5% by usage of L filter as shown in Figure 5.35

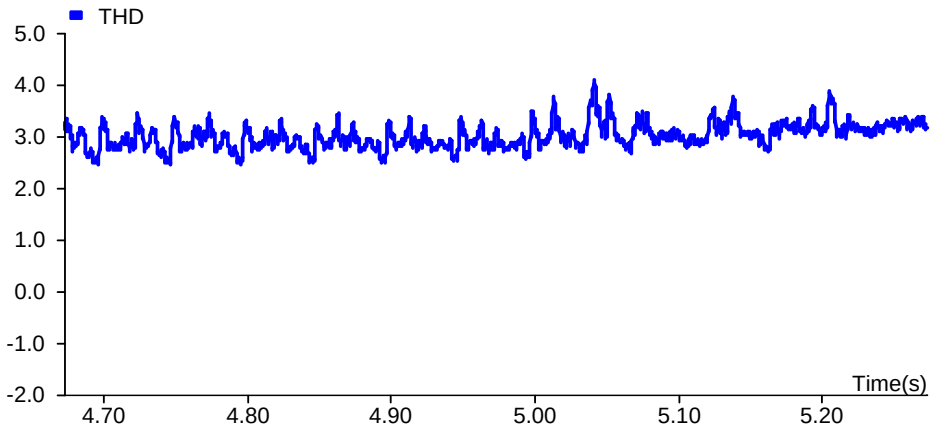

Figure 5.35. THD value of the injected grid current with the ANN MPPT technique

The fluctuation of the inverter output current with the change of the irradiance is showed in Figure 5.36 (a) and (b).

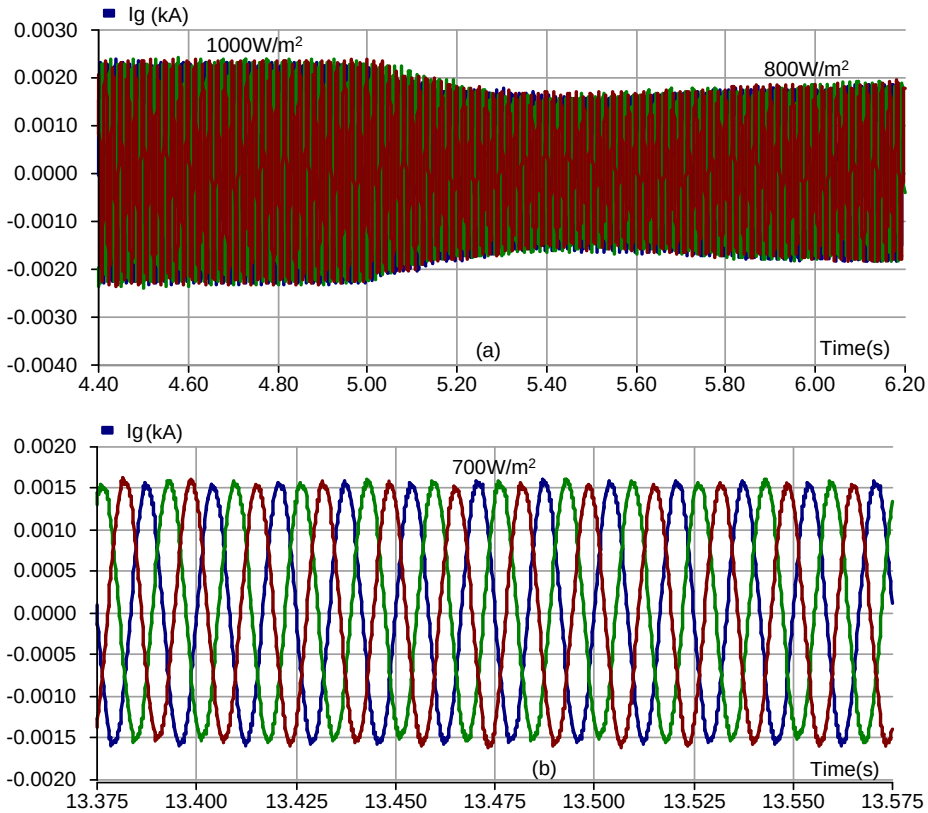

Figure 5.36. The fluctuation of the inverter output current with the irradiance change (a) from 1000W/m^2 to 800W/m^2 (b) 700W/m^2

Grid synchronization of the inverter is showed in Figure 5.37.

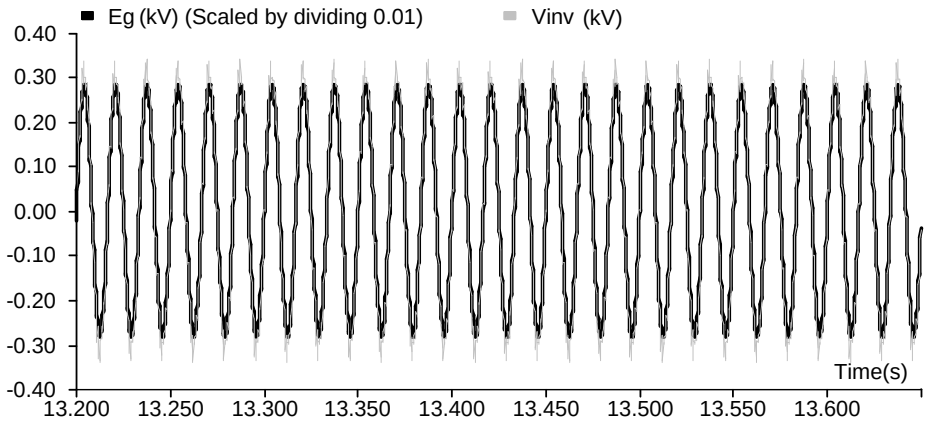

Figure 5.37. Grid synchronization of the system with the ANN MPPT technique

5.6. Photovoltaic System with Proposed Hybrid MPPT Technique

To evaluate power output and robustness of the proposed MPPT technique and compare it with other conventional MPPT techniques same signal generator is employed as an irradiance source. It can be clearly concluded that when a significant change occurs in irradiance, proposed algorithm supplies a remarkable results in terms of convergence speed and determining perturbation direction as seen in Figure 5.38.

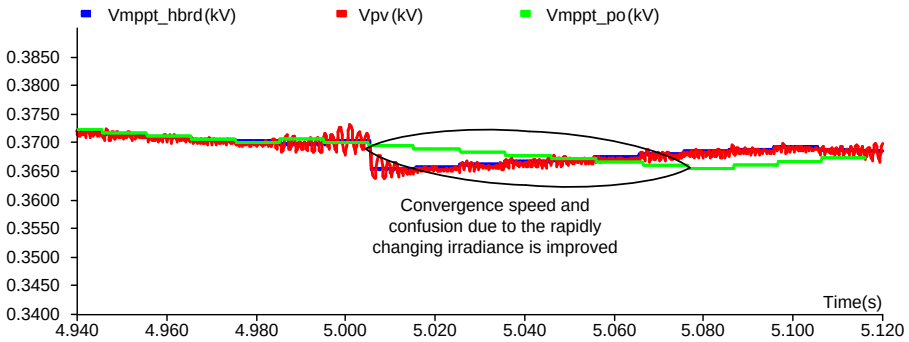

Figure 5.38. Robustness of the proposed algorithm against to sudden drop of the irradiance

When the power output of a branch is examined, it is not possible to see a considerable change compared to other conventional methods as seen in Figure 5.39.

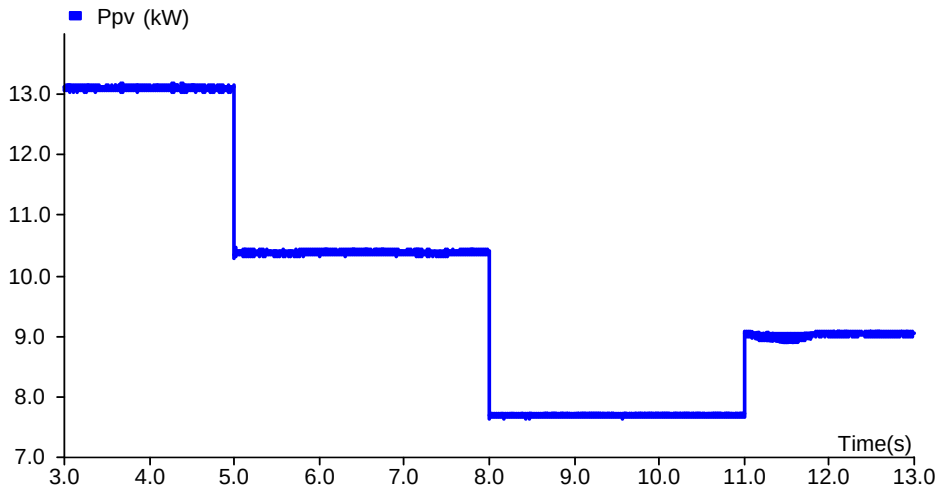

Figure 5.39. The output power of the PV array with Hybrid MPPT technique

To make a deeply evaluation and demonstrate the superiorities of proposed technique a different signal generator, which instantaneously changes the value of the irradiance is presented and used as an irradiance source. Advantages of the proposed Hybrid MPPT technique can be clearly illustrated with the help of this signal generator. The simulation is run at t=0s to 15s. Output of the generator is demonstrated in Figure 5.40.

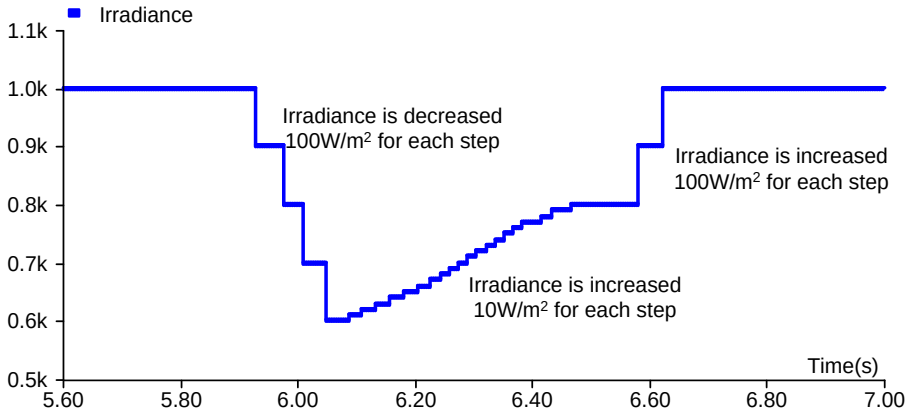

Figure 5.40. Output of the signal generator that used for testing Hybrid MPPT technique

The output power of the PV varies from 13.1kW to 7.69kW as shown in Figure 5.38 due to the change of irradiance. The system is operated at reference voltage (V_{ref}), which is obtained from the proposed Hybrid algorithm to achieve the

maximum output power. Also, Figure 5.41 demonstrates the fluctuations on the output power due to the rapidly variations of the atmospheric conditions are reduced.

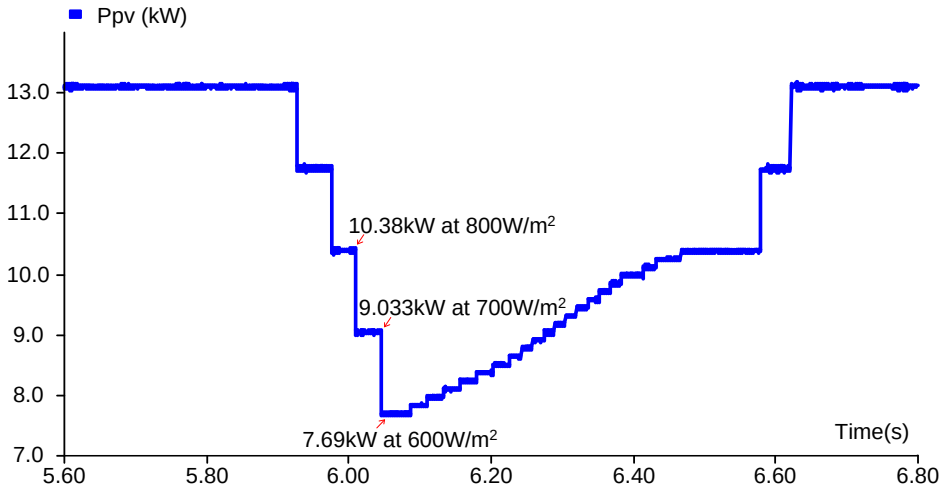

Figure 5.41. The output power of the PV array with Hybrid MPPT technique

The effect of rapidly changed irradiance on the I/V and P/V characteristics of PV array is demonstrated in Figure 5.42. V_{MPP} is successfully changed with the variation of the irradiation by the proposed Hybrid algorithm. Reference operating voltage is maintained at V_{MPP} even with modest and major changes in irradiance.

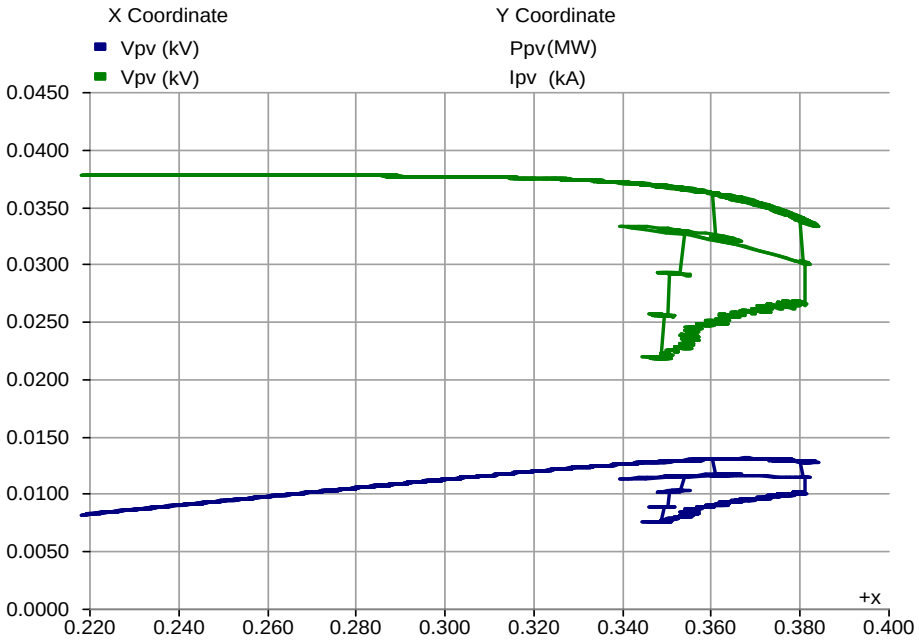

Figure 5.42. I/V and P/V characteristic of PV string with Hybrid MPPT technique

It can be clearly seen that the convergence speed and tracking accuracy is considerably improved. The presented hybrid MPPT technique works well under variable irradiance compared to P&O and INC MPPT technique. The proposed algorithm has demonstrated its robustness for variation of the irradiance even with a sudden drop of the irradiance. The reference voltage is updated instantaneously and the algorithm can immediately specify the new reference voltage value. This improves the convergence speed. In addition, deficiencies of the conventional MPPT techniques like determining correct perturbation side when a sudden change occurs in irradiance, restoring the reference voltage and numbers of oscillations are improved as shown in Figure 5.43. Consequently, the results are obviously demonstrated that P&O algorithm is improved.

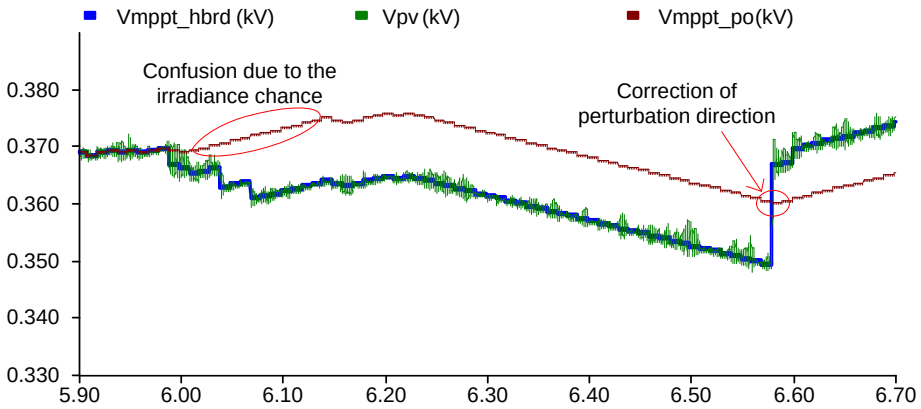

Figure 5.43. Reference voltage perturbation under rapidly changing irradiance

It can be concluded that the results realized by hybrid MPPT technique are more efficient than those obtained with the conventional MPPT techniques and ANN based MPPT technique. Also, dependency on PV panel characteristics is removed. This is the property of the ANN based MPPT technique and reduces the efficiency with aging. The modest changes in the irradiance are properly tracked by the proposed algorithm as illustrated in Figure 5.44.

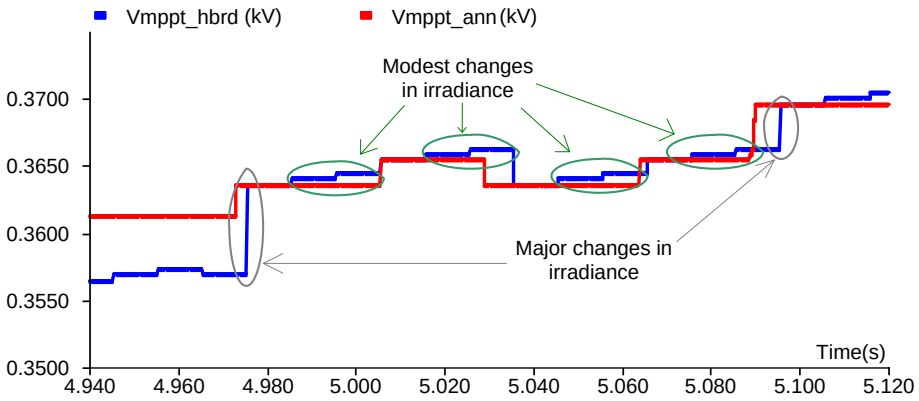

Figure 5.44. Reference voltage perturbation of ANN and Hybrid MPPT method

The DC link voltage is almost kept constant at 700V as demonstrated in Figure 5.45.

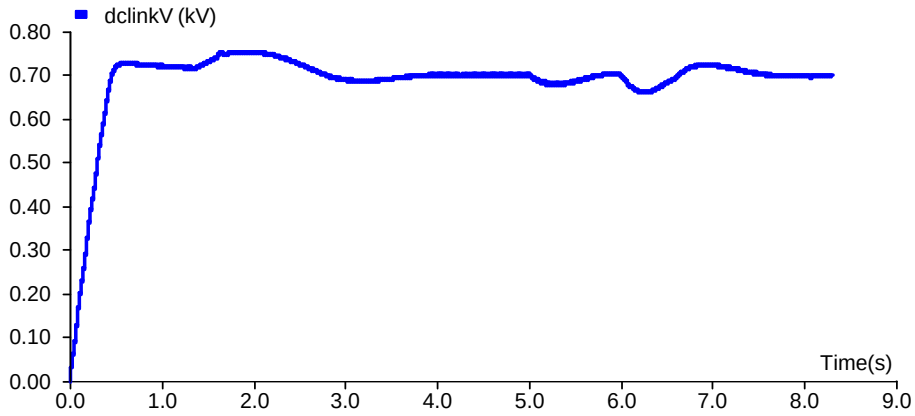

Figure 5.45. The DC link voltage of the system under variable atmospheric conditions

The injected reactive and active power to the grid is demonstrated in Figure 5.46 and Figure 5.47, respectively. As seen in Figure 5.46 the amount of injected reactive power is successfully controlled by the controller of the inverter and the system is operated at unity power factor.

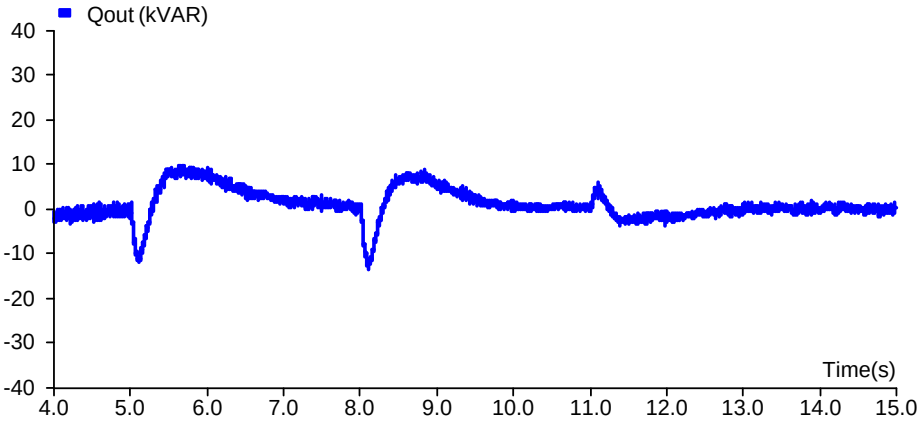

Figure 5.46. Reactive power output of the system with Hybrid MPPT technique

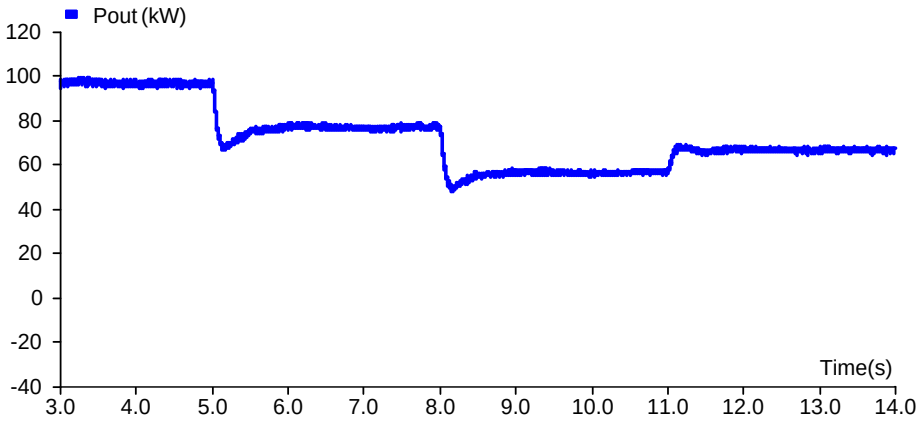

Figure 5.47. Active power output of the system with Hybrid MPPT technique

To show the system is operating at unity power factor output voltage and current of the inverter is overlapped in Figure 5.48.

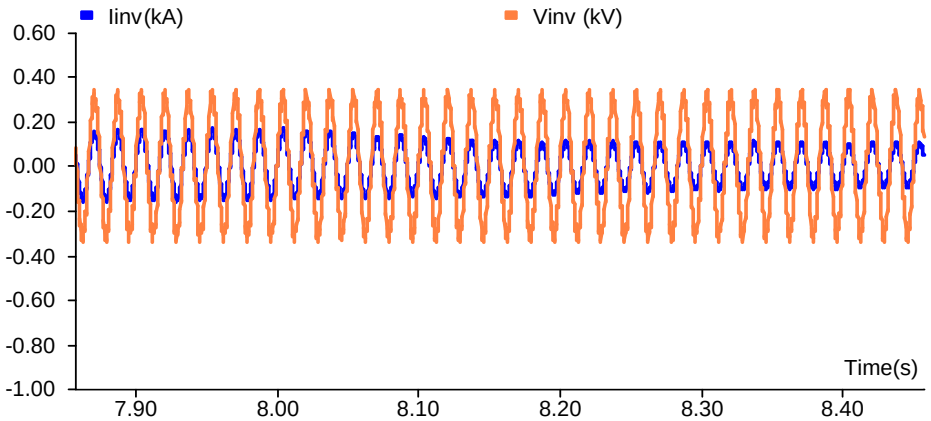

Figure 5.48. Inverter operation at unity power factor

THD value of the injected current is decreased below 5% by usage of L filter as shown in Figure 5.49

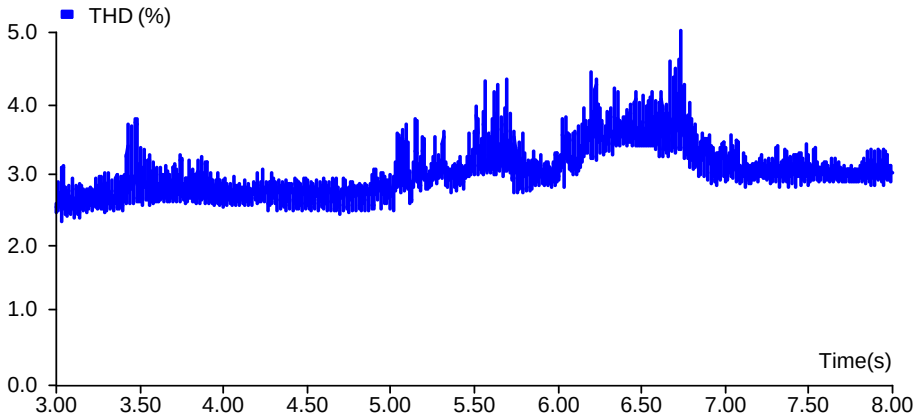

Figure 5.49. THD value of the injected grid current with Hybrid MPPT technique

The fluctuation of the inverter output current with the change of the irradiance is showed in Figure 5.50 (a) and (b).

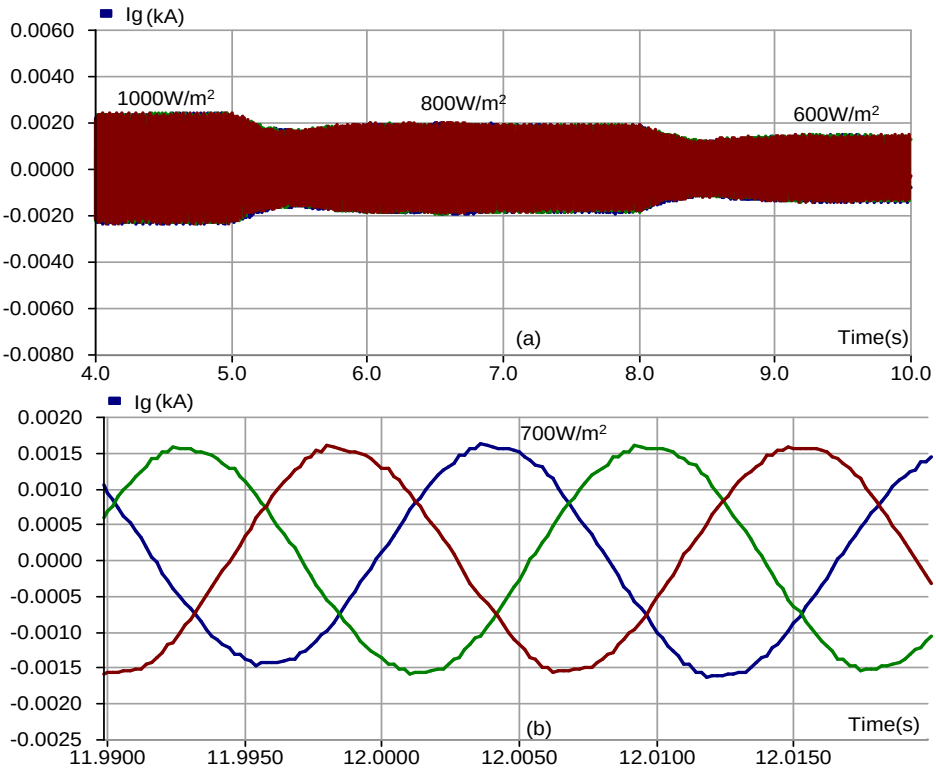

Figure 5.50. The fluctuation of the inverter output current with the irradiance change (a) from 1000W/m^2 to 800W/m^2 (b) 700W/m^2

Grid synchronization of the system is illustrated in Figure 5.51.

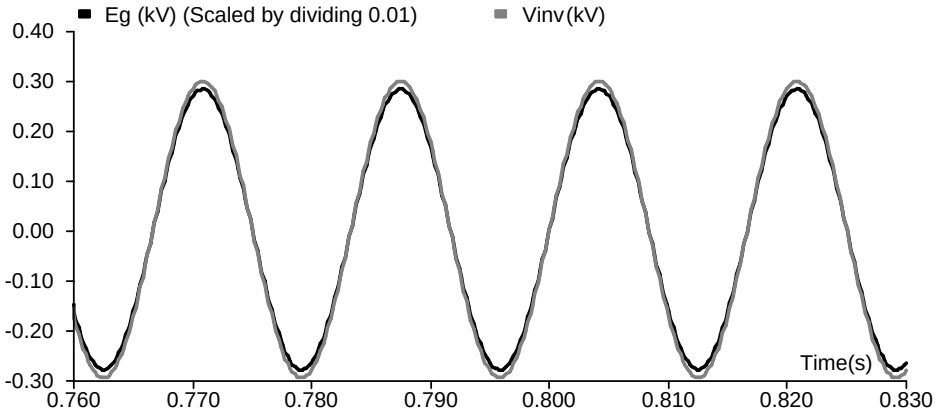

Figure 5.51. Grid synchronization of the system with Hybrid MPPT technique

5.7. Proposed MPPT Techniques vs. Conventional MPPT Techniques

The power rating of our system indicates that the generation capacity of the installed system. It does not demonstrate the produced energy output. In brief to evaluate the all components of the system especially controllers we need to know the produced amount of the electricity. The amount of energy that our systems produce highly depends on irradiance and temperature. In addition, the orientation and tilt of our installation, intensity of irradiance, sunshine duration and shadow conditions are affects the energy output of the system.

To show the robustness of the MPPT methods the modeled PV arrays are subjected to 1000W/m^2, 800W/m^2, 600W/m^2 and 700W/m^2 of solar irradiance, respectively. Daily mean sunshine duration is taken as 5.2 hour for Adana.

Calculated amount of energy production per hour according to employed MPPT techniques is given in Table 5.4.

Table 5.4. Amount of energy production according to employed MPPT techniques

MPPT Techniques	Energy Production
P&O MPPT Technique	76.21270 kWh
INC MPPT Technique	76.31548 kWh
ANN MPPT Technique	76.35690 kWh
Hybrid MPPT Technique	76.41987 kWh

Daily energy production of the system for 5.2 hour is provided in Table 5.5.

Table 5.5. Daily and monthly energy production of the system

MPPT Techniques	Energy Production (Daily)	Energy Production (Monthly)
P&O MPPT Technique	396.30604 kWh	11889.1812 kWh
INC MPPT Technique	396.84158 kWh	11905.2474 kWh
ANN MPPT Technique	397.05588 kWh	11911.6764 kWh
Hybrid MPPT Technique	397.38332 kWh	11921.4996 kWh

As seen from the tables the best results are obtained with the usage of Hybrid MPPT technique under rapidly changed uniform irradiance.

Furthermore, for analyzing the superiority of the presented MPPT techniques, one of the created PV string is partially shaded as shown in Figure 5.52.

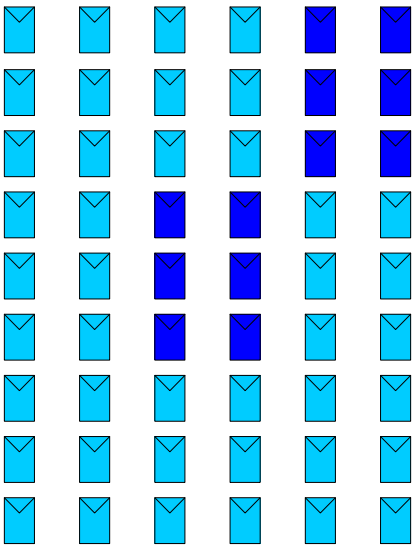

Figure 5.52. Partially shaded PV string

When the presented MPPT techniques are independently applied to the partially shaded string, amount of output energy production of the string according to employed MPPT techniques is provided in Table 5.6.

Table 5.6. Energy production of a PV string under partially shading condition

MPPT Techniques	Energy Production
P&O MPPT Technique	10,99369 kWh
INC MPPT Technique	10,92687 kWh
ANN MPPT Technique	11,00265 kWh
Hybrid MPPT Technique	11,01250 kWh

As seen from the Table 5.6 under partially shading conditions Hybrid MPPT technique supplies the better energy output than the other conventional MPPT techniques.

5.8. Summary

In this section, the developed MPPT techniques are simulated for several irradiation levels, which adjusted by a signal generator, and their superiorities compared with each other. The proposed ANN based and Hybrid MPPT techniques exhibits faster response and more accurate results than the P&O and INC MPPT techniques. Furthermore, partial shading condition is analyzed for developed MPPT techniques, and the results are compared with each other in terms of generated hourly, daily and monthly energy. In addition, the inverter control scheme is tested under various irradiance levels and it can keep the DC-link's voltage constant at desired value and able to adjust the injected reactive power near to zero.

6. CONCLUSIONS, CHALLENGES AND FUTURE WORKS

In this thesis, a rigorous model of two stage grid connected PV system is developed and then MPPT techniques are highlighted. The proposed system is based on the use of a multi string inverter, which comprises an interleaved DC-DC boost converter, a 3-phase full bridge DC-AC inverter with a L filter as the grid interface. A novel Hybrid MPPT technique and ANN based MPPT techniques are incorporated with this system. Also, the comprehensive literature research is conducted to understand and design the proposed MPPT techniques. Various simulations are performed with PSCAD/EMTDC 4.2.1 simulation software. Based on the obtained results, the proposed algorithms operates effectively compared to mostly used conventional MPPT algorithms even in cases of rapidly changing atmospheric conditions and partial shading conditions. The deficiencies of the conventional MPPT techniques are defined and the main components and operation principle of entire of the grid-tied PV system particularly MPPT techniques are explained in Chapters 1 to 3. In Chapter 4, the design of the proposed MPPT techniques and is clarified in detail. The performance and efficiency of the proposed system are tested with different simulation cases by PSCAD/EMTDC program in Chapter 5.

The main findings of the thesis are outlined in below.

- The simulation results of the modeled PV panels shows that the simulated models are accurate to determine the I/V when compared with the characteristics given from the data sheet.
- The simulations of the modeled PV panels demonstrate that the models used in this thesis are adequate to test the MPPT algorithm and to show effect of partial shading conditions.
- P&O algorithm has some drawbacks such as it cannot track the MPPT voltage when a sudden change occurs in irradiance. It remains under the generated MPPT voltage, cannot quickly restore itself and also suffers from high oscillations.

- The INC technique suffers also from a relatively slow dynamic response time due to the complex computations to calculate the instantaneous and incremental changes and then compare them to each other.
- An ANN based MPPT technique and Hybrid MPPT technique is proposed, which predicts the appropriate reference voltage for generating control signal of DC-DC converter and removes the disabilities of conventional MPPT techniques.
- Proposed MPPT algorithms are validated for several case studies, and the obtained results are compared with that of conventional MPPT algorithms in terms of convergence speed, specifying of correct direction side, oscillations and overall system efficiency under rapidly changing atmospheric conditions and partial shading conditions.
- Interleaved DC-DC boost converter topology, which provides fast dynamic response and reduced ripples on input and output waveforms, is presented.
- Multi-string inverter type, which supplies extra input ports of inverter ensure efficient control of the entire system by controlling of MPP in small strings of PV systems, is simulated.
- A DC link voltage controller and reactive power flow controller are presented in order to solve the problem of regulating the voltage at the input of the three phase VSI and reducing the reactive power flow.
- L filter has the advantage of lower cost and higher dynamic response since smaller area is needed to achieve required performance in damping the switching harmonics comparing with LC or LCL filters.
- The THD value of the output current is less than 5%, which is within IEEE-519 & IEC-6000-3 standards.
- Injected reactive power of established PV system is compensated and the power factor is always kept at higher than 0.98.

MPPT controllers are well founded in the literature and market. However, some subjects still need further research and analysis. The recommendations for the future works can be summarized as follows:

- The constructed two stage grid-tied PV system and proposed MPPT techniques can be tested by implementation of a physical model where the efficiency and accuracy of the proposed system can be better evaluated.
- Different DC-DC converter configurations, which affect the MPPT capability of the system, can be developed and evaluated for PV applications.
- DC-AC inverter controller part can be improved and tested for different cases and fault analysis can be performed to specify the optimal control strategy.
- Several filter types such as L, LC, LCL and etc., can be integrated to output of the inverter and an evaluation can be realized in terms of damping the switching harmonics, dynamic response and cost.
- Islanding issue and anti-islanding protection application for grid tied PV systems can be investigated.
- Optimal layout with the use of a minimum number of solar irradiation measurement sensors can be approved experimentally.

REFERENCES

ABDELSALAM A. K., MASSOUD A. M., AHMED S., ENJETI P. N., 2011. High-Performance Adaptive Perturb and Observe MPPT Technique for Photovoltaic- Based Microgrids, IEEE Transactions on Power Electronics, Vol. 26, No. 4, 1010-1021.

Annual Energy Outlook 2010 with Projections to 2035, 2010. U. S. Energy Information Administration (EIA), available at http://www.eia.gov/oiaf/archive/aeo10/pdf/0383 (2010).pdf [accessed18.05.20 15].

BARIS K., KUCUKALI S., 2012. Availability of Renewable Energy Sources in Turkey: Current Situation, Potential, Government Policies and the EU Perspective, Energy Policy 42 (2012) 377–391.

BENNETT T., ZILOUCHIAN A., MESSENGER R., 2013. A proposed maximum power point tracking algorithm based on a new testing standard, Solar Energy 89 (2013) 23–41.

BIANCONI E, CALVENTE J, GIRAL R, MAMARELIS E, PETRONE G, RAMOS-PAJA C. A., SPAGNUOLO G., VITELLI M., 2013. Perturb and observe MPPT algorithm with a current controller based on the sliding mode. Electrical Power and Energy Systems 44 (2013) 346–356.

BLAS B. A., TORRES J. L., PRIETO E., GARCIA A., 2002. Selecting a suitable model for characterizing photovoltaic devices, Renewable Energy 25 (2002) 371–380.

BLAS M. A., TORRES J. L., PRIETO E., GARCIA A., 2001. Selecting a suitable model for characterizing photovoltaic devices, Renewable Energy 25 (2002) 371–380

BOICO, F., LEHMAN, B., SHUJAEE, K., 2007. Solar battery chargers for NiMH Batteries. IEEE Transactions on Power Electronics 22, 1600–1609.

BP Statistical Review of World Energy 2014, 2014. Available at http://www.bp.com/content/dam/bp/pdf/Energy-economics/statistical-review-

2014/BP-statistical-review-of-world-energy-2014-full-report.pdf [accessed 18.05.2015].

CAN H., 2013. Model of a photovoltaic panel emulator in MATLAB-Simulink, Turkish Journal of Electrical Engineering & Computer Sciences Sci 21: 301 – 308.

CELIK A. N. and ACIKGOZ N., 2007. Modelling and experimental verification of the operating current of mono-crystalline photovoltaic modules using four- and five- parameter models," Appl. Energy, vol. 84, no. 1, pp. 1–15.

CHAOUI A., GAUBERT J.P., KRIM F. and RAMBAULT L., 2008. On the Design of Shunt Active Filter for Improving Power Quality, IEEE International Symposium on Industrial Electronics, pp. 31-37.

CHIU C. S., OUYANG Y. L., KU C. Y., 2012. Terminal Sliding Mode Control for Maximum Power Point Tracking of Photovoltaic Power Generation Systems, Solar Energy 86 (2012) 2986–2995.

EL CHAAR L., IAMONT L. A., EL ZEIN N., 2011. Review of Photovoltaic Technologies, Renewable and Sustainable Energy Reviews 15 (2011) 2165–2175.

Elektrik Piyasası Şebeke Yönetmeliği (EPŞY), available at http://www.epdk.gov.tr/index.php/elektrik-piyasasi/mevzuat?id=89 [accessed 11.06.2015]

ELTAWIL M. A., ZHAO Z., 2013. MPPT techniques for photovoltaic applications, Renewable and Sustainable Energy Reviews 25(2013)793–813.

Energy Informative (EI), available at http://energyinformative.org/ [accessed 24.06.2015]

Enerji Enstitüsü (EE). available at http://enerjienstitusu.com/turkiye-kurulu-elektrik-enerji-gucu-mw/, [accessed 04.06.2015].

ENRIQUE J. M., DURAN E., CARDONA M. S., ANDUJAR J. M., 2007. Theoretical assessment of the maximum power point tracking efficiency of photovoltaic facilities with different converter topologies, Solar Energy 81 (2007) 31–38.

ENRIQUE, J. M., ANDUJAR, J. M., BOHORQUEZ, M. A., 2010. A reliable, fast and low cost maximum power point tracker for photovoltaic applications. Solar Energy 84, 79–89.

ESRAM, T., CHAPMAN, P. L., 2007. Comparison of photovoltaic array maximum power point tracking techniques. IEEE Transactions on Energy Conversion 22, 439–449.

EVJU S. E., 2007. MSc Thesis, Norwegian University of Science and Technology, Department of Electrical Power Engineering, 164 pages.

EXPOSITO A. G., CONEJO A. J., CANIZARES C., 2009. Electric Energy Systems, CRC Press, 648 pages.

FEMIA N, PETRONE G, SPAGNUOLO G VITELLI M., 2004. Optimizing sampling rate of P&O MPPT technique. In: 351k annual IEEE power electronics specialists conference, Aachen, Germany; April-2004. p 1945–9, ZW4.

GOW J. A., MANNING C. D., 1999. Development of a photovoltaic array model for use in power-electronics simulation studies, IEE Proc.-Electr. Power Appl., Vol. 146, No.2.

HART D. W., 2011. Power Electronics, McGraw-Hill, 477 pages.

HASNI A., SEHLI A., DRAOUI B., BASSOU A., AMIEUR B., 2012. Estimating global solar radiation using artificial neural network and climate data in the south-western region of Algeria, Energy Procedia 2012; 18:531-7.

HUSSEIN, K. H., MUTA, I., HOSHINO, T., OSAKADA, M., 1995. Maximum photovoltaic power tracking: an algorithm for rapidly changing atmospheric conditions. IEE Proceedings on Generation, Transmission and Distribution 142, 59–64.

ISHAQUE K., SALM Z., TAHERI H., SYAFARUDDIN, 2011.Modeling and Simulation of Photovoltaic (PV) System during Partial Shading Based on a Two-Diode Model. Simulation Modeling Practice and Theory 19 (2011) 1613–1626.

JUNG D. Y., JI H. Y., PARK S. H., JUNG J. C., WON C. Y., 2011. Interleaved Soft-Switching Boost Converter for Photovoltaic Power-Generation System, IEEE Transactions on Power Electronics, Vol. 26, No. 4, 1137-1145.

KALBAT A. Y., 2013. PSCAD simulation of grid-tied photovoltaic systems and Total Harmonic Distortion analysis, Electric Power and Energy Conversion Systems (EPECS), 2013 3rd International Conference.

KEREKES T., TEODORESCU R., BORUP U., 2007. Transformerless Photovoltaic Inverters Connected to the Grid. IEEE 2007 Applied Electronics Conference, (APEC), 2007, pp 1733-1737.

KJAER S. B., PEDERSEN J. K., BLAABJERG F., 2005. A Review of Single–Phase Grid-Connected Inverters for Photovoltaic Modules, IEEE Transactions on Industry Applications, Vol. 41, No. 5.

KOLIC Y., GAUTHIER E., PEREZ G. M. A., SIBAI A., DUPUY J. C., PINARD P., M'GHAIETH R., MAAREF H., 1995. Electron powder ribbon polycrystalline silicon plates used for porous layer fabrication, Thin Solid Films 255 (1995) 159-162.

KUNG S. Y., 1993. Digital Neural Networks, PTR Prentice-Hall. 444 pages.

LEE P. W. , LEE Y. S., CHENG D. K. W., LIU X. C., 2000. Steady-State Analysis of an Interleaved Boost Converter with Coupled Inductors, IEEE Transactions on Industrial Electronics, Vol. 47, No. 4, 2000.

LIPPMANN R. P., 1987. An Introduction to Computing with Neural Nets, ASSP Magazine IEEE 1987; 4-2:4-22.

LIU Y. H., LIU C. L., HUANG J. W., CHEN J. H., 2013. Neural-network-based maximum power point tracking methods for photovoltaic systems operating under fast changing environments, Solar Energy 89 (2013) 42–53.

LIU Y., 2009. Advanced Control of Photovoltaic Converters, PhD Thesis, University of Leicester, Department of Engineering, 141 Pages.

LYNN P.A., 2010. Electricity from Sunlight. An Introduction to Photovoltaics. WILEY, 221 pages.

MAHMOUD Y., XIAO W., ZEINELDIN H. H., 2012. A Simple Approach to Modeling and Simulation of Photovoltaic Modules, IEEE Transactions on SustainableEnergy, Vol. 3, No. 1.

MASSAWE H. B., 2013. Grid Connected Photovoltaic Systems with Smart Grid functionality, M.S. Thesis, Norwegian University of Science and Technology, Department of Electric Power Engineering, 66 Pages.

MASTERS G. M., 2013. Renewable and Efficient Electric Power Systems, WILEY, 383 pages.

MAYCOCK P., 2015. 2006-2015 World PV Market: Technology & Cost, available at http://www.ncsl.org/print/energy/PMaycockSolar1007.pdf [accessed 27.05.2015].

MEI Q., SHAN M., LIU L., GUERRERO J. M., 2011. A Novel Improved Variable Step-Size Incremental-Resistance MPPT Method for PV Systems. IEEE Transactions On Industrial Electronics, Vol. 58, No. 6, 2427-2434.

MELLIT A., BENGHANEM M., KALOGIROU S. A., 2007. Modeling and simulation of a stand-alone photovoltaic system using an adaptive artificial neural network: Proposition for a new sizing procedure, Renewable Energy 32 (2007) 285–313.

MELLIT A., KALOGIROU A. S., 2014. MPPT-based artificial intelligence techniques for photovoltaic systems and its implementation into field programmable gate array chips: Review of current status and future perspectives, Energy 70 (2014) 1-21.

MEZA, C., NEGRONI, J.J., GUINJOAN, F. AND BIEL, D., 2007. Inverter Configuration Comparative for Residential PV-grid connected systems, 32nd Annual Conference on IEEE Industrial Electronics, IECON 2006, pp. 4361 - 4366.

MORADI M. H., TOUSI S. M. R., NEMATI M., BASIR N. S., SHALAVI N., 2013. A robust hybrid method for maximum power point tracking in photovoltaic systems, Solar Energy 94 (2013) 266–276.

MULJADI E., SINGH M., GEVORGIAN V., 2013. PSCAD Modules Representing PV Generator, National Renewable Energy Laboratory. Technical Report NREL/TP-5500-58189.

MURTAZA A., CHIABERGE M., GIUSEPPE M. D., BOERO D., 2014. A duty cycle optimization based hybrid maximum power point tracking technique for photovoltaic systems, Electrical Power and Energy Systems 59 (2014) 141–154.

NATIONAL RENEWABLE ENERGY LABORATORY (NREL), available at http://www.nrel.gov/learning/re_photovoltaics.html [accessed 18.05.2015]. National Renewable Energy Laboratory (NREL), available at http://www.nrel.gov/pv/ [accessed 18.05.2015]

NEMA R. K., BHATNAGAR P., 2013. Maximum power point tracking control techniques: State-of-the-art in photovoltaic applications, Renewable and Sustainable Energy Reviews 23 (2013) 224–241.

PATEL H., AGARWAL V., 2008. MATLAB-Based Modeling to Study the Effects of Partial Shading on PV Array Characteristics, IEEE Transactions On EnergyConversion, Vol. 23, No. 1,

RAHMAN S. A., VARMA R. K., 2011. PSCAD/EMTDC model of a 3-phase grid connected photovoltaic solar system, in Proc. 2011 North American Power Symp., pp. 1-7.

RAI A. K., KAUSHIKA N. D., SINGH B., AGARWAL N., 2011. Simulation Model of ANN Based Maximum Power Point Tracking Controller for Solar PV System, Solar Energy Materials & Solar Cells 95 (2011) 773–778.

RAJAPAKSE A. D., MUTHUMUNI D., 2009. Simulation tools for photovoltaic system grid integration studies, Electrical Power & Energy Conference (EPEC), 2009 IEEE.

RAMAPRABHA R., BALAJI K., RAJ S. B., LOGESHWARAN V. D., Comparison of Interleaved Boost Converter Configurations for Solar Photovoltaic System Interface, TJER 2013, Vol. 10, No. 2, 87-98.

RASHID M. H., 2007. Power Electronics Handbook Devices, Circuits, and Applications. Elsevier, 1172 pages.

RAZYKOF T. M., FEREKIDES C. S., MOREL D., STEFENAKOS E., ULLAL H. S., UPADHYAYA H. M., 2011. Solar photovoltaic electricity: Current status and future prospects, Solar Energy 85 (2011) 1580–1608.

REISI A. R., MORADI M. H., JAMASB S., 2013. Classification and comparison of maximum power point tracking techniques for photovoltaic system: A review, Renewable and Sustainable Energy Reviews 19 (2013) 433–443.

RENEWABLE ENERGY POLICY NETWORK FOR THE 21st CENTURY, 2014. Renewables 2014 Global Status Report, available at http://www.ren21.net/portals/0/documents/resources/gsr/2014/gsr2014_full%20report_low%20res.pdf.

REPUBLIC OF TURKEY MINISTRY OF ENERGY AND NATURAL RESOURCES (YEGM), available at http://www.eie.gov.tr/ [accessed 27.05.2015].

SAFARI A., MEKHILEF S., 2011. Simulation and Hardware Implementation of Incremental Conductance MPPT with Direct Control Method Using Cuk Converter, IEEE Transactions On Industrial Electronics, Vol. 58, No. 4, 1154- 1161.

SAGBAS A., KARAMANLIOGLU T., 2011. A Study on Potential and Utilization of Renewable Energy Sources in Turkey, 6th International Advanced Technologies Symposium (IATS'11), May 2011, Elazığ, Turkey.

SAID S., MASSOUD A., BENAMMAR M., AHMED S., 2012. A Matlab /Simulink- Based Photovoltaic Array Model Employing SimPowerSystems Toolbox, Journal of Energy and Power Engineering 6 (2012) 1965-1975.

SALAM Z., AHMED J., MERUGU B. S., 2013. The Application of Soft Computing Methods for MPPT of PV System: A Technological and Status Review, Applied Energy 107 (2013) 135-148.

SALAS V., OLIAS E., BARRADO A., LAZARO A., 2006. Review of the Maximum Power Point Tracking Algorithms for Stand-Alone Photovoltaic Systems, Solar Energy Materials & Solar Cells 90 (2006) 1555–1578.

SARIBULUT L., 2012. Detection and Mitigation Methods of Power Quality Disturbances, PhD Thesis, Çukurova University, Institute of Natural and Applied Sciences, 291 pages.

SCHIMPF F., NORUM E. L., 2008. Grid Connected Converters for Photovoltaic, State Of The Art, Ideas for Improvement of Transformerless Inverters, Nordic Workshop on Power and Industrial Electronics (NORPIE), June 9-11, 2008.

SHIN H. B., PARK J. G., CHUNG S. K., LEE H W., LIPO T A., 2005. Generalized steady-state analysis of multiphase interleaved boost converter with coupled inductors. Proc. IEE Electronics Power Application 152:584-594.

SOTO W., KLEIN S. A., BECKMAN W. A., 2006. Improvement and validation of a model for photovoltaic array performance, Solar Energy 80 (2006) 78–88.

SUBUDHI B., PRADHAN R., 2013. A Comparative Study on Maximum Power Point Tracking Techniques for Photovoltaic Power Systems, IEEE Transactions on Sustainable Energy, Vol. 4, No. 1, 89-98.

SULLIVAN, C. R., POWERS, M. J., 1993. A high-efficiency maximum power point tracker for photovoltaic arrays in a solar-powered race vehicle. IEEE Power Electronics Specialists Conference, June 1993, pp. 574–580.

TAFTICHT T., AGBOSSOU K., DOUMBIA M. L., CHERITI A., 2007. An improved maximum power point tracking method for photovoltaic systems, Renewable Energy 33 (2008) 1508–1516.

TEKE A., 2011. Unified Power Quality Conditioner: Design, Simulation and Experimental Analysis, PhD Thesis, Çukurova University, Institute of Natural and Applied Sciences, 204 pages.

Texas Instrument, (TI) AN-1820 LM5032 Interleaved Boost Converter Application Report, 2013. Available at http://www.ti.com/lit/an/snva335a/snva335a.pdf [accessed 29.05.2015].

TSENG S. Y., WANG H. Y., 2013. A Photovoltaic Power System Using a High Step-up Converter for DC Load Applications, Energies 2013, 6, 1068-1100.

U.S. ENERGY INFORMATION ADMINISTRATION (EIA) available at http://www.eia.gov/renewable/annual/solar_photo/ [accessed 18.05.2015].

VEERACHARY M., 2008. Maximum power point tracking algorithm for nonlinear DC sources 2008. In: IEEE region 10 colloquium and the third international conference on industrial and information systems, Kharagpur, India; Paper no: 507.

VEERACHARY M., SENJYU T., UEZATO K., 2003. Neural-Network-Based Maximum-Power-Point Tracking of Coupled-Inductor Interleaved-Boost-Converter-Supplied PV System Using Fuzzy Controller, IEEE Transactions On Industrial Electronics, Vol. 50, No. 4, 749-758.

VILLALVA M. G., GAZOLI J. R., FILHO E. R., 2009. Comprehensive Approach to Modeling and Simulation of Photovoltaic Arrays, IEEE Transactions on Power Electronics, Vol. 24, No. 5.

WURFEL P., 2009. Physics of Solar Cells, WILEY-VCH, 244 pages.

XIAO W., OZOG N., DUNFORD W. G., 2007. Topology Study of Photovoltaic Interface for Maximum Power Point Tracking, IEEE Transactions on Industrial Electronics, Vol. 54, No. 3, 1696-1704.

XIAOW., DUNFORDW. G., and CAPEL A., 2004. A novel modeling method for photovoltaic cells, IEEE 35th Ann. Power Electron. Spec. Conf. (PESC), vol. 3,pp.1950–1956.

CURRICULUM VITAE

Özgür ÇELİK was born in Ankara, Turkey in 1990. He graduated from Sincan Süleyman Demirel Anatolian High School in 2008. He received his BSc degree in Electrical and Electronics Engineering from Çukurova University in 2013. After graduation, he has specialized on transmission and distribution systems in private sector for 1-year. In 2013, he started his MSc education in Electrical and Electronics Engineering in Çukurova University. He has been working as a Research Assistant in Electrical and Electronics Engineering Department of the Adana Science and Technology University since 2014.

His research areas are renewable energy systems, generation, transmission and distribution of electrical energy, power electronic converters and energy efficiency applications.

He is a member of Institute of Electrical and Electronics Engineer (IEEE) and Turkish Chamber of Electrical Engineers (UCTEA).

APPENDIX

APPENDIX A: Datasheet of SUNPOWER E19 / 240 Solar Panel

BENEFITS

Highest Efficiency
SunPower™ Solar Panels are the most efficient photovoltaic panels on the market today.

More Power
Our panels produce more power in the same amount of space—up to 50% more than conventional designs and 100% more than thin film solar panels.

Reduced Installation Cost
More power per panel means fewer panels per install. This saves both time and money.

Reliable and Robust Design
Proven materials, tempered front glass, and a sturdy anodised frame allow panel to operate reliably in multiple mounting configurations.

SPR-240E-WHT-D

E19 SERIES

The SunPower™ 240 Solar Panel provides today's highest efficiency and performance. Utilising 72 SunPower back-contact solar cells, the SunPower 240 delivers a total panel conversion efficiency of 19.3%. The panel's reduced voltage-temperature coefficient, anti-reflective glass and exceptional low-light performance attributes provide outstanding energy delivery per peak power watt.

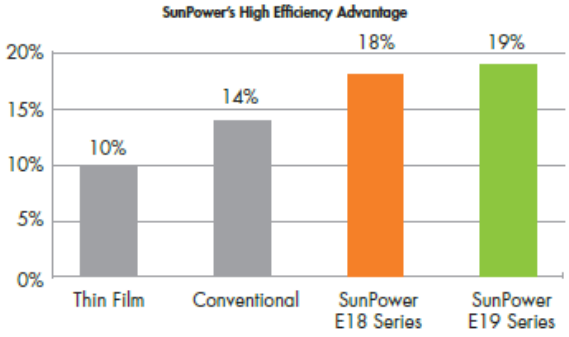

Electrical Data

Measured at Standard Test Conditions (STC): Irradiance 1000W/m², AM 1.5, and cell temperature 25° C

Nominal Power (+5/-3%)	P_{nom}	240 W
Efficiency	η	19.3 %
Rated Voltage	V_{mpp}	40.5 V
Rated Current	I_{mpp}	5.93 A
Open Circuit Voltage	V_{oc}	48.6 V
Short Circuit Current	I_{sc}	6.30 A
Maximum System Voltage	IEC	1000 V
Temperature Coefficients	Power (P)	-0.38% / K
	Voltage (V_{oc})	-132.5mV / K
	Current (I_{sc})	3.5mA / K
NOCT		45° C +/-2° C
Series Fuse Rating		20 A
Limiting Reverse Current (3-strings)	I_r	15.8 A

Electrical Data

Measured at Nominal Operating Cell Temperature (NOCT): Irradiance 800W/m², 20° C, wind 1 m/s

Nominal Power	P_{nom}	178 W
Rated Voltage	V_{mpp}	37.3 V
Rated Current	I_{mpp}	4.77 A
Open Circuit Voltage	V_{oc}	45.5 V
Short Circuit Current	I_{sc}	5.10 A

I-V Curve

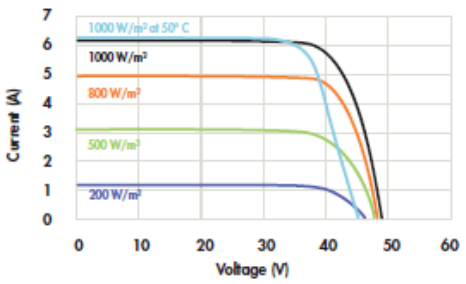

Current/voltage characteristics with dependence on irradiance and module temperature.

Tested Operating Conditions

Temperature	-40° C to +85° C
Max load	550 kg / m² (5400 Pa) front - e.g. snow 245 kg / m² (2400 Pa) front and back - e.g. wind
Impact Resistance	Hail – 25 mm at 23 m/s

Warranties and Certifications

Warranties	25 year limited power warranty
	10 year limited product warranty
Certifications	IEC 61215 Ed. 2, IEC 61730 (SCII)

Mechanical Data

Solar Cells	72 SunPower all-back contact monocrystalline
Front Glass	High transmission tempered glass with anti-reflective (AR) coating
Junction Box	IP-65 rated with 3 bypass diodes
	32 x 155 x 128 (mm)
Output Cables	1000mm length solar cables / MultiContact (MC4) connectors
Frame	Anodised aluminium alloy 6063 (black)
Weight	15.0 kg

Dimensions